



MRes Venugopal Gudipati

The Yeast quinone reductase Lot6p and its cellular functions

DISSERTATION

zur Erlangung des akademischen Grades eines

Doktors der Naturwissenschaften

erreicht an der

Technischen Universität Graz

Betreuer: Univ.-Prof. Mag. *rer. nat.* Dr. *rer. nat.* Peter Macheroux

Institut für Biochemie, Technische Universität Graz

Graz, 2014

Acknowledgments

The part of my life dedicated to produce this dissertation was wonderfully frustrating. Nevertheless, I made good friends, learned a lot, improved my criticality and most importantly performed research which I like the most. Even though the writings in this thesis are mine, the work described in this thesis would not have been possible without the knowledge & support of my colleagues, beautiful friendships and the love of my family. Especially, I am immensely grateful to the Republic of Austria and its people for hosting me and providing me the opportunity to start a research career.

My supervisor Prof. Peter Macheroux owes my gratitude for offering me this position and mentoring me on matters both professional and personal throughout my doctoral thesis. All the past and present colleagues of the Macheroux lab who later became good friends, made my long days in the lab pleasant, discussed trivial and essential topics, offered assistance and advice whenever possible. It was my privilege to mentor Anna Hatzl, Florian Sarkleti, Alin Ionas, David Rantasa and Karin Koch during my thesis.

I am really fortunate for the time i spent with friends and i wouldn't have been able to enjoy my time working on this thesis if it was not for them. Especially, Vasyl Ivashov, Domen Zafred, Wolf-Dieter Lienhart, Zalina Magomedova and all my friends from Elisabethheim.

I spent six wonderful months in the lab of Prof. Jürgen Dohmen at the University of Cologne and I am extremely grateful to Jürgen for teaching me how to look at the intricacies of ubiquitin proteasome system in an *in vivo* context. Those six months would not have been so beautiful without the friendship and assistance from of all the members of Jürgen lab.

I am very thankful to all the members of thesis committee for valuable suggestions. I would like to thank Fonds zur Förderung der wissenschaftlichen Forschung (FWF) and the PhD program DK Molecular Enzymology for funding this thesis.

I have no words to describe how much gratitude I owe my parents and family, without their constant support and understanding I would not have been able to come to this point in my career. I lovingly acknowledge Giulia Di Giglio who loved me and offered me unwavering support for the last three years.

Abstract

Quinone reductases (QR) are flavin dependent enzymes present in bacteria, fungi, plants and mammals. QR were shown to prevent quinone mediated oxidative stress by catalyzing the obligatory two electron reduction of quinones to hydroquinones, thereby preventing the formation of semi quinone radicals. Recently, it was proposed that two QR, Lot6p from the yeast *Saccharomyces cerevisiae* and NAD(P)H:quinone oxidoreductase 1 (NQO1) from humans function as regulators of the 20S proteasome. These QR were shown to bind the 20S proteasome and prevent the *in vitro* ubiquitin independent degradation of the transcription factors Yap4p and p53, respectively. Currently, structural information detailing the mode of QR interaction with the 20S proteasome and transcription factors is lacking.

In order to structurally characterize Lot6p's interaction with the 20S proteasome, three amino acid residues at the proposed interaction site were exchanged to generate variants, Lot6p N96C, W97A and G98L. Two variants, Lot6p N96C and G98L, were unable to bind the FMN cofactor. Probably these variants are not able to bind the 20S proteasome, since it was previously shown that apo-Lot6p is unable to bind the 20S proteasome. The variant Lot6p W97A retains the FMN cofactor and exhibits similar FMN reductase activity compared to Lot6p. However, Lot6p W97A was unable to bind the 20S proteasome and the reasons for this are still unexplained. Simultaneously, the *in vivo* role of Lot6p in the regulation and ubiquitin independent degradation of Yap4p was also studied. It has been shown that intracellular levels of Yap4p are independent of Lot6p and also that ubiquitination is essential for the degradation of Yap4p. However, it is still not clear if an alternate *in vivo* mechanism exists where Yap4p is degraded in an ubiquitin independent manner.

NQO1 is known to regulate the ubiquitin independent degradation of tumour suppressors (e.g. p53, p33 and p73). Contrastingly, a prevalently occurring variant (*NQO1**2, NQO1 P187S) is known to be dysfunctional in its enzymatic and interaction properties. However, the exact structural and biochemical basis for the dysfunctionality of NQO1 P187S was not known. We have shown for the first time that the amino acid exchange P187S destabilizes a crucial interdomain contact between the C-terminal domain and the core domain. The destabilization of the interdomain contact consequently compromises the FAD cofactor binding and catalytic efficiency leading to the loss of function.

Kurzfassung

Chinon-Reduktasen (QR) sind flavinabhängige Enzyme, welche in Bakterien, Pilzen, Pflanzen und Säugetieren gefunden werden. Es konnte gezeigt werden, dass QR den durch Chinone ausgelösten oxidativen Stress verringern können, indem sie die Bildung eines radikalischen Semichinons verhindern. Kürzlich wurde gezeigt, dass die QR, aus *Saccharomyces cerevisiae* (Lot6p) und die im Menschen vorkommende NAD(P)H:Chinon Oxidoreduktase 1 (NQO1) als Regulatoren des 20S-Proteasoms fungieren. Darüber hinaus konnte gezeigt werden, dass diese zwei QR *in vitro* an das 20S-Proteasom binden und den Ubiquitin-unabhängigen Abbau von Transkriptionsfaktoren (z.B. Yap4p in der Hefe bzw. p53 beim Menschen) beeinflussen. Derzeit gibt es keine strukturellen Informationen über die genaue Interaktion der QR mit dem 20S-Proteasom sowie den Transkriptionsfaktoren.

Um die molekularen Wechselwirkungen von Lot6p mit dem 20S-Proteasom zu charakterisieren wurden drei Aminosäuren an der vermuteten Interaktionsstelle ausgetauscht. Es konnte gezeigt werden, dass zwei dieser Varianten, Lot6p N96C und G98L, den FMN-Kofaktor nicht binden können. Nachdem bereits bekannt ist, dass Apo-Lot6p nicht an das 20S-Proteasom binden kann, ist auch bei diesen beiden Varianten eine Bindung mit hoher Wahrscheinlichkeit auszuschließen. Lot6p W97A hingegen behält die Fähigkeit FMN zu binden und zeigt auch eine, dem Wildtyp vergleichbare, FMN-Reduktase-Aktivität. Trotzdem konnte Lot6p W97A nicht an das Proteasom binden – hierbei sind die Ursachen jedoch noch unbekannt. Parallel dazu wurde auch die Rolle von Lot6p im vom Ubiquitin unabhängigen Abbau von Yap4p *in vivo* untersucht. Es erwies sich, dass der intrazelluläre Yap4p-Level von Lot6p unabhängig ist und die Ubiquitinierung für den Abbau von Yap4p essentiell ist. Jedoch bleibt weiterhin unklar ob ein alternativer, ubiquitin-unabhängiger, Abbauweg ebenfalls für Yap4p *in vivo* existiert.

NQO1 wurde als Regulator für den Ubiquitin-unabhängigen Abbau von Tumorsuppressoren (z. B. p53, p33 und p73) identifiziert. Eine häufig auftretende Variante des Enzyms (NQO1*2, NQO1 P187S) ist sowohl in den enzymatischen als auch regulatorischen Eigenschaften dysfunktional. Bisher waren die strukturellen und biochemischen Ursachen für diese Dysfunktionalität unbekannt. Wir konnten nun erstmals zeigen, wie der Aminosäureaustausch eine wichtige Kontaktstelle zwischen der Kerndomäne und der C-terminalen Domäne des Proteins destabilisiert. Diese Störung der Kontaktstelle der beiden Domänen schwächt die Bindung des FAD-Kofaktors und die Effizienz der katalytischen Eigenschaften, was in weiterer Folge zum Funktionsverlust des Proteins führt.

EIDESSTATTLICHE ERKLÄRUNG

Ich erkläre an Eides statt, dass ich die vorliegende Arbeit selbstständig verfasst, andere als die angegebenen Quellen/Hilfsmittel nicht benutzt, und die den benutzten Quellen wörtlich und inhaltlich entnommene Stellen als solche kenntlich gemacht habe.

STATUTORY DECLARATION

I declare that I have authored this thesis independently, that I have not used other than the declared sources / resources, and that I have explicitly marked all material which has been quoted either literally or by content from the used sources.

Graz, 11.02.2014

Venugopal Gudipati

Instructions for the reader

Parts of this thesis have already been published or will be published in the near future. Thus, an unconventional arrangement of contents has been chosen. Each chapter is either a publication or a manuscript in submission or unpublished results. Every single chapter represents a closed entity and can be read without detailed knowledge of the entire content. The contributions of all the authors are clearly stated for all the publications and manuscripts. In case of chapters where contributions are not mentioned all the work has been done by me.

Table of Contents

Introduction to this thesis.....	1
Chapter 1 (Review article)	
Author contributions	3
The flavoproteome of the yeast <i>Saccharomyces cerevisiae</i>	4
Chapter 2 (Unpublished results)	
Quinone reductases and their role in regulating 20S proteasome	
2.1 Introduction	14
2.1.1 Quinone reductases are essential for combating oxidative stress.....	15
2.1.2 Yeast quinone reductase Lot6p.....	16
2.1.3 Biochemical and Structural properties of Lot6p	16
2.1.4 Physiological role of quinone reductase Lot6p	19
2.2 Materials and methods	22
2.3 Results	24
2.4 Discussion.....	31
References.....	33
Chapter 3 (Unpublished results)	
In vivo role of Lot6p in the regulation of transcription factor Yap4p	
3.1 Introduction	36
3.1.1 The leucine-zipper coiled-coil domain	36
3.1.2 Yeast activator protein family	37
3.1.3 Yeast activator protein Yap4p	38
3.2 Materials and methods	40

3.3 Results and discussion.....	43
References.....	49
Chapter 4 (Review article)	
Author contributions	53
The human flavoproteome	54
Chapter 5 (Manuscript in submission)	
Collapse of the native structure by a single amino acid exchange in human NAD(P)H:quinone oxidoreductase (NQO1)Title page & contributions	
Title page & contributions.....	67
Abstract.....	68
Significance statement	68
Introduction	69
Results and discussion.....	69
Figures	74
Supplementary figures	78
Materials & Methods.....	85
Acknowledgments	91
References.....	91
Chapter 6 (Unpublished results)	
Biochemical characterization of human NAD(P)H:quinone oxidoreductase (NQO1) variant NQO1 R139W	
6.1 Introduction	94
6.2 Results, discussion and future work.....	96
References.....	97

Appendix

Curriculum vitae	98
------------------------	----

Introduction to this thesis

Flavoproteins are ubiquitous proteins involved in a wide range of biological processes ranging from electron transport, cofactor synthesis, light emission and DNA repair. Flavoproteins typically contain a flavin mononucleotide (FMN) and/or flavin adenine dinucleotide (FAD) coenzyme bound to the protein either covalently or non-covalently. Otto Warburg and collaborators discovered the first flavoprotein from *Saccharomyces cerevisiae* called “yellow ferment” which was later renamed as OYE (Old yellow enzyme). Since the discovery of OYE, numerous flavoproteins (374 until the year 2011) were discovered in all forms of life. The information regarding flavoproteins is dispersed throughout the literature. For the first time this thesis reviews the flavoproteomes of model organism *Saccharomyces cerevisiae* and *Homo sapiens sapiens* in detail. Two flavoproteins, Lot6p from *S. cerevisiae* and NAD(P)H:quinone oxidoreductase (NQO1) from *H. sapiens sapiens* were of particular interest in the context of this thesis.

This thesis is divided into six chapters and the information provided in each chapter is briefly summarized below.

Chapter I reviews the flavoproteome of the yeast *S. cerevisiae*. This chapter discusses the discovery, general aspects of the yeast flavoproteome and also provides a general overview on the role of yeast flavoproteins in iron metabolism, redox balancing and flavin biosynthesis. Furthermore, an overview table listing all yeast flavoproteins identified so far is presented along with an additional overview of yeast flavoproteins used as models for studying human diseases.

Chapter II discusses the role of yeast quinone reductase Lot6p in regulation of 20S proteasome. Information regarding the biochemical characterization of Lot6p variants, Lot6pN96C, Lot6p W97A, and Lot6p G98L is presented in this chapter. This chapter also discusses the interaction properties of Lot6p W97A with the 20S proteasome.

Chapter III discusses the *in vivo* role of Lot6p in the regulation of bZIP transcription factor Yap4p. This chapter also provides information regarding the involvement of Yap4p in oxidative and osmotic stress conditions. Additionally, information regarding the degradation pathways of Yap4p is also provided.

Chapter IV describes the human flavoproteome. This chapter provides cumulative information regarding the role of flavoproteins in the biosynthesis of various cofactors, e.g. folate, heme, pyridoxal 5'-phosphate, coenzyme-A and coenzyme-Q. Tabular forms listing all the human

flavoproteins identified and the human flavoproteins involved in diseases and syndromes are also presented.

Chapter V & VI detail the biochemical and structural characterization of two naturally occurring human NQO1 variants, NQO1 P187S and NQO1 R139W. Chapter V provides conclusive biochemical and structural evidence explaining the loss of function in NQO1 P187S variant. Chapter VI provides the current status of the NQO1 R139W characterization together with details of further experiments which will be performed in the near future.

The flavoproteome of the yeast *Saccharomyces cerevisiae*

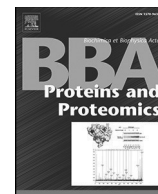
Author contributions

The idea to write this review article was conceived by Peter Macheroux. Peter Macheroux wrote the sub section introduction to the history of flavoprotein discovery. Karin Koch compiled the list of flavoproteins. The list was further verified and validated by me. Karin Koch and Wolf-Dieter Lienhart wrote the sub section on flavin biosynthesis and transport. I wrote the subsection and compiled the list of yeast flavoproteins as models for human diseases. All the authors contributed equally to the remaining sections of manuscript.



Contents lists available at ScienceDirect

Biochimica et Biophysica Acta

journal homepage: www.elsevier.com/locate/bbapap

Review

The flavoproteome of the yeast *Saccharomyces cerevisiae* [☆]Venugopal Gudipati, Karin Koch, Wolf-Dieter Lienhart, Peter Macheroux ^{*}

Graz University of Technology, Institute of Biochemistry, Petersgasse 12, A-8010 Graz, Austria

ARTICLE INFO

Article history:

Received 4 November 2013
 Received in revised form 18 December 2013
 Accepted 21 December 2013
 Available online 27 December 2013

Keywords:

Iron metabolism
 Mitochondrion
 Redox balance
 tRNA-modifications
 Membrane transporters

ABSTRACT

Genome analysis of the yeast *Saccharomyces cerevisiae* identified 68 genes encoding flavin-dependent proteins (1.1% of protein encoding genes) to which 47 distinct biochemical functions were assigned. The majority of flavoproteins operate in mitochondria where they participate in redox processes revolving around the transfer of electrons to the electron transport chain. In addition, we found that flavoenzymes play a central role in various aspects of iron metabolism, such as iron uptake, the biogenesis of iron-sulfur clusters and insertion of the heme cofactor into apocytochromes. Another important group of flavoenzymes is directly (Dus1-4p and Mto1p) or indirectly (Tyw1p) involved in reactions leading to tRNA-modifications. Despite the wealth of genetic information available for *S. cerevisiae*, we were surprised that many flavoproteins are poorly characterized biochemically. For example, the role of the yeast flavodoxins Pst2p, Rfs1p and Ycp4p with regard to their electron donor and acceptor is presently unknown. Similarly, the function of the heterodimeric Aim45p/Cir1p, which is homologous to the electron-transferring flavoproteins of higher eukaryotes, in electron transfer processes occurring in the mitochondrial matrix remains to be elucidated. This lack of information extends to the five membrane proteins involved in riboflavin or FAD transport as well as FMN and FAD homeostasis within the yeast cell. Nevertheless, several yeast flavoproteins, were identified as convenient model systems both in terms of their mechanism of action as well as structurally to improve our understanding of diseases caused by dysfunctional human flavoprotein orthologs.

© 2013 The Authors. Published by Elsevier B.V. All rights reserved.

1. Introduction to the history of Flavoprotein discovery

The yeast *Saccharomyces cerevisiae* played a central role in the discovery of flavoproteins as Otto Warburg and his collaborators were the first to isolate a “yellow ferment” from yeast cells [1]. Further studies by Theorell led to the concept of reversible association of co-enzyme and apo-enzyme to form the active holo-enzyme [2]. The isolation of other (new) yellow ferments from yeast prompted the renaming of the original ferment in to “old yellow ferment” (old yellow enzyme = OYE) [3]. Although it was demonstrated that OYE is reduced by NADPH [1,4] the physiological electron accepting substrate(s) remains uncertain despite its reported role in the maintenance of the cytoskeleton [5]. This may have contributed

to the persistent use of OYE instead of the official classification as NAD(P)H dehydrogenase (EC 1.6.99.1).

Despite the elusive nature of the physiological substrate(s), OYE rapidly developed in to an important model flavoenzyme culminating in the determination of the nucleotide sequence of *oye2* and *oye3* as well as the elucidation of its three-dimensional structure by X-ray crystallography [6–8]. The detailed biochemical characterisation of OYE also led to the identification of a number of artificial substrates, such as *N*-ethylmaleimide, cyclohex-2-enone and nitroolefins [8–10]. All of these substrates share a common structural motif consisting of an electron-withdrawing group (e.g. a carbonyl or nitro group) in α -position of a carbon-carbon double bond. The remarkably broad range of accepted substrates rendered OYE an ideal tool for biocatalytic applications exploited in numerous studies [11–15]. These efforts were further stimulated by the discovery of OYE homologs in many eubacteria as well as plant species in the 1990s [16–23]. Plant OYE homologs were of particular interest because of their well-defined role in the biosynthesis of the plant hormone jasmonate, which plays a crucial role in the plant's defense response to pathogens [24,25]. In all reported cases, the natural substrates exhibited the structural motif discovered in previous studies with yeast OYE. Hence, the yeast enzyme also became the paradigm for the class of “ene-reductases” now widely used for the synthesis of a variety of useful chemicals. Curiously, the broad range of activated “enes” accepted by OYEs as substrates is in stark contrast to its

Abbreviations: DHAP, dihydroxy acetone phosphate; DHBP, 3,4-dihydroxy-2-butanone-4-phosphate; DRAP, 2,5-diamino-6-(ribosylamino)-4-(3H)-pyrimidinone 5'-phosphate; ER, endoplasmic reticulum; ETC, electron transport chain; Gly3p, glycerol 3-phosphate; gluSA, γ -glutamic acid semialdehyde; Mia(40), mitochondrial intermembrane space import and assay/oxidoreductase 40; ORF, open reading frame; Q, ubiquinone

[☆] This is an open-access article distributed under the terms of the Creative Commons Attribution-NonCommercial-No Derivative Works License, which permits non-commercial use, distribution, and reproduction in any medium, provided the original author and source are credited.

^{*} Corresponding author. Tel.: +43 316 873 6450; fax: +43 316 873 6952.

E-mail address: peter.macheroux@tugraz.at (P. Macheroux).

Table 1
Yeast flavoproteins and genes.

No.	E.C.	Enzyme	Cofactor	Structure clan (family) ^a	Localization	Abbrev.	Syst. name
1	1.1.2.3	L-Lactate:cytochrome c oxidoreductase (flavo-cytochrome b ₂)	FMN/heme	TIM_barrel (FMN_dh)	Mito. intermembr. sp.	<i>cyb2</i>	YML054C
2	1.1.2.4	D-Lactate dehydrogenase	FAD/heme	–	I. mito. membr. Mito. matrix Cytoplasm	<i>dld1</i> <i>dld2</i> <i>dld3</i>	YDL174C YDL178W YEL071W
3	1.1.3.37	D-Arabino-1,4-lactone oxidase	8 α -(N3-His)-FAD	<i>FAD_PCMH</i>	O. mito. membr.	<i>alo1</i>	YML086C
4	1.1.5.3	Glycerol-3-phosphate dehydrogenase	FAD	<i>NADP_Rossmann (DAO)</i>	I. mito. membr.	<i>gut2</i>	YIL155C
5	1.3.1.90	tRNA dihydrouridine synthase	FMN	<i>TIM_barrel (Dus)</i>	Nucleus Nucleus/cytoplasm Nucleus/cytoplasm	<i>dus1</i> <i>dus2</i> <i>dus3</i> <i>dus4</i>	YML080W YNR015W YLR401C YLR405W
6	1.3.3.1	Dihydroorotate dehydrogenase	FMN	<i>TIM_barrel (DHO_dh)</i>	Cytoplasm	<i>ura1</i>	YKL216W
7	1.3.3.4	Protoporphyrinogen IX oxidase	FAD	<i>NADP_Rossmann (Amino_oxidase)</i>	I. mito. membr.	<i>hem14</i>	YER014W
8	1.3.3.6	Acyl-CoA oxidase	FAD	<i>Acyl-CoA_dh (ACOX, acyl-CoA_dh_1)</i>	Peroxisome	<i>pox1</i>	YGL205W
9	1.3.5.1	Succinate dehydrogenase Flavoprotein subunit A	8 α -(N3-His)-FAD/2Fe-2S/–	<i>NAPH_Rossmann (FAD_binding_2)</i>	I. mito. membr.	<i>sdh1</i> <i>sdh1b</i>	YKL148C YJL045W
10	1.4.1.14	Protein required for flavinylation of sdh NAD-dependent glutamate synthase	– FMN/3Fe-4S	<i>Glu_synthase/ Glu_syn_central</i>	I. mito. membr. Mito. matrix	<i>emi5</i> <i>glt1</i>	YOL071W YDL171C
11	1.4.3.5	Pyridoxal 5'-phosphate oxidase	FMN	FMN-binding (Pyridox_oxidase)	Mito. intermembr. sp.	<i>pdx3</i>	YBR035C
12	1.4.3.17	Pyridoxine 5'-phosphate oxidase Polyamine oxidase	FAD	<i>NADP_Rossmann (FAD_binding_2)</i>	cytoplasm	<i>fms1</i>	YMR020W
13	1.5.1.20	Methylenetetrahydrofolate reductase	FAD	<i>FAD_oxidored (MTHFR)</i>	– Mito.	<i>met12</i> <i>met13</i>	YPL023C YGL125W
14	1.5.5.1	Electron-transferring flavoprotein-ubiquinone oxidoreductase	FAD/4Fe-4S	<i>4Fe-4S (ETF_QO)</i>	I. mito. membr.	<i>cir2</i>	YOR356W
15	–	Electron transferring flavoprotein	FAD	<i>FAD_DHS (ETF_alpha)</i>	Mito. matrix	<i>aim45</i>	YPR004C
16	1.5.99.8	Proline dehydrogenase	FAD	<i>FAD_oxidored (Pro_dh)</i>	Mito. matrix	<i>put1</i>	YLR142W
17	1.6.2.2	Cytochrome-b5 reductase	FAD	<i>FAD_Lum_binding (FAD_binding_6)</i>	ER & o. mito. membr. ER & plasma membr.	<i>cbr1</i> <i>pga3</i>	YIL043C YML125C
18	1.6.2.4	NADPH-hemoprotein reductase (cytochrome P450 reductase)	FMN/heme FAD	Flavoprotein (Flavodoxin_1) FAD_Lum_binding (FAD_binding_1)	O. mito. membr., ER & plasma membr.	<i>ncp1</i>	YHR042W
19	1.6.5.2	NAD(P)H quinone oxidoreductase	FMN	Flavoprotein (Flavodoxin_2)	cytoplasm	<i>lot6</i>	YLR011W
20	1.6.5.9	NADH-ubiquinone oxidoreductase (rotenone-insensitive)	FAD/Fe-S	<i>NADP_Rossmann (Pyr_redox_2)</i>	I. mito. membr.	<i>ndi1</i>	YML120C
21	1.6.99.1	NADPH dehydrogenase	FMN	TIM_barrel (Oxidored_FMN)	Cytoplasm	<i>oye2</i>	YHR179W
22	1.–.–.–	External NADH dehydrogenase	FAD	–	I. mito. membr. I. mito. membr.	<i>oye3</i> <i>nde1</i> <i>nde2</i>	YPL171C YMR145C YDL085W
23	1.6.–.–	NADPH-dep. diflavin oxidoreductase	FMN FAD	Flavoprotein (Flavodoxin_1) FAD_Lum_binding (FAD_binding_1)	Mito. matrix	<i>tah18</i>	YPR048W
24	–	5-Carboxymethylaminomethylation of uridine (heterodimer with Mss1p)	FAD	<i>GIDA</i>	Mito.	<i>mto1</i>	YGL236C
25	–	Wybutosine biosynthesis, a tRNA-modification	FMN/4Fe-4S	Flavoprotein	ER	<i>tyw1</i>	YPL207W
26	1.8.1.2	Sulphite reductase (beta subunit)	FMN/heme FAD	Flavoprotein (Flavodoxin_1) FAD_Lum_binding (FAD_binding_1)	Cytoplasm	<i>met5</i>	YJR137C
27	1.8.1.4	Dihydrolipoyl dehydrogenase	FAD	<i>NADP_Rossmann (Pyr_redox_2)</i>	Mito. matrix	<i>lpd1</i>	YFL018C
28	1.8.1.7	Glutathione-disulfide reductase	FAD	<i>NADP_Rossmann (Pyr_redox_2)</i>	Cytoplasm & mito.	<i>glr1</i>	YPL091W
29	1.8.1.9	Thioredoxin-disulfide reductase	FAD	<i>NADP_Rossmann (Pyr_redox_2)</i>	Cytoplasm & mito. intermembr. sp.	<i>trr1</i>	YDR353W
30	–	Microtubule associated protein	FAD	<i>NADP_Rossmann? (Pyr_redox_2)</i>	Cytoplasm & mito. cytoplasm microtubule	<i>trr2</i> <i>irc15</i>	YHR106W YPL017C
31	1.8.3.2	Sulfhydryl oxidase	FAD/Fe-S cluster/ Heme	<i>Erv1_Alr</i>	Mito. intermembr. sp. ER membr.	<i>erv1</i> <i>erv2</i>	YGR029W YPR037C
32	1.8.4.–	Endoplasmic oxidoreductin 1	FAD	<i>Ero1</i>	ER & ER membr.e	<i>ero1</i>	YML130C
33	1.14.12.17	Nitric oxide oxidoreductase (flavo-hemoglobin)	FAD/heme	FAD_Lum_Binding (FAD_binding_6)	Cytoplasm	<i>yhb1</i>	YGR234W
34	1.14.13.–	Oxidase of thiols in the ER	FAD	–	Mito. matrix	<i>fmo1</i>	YHR176W
35	1.14.13.9	Kynurenine 3-monooxygenase	FAD	–	O. mito. membr.	<i>bnaf4</i>	YBL098W

Table 1 (continued)

No.	E.C.	Enzyme	Cofactor	Structure clan (family) ^a	Localization	Abbrev.	Syst. name
				NADP_Rossmann (FAD_Binding_3)			
36	1.14.99.7	Squalene monooxygenase	FAD	–	ER membr.	<i>erg1</i>	YGR175C
37	1.14.99.-	Monooxygenase in coenzyme Q biosyn.	FAD	–	I. mito. membr.	<i>coq6</i>	YGR255C
38	1.-.-.-	Ferric reductase	FAD/heme	–	Plasma membr.	<i>fre1</i>	YLR214W
					Plasma membr.	<i>fre2</i>	YKL220C
					Plasma membr.	<i>fre3</i>	YOR381W
					Plasma membr.	<i>fre4</i>	YNR060W
					Plasma membr.	<i>fre5</i>	YOR384W
					Vacuole membr.	<i>fre6</i>	YLL051C
					Plasma membr.	<i>fre7</i>	YOL152W
					–	<i>fre8</i>	YLR047C
39	1.-.-.-	NADPH oxidase	FAD/heme	–	Perinucl. ER membr.	<i>aim14</i>	YGL160W
40	1.-.-.-	NAD(P)H-dep. heme reductase	FAD	–	Inner mito. membr.	<i>cyc2</i>	YOR037W
41	2.2.1.6	Acetolactate synthase	FAD/TPP	FAD_DHS (TPP_enzyme_M)	Mito.	<i>ihv2</i>	YMR108W
42	2.3.1.86	Fatty acid synthase, subunit β, chain I	FMN	Not reported	Cytoplasm & mito.	<i>fas1</i>	YKL182W
43	4.1.1.36	4'-Phosphopantothencycysteine decarboxylase (forms a heterotrimeric complex with Sis2p and Vhs3p)	FMN	<i>Flavoprotein</i>	Cytoplasm	<i>cab3</i>	YKL088W
44	4.1.99.3	Deoxyribodipyrimidine photo-lyase	FAD	<i>HUP (DNA_photolyase)</i>	Cytoplasm, mito. & nucleus	<i>phr1</i>	YOR386W
45	4.2.3.5	Chorismate synthase	FMN	<i>Chorismate_synt</i>	Cytoplasm	<i>aro2</i>	YGL148W
46	–	Flavodoxin-like protein	FMN	<i>Flavoprotein</i> (<i>Flavodoxin_1</i>)	Cytoplasm, mito.	<i>pst2</i>	YDR032C
	–	Flavodoxin-like protein	FMN	<i>Flavoprotein</i> (<i>Flavodoxin_1</i>)	Cytoplasm	<i>rfs1</i>	YBR052C
	–	flavodoxin-like protein	FMN	<i>Flavoprotein</i> (<i>Flavodoxin_1</i>)	Cytoplasm, mito.	<i>ycp4</i>	YCR004C
47	–	Apoptosis-inducing factor	FAD	–	O. mito. membr., plasma membr. & nucleus	<i>aif1</i>	YNR074C

Abbreviations used in Table 1: biosyn., biosynthesis; dh, dehydrogenase; degr., degradation; dep., dependent; i., inner; ER, endoplasmic reticulum; mito., mitochondrion; o., outer; perinucl., perinuclear; red., reductase; sp., space.

^a Pfam classification given in plain text is for yeast proteins and those in italics are for homologs from other species.

invoked physiological role as a reductase of disulphide bonds in oxidatively damaged proteins of the cytoskeleton, such as actin [5].

2. General aspects of the yeast flavoproteome

The yeast genome contains 68 genes encoding for a flavin-dependent protein and thus 1.1% of all yeast proteins (5885 protein-encoding genes [26]) have a requirement for either FMN or FAD. Owing to the presence of several flavoprotein families, which will be discussed further below, these 68 genes give rise to 47 defined biochemical roles. Thirty-five flavoproteins require FAD (74%) and fifteen require FMN (26%). Yeast also possesses three diflavin enzymes, which harbor both FMN and FAD (Table 1). The utilization of FMN and FAD in yeast flavoproteins is very similar to the distribution found in a global analysis across all kingdoms of life [27] and does not have the bias towards FAD as found for the human flavoproteome [28]. Covalent flavinylation, which is statistically found in ca. 10% of flavoproteins, is underrepresented in the yeast flavoproteome with only two enzymes, succinate dehydrogenase (Sdh1p) and L-arabinono-1,4-lactone oxidase (Alo1p) featuring a covalent bond between the N(3)-nitrogen of a histidine residue and the 8-methyl group of the isoalloxazine ring system (Table 1). Both of these enzymes operate in yeast mitochondria and are located in the inner (Sdh1p) and outer (Alo1p) membrane. The scarcity of covalent flavoproteins is linked to the relative absence of the structural clan FAD_PCMH (with the exception of Alo1p), which features many examples of mono- and even bi-covalent flavinylation [27,28].

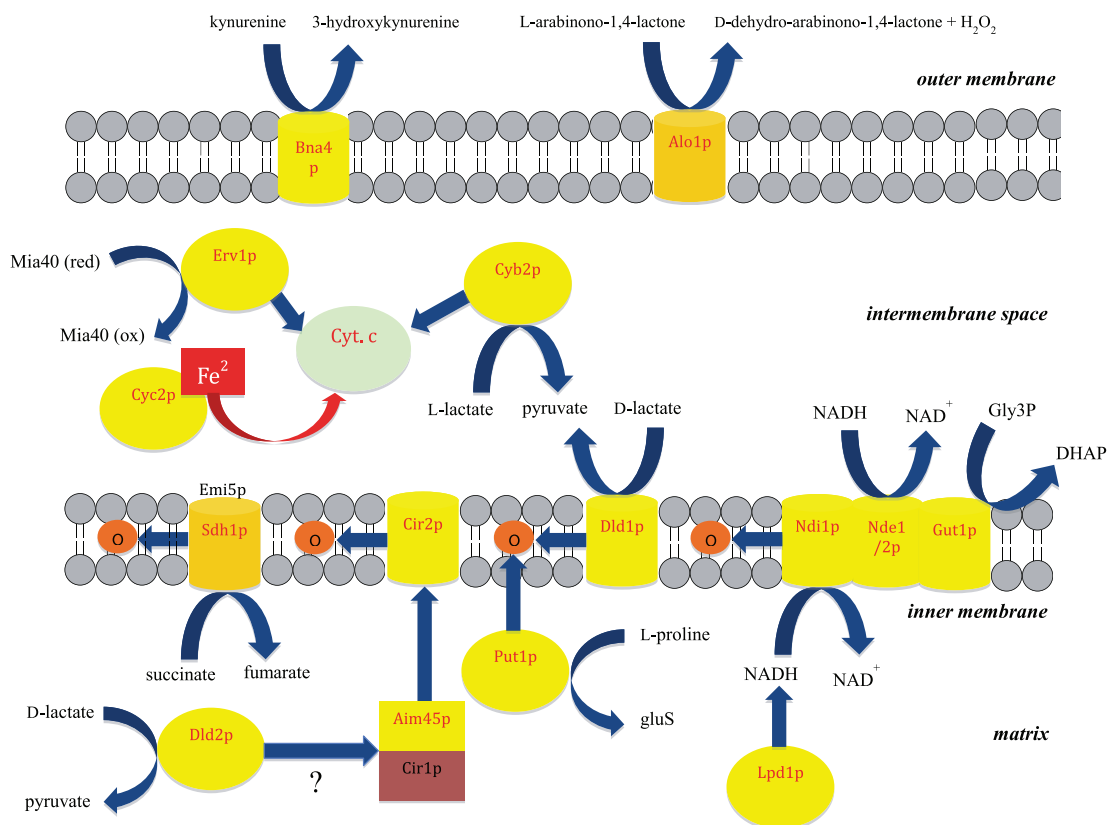
Structural information through X-ray crystallographic analysis is available for about one third of yeast flavoproteins listed in Table 1 (plain font in column “Structure clan/family”). In addition, the three-dimensional structure can be inferred from the known structure of homologs from other species (italics in column “Structure clan/family”). In some cases the structure of yeast flavoproteins served as paradigms for a family of enzymes, for example yeast OYE [6,29] and more recently kynurenine monooxygenase [30].

The general difficulties to elucidate the structure of integral or membrane associated proteins is also seen for flavoproteins (see Table 1).

Table 1 also provides information on the localisation of flavoproteins in the yeast cell. More than half of yeast flavoproteins (36 entries in Table 1) operate in the mitochondrion. Many of these are directly participating in redox reactions connected to the electron transport chain (ETC) (see also next section). Seventeen flavoproteins are located in the cytoplasm and only a few in the nucleus (Dus1-4p, Phr1p, Aif1p), endoplasmic reticulum (Aim14p, Cbr1p, Erg1p, Ero1p, Erv2p, Fmo1p, Ncp1p, Pga3p, Tyw1p) or the peroxisome (Pox1p). Requirement for the same flavoenzyme activity in different cellular compartments is either satisfied by expression of isozymes (e.g. Dld1-3p are found in either the cytoplasm, the inner mitochondrial membrane or the matrix) or the same flavoenzyme is present in multiple compartments (e.g. Cbr1p, Pga3p, Ncp1p, Trr1/2p, Yhb1p, Fas1p, Phr1p, Aif1p).

3. Flavoproteins, the stewards of iron

A remarkable result of our analysis concerns the multi-layered relationship between flavins and iron. As discussed in more detail in the next section, flavin-dependent ferric reductases (Fre1p-8p) are essential for reduction of ferric iron (and copper), which is prerequisite for iron (and copper) uptake by yeast transporters (permeases). Moreover, in several flavoproteins the flavin is responsible for the reduction of either heme iron or an iron-sulfur cluster (Table 1 and Scheme 1). Prominent examples include succinate dehydrogenase (Sdh1p), (Aim1p), nitric oxide oxidoreductase and L-lactate:cytochrome c oxido reductase (flavocytochrome b₂). In addition to this intramolecular electron transfer, two yeast flavoproteins, Cyc2p and Tah18p, are involved in intermolecular electron transfer. In the case of Cyc2p, which is located in the inner mitochondrial membrane with its FAD-containing active site exposed to the intermembrane space, the enzyme reduces Fe(III) and participates in the incorporation of the heme prosthetic group into apocytochrome c and c1 [31,32]. Similarly, the diflavin reductase Tah18p forms a complex



Scheme 1. Flavoproteins in mitochondrial redox processes. Flavoproteins are represented by yellow spheres (soluble flavoproteins in the matrix or intermembrane space) or barrels (inner or outer mitochondrial membrane). Flavoproteins with a covalently bound FAD (Sdh1p in the inner and Alo1p in the outer membrane) are shown in light orange. Cytochrome c is shown as a light green sphere. Curved blue arrows indicate redox reactions and straight arrows electron transfer. For further explanations and comments see main text. Several flavoproteins appear to participate in a multi-protein complex in the inner mitochondrial membrane [57]. For clarity, we have shown only a complex consisting of Ndi1p, Nde1/2p and Gut1p. Abbreviations used are: DHAP, dihydroxy acetone phosphate; Gly3p, glycerol 3-phosphate; GluS, γ -glutamic acid semialdehyde; Mia(40), mitochondrial intermembrane space import and assay/oxidoreductase 40 (ox, oxidized; red, reduced); Q, ubiquinone.

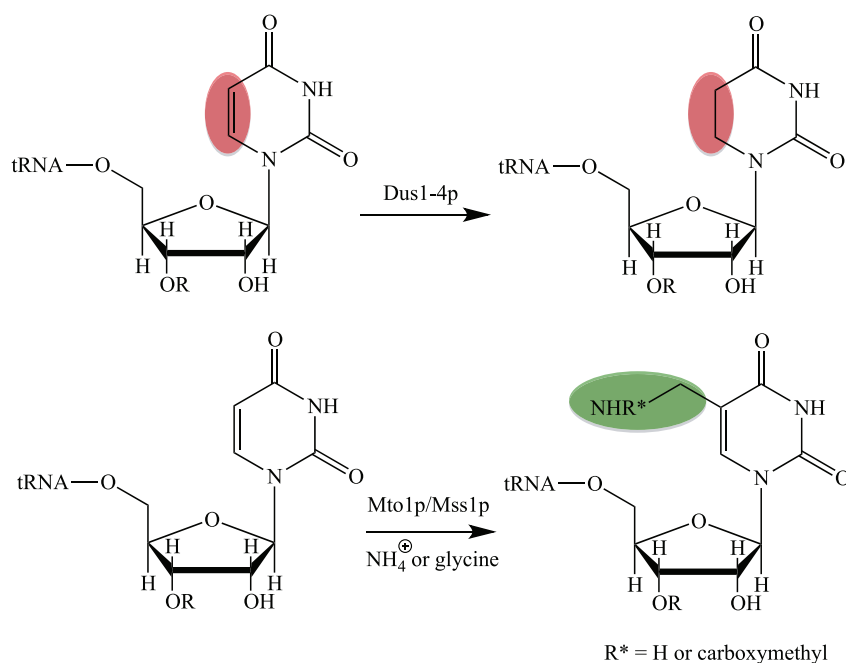
with Dre2p and provides electrons derived from NADPH to support the biosynthesis of two iron–sulfur clusters [33]. Recently, Tah18p was reported to be involved in NO generation in yeast and hence it is conceivable that it has more clients than Dre2p [34]. Thus flavoproteins fulfill various crucial tasks ranging from iron uptake, delivery of electrons to the mitochondrial electron transport chain, reduction of cytochrome-dependent reductases, biogenesis of iron–sulfur clusters and insertion of the heme cofactor into apocytochromes.

4. Flavoprotein families in yeast

As mentioned above, the yeast flavoproteome contains several families of flavoproteins, which catalyze identical or similar reactions. The largest group are the ferric/cupric reductases encoded by *fre1*–8 (see Table 1, entry 38). *Fre1* and *fre2* are metalloregulated by either iron or copper availability and the encoded metalloreductases reduce Fe(III) and Cu(II) at the expense of NADPH [35]. In addition to *fre1* and *fre2*, the yeast genome contains six homologous genes, termed *fre3*–8. *Fre3*–6 are regulated by iron whereas *fre7* is copper-regulated [36,37]. *Fre8* and the homologous *aim14* are not regulated by iron or copper suggesting a different role for these proteins [36]. Recently, it was demonstrated that *aim14* encodes an NADPH-oxidase, which produces superoxide in the endoplasmic reticulum [38] and it is thus conceivable that *fre8* also encodes an enzyme with similar properties. This notion is also supported by pair-wise sequence alignments showing the highest identity (30.6%) and similarity (56.5%) on the amino acid level between *fre8* and *aim14* within this family of flavoproteins [36]. Again, these functions highlight the importance of flavoenzymes for iron uptake and reduction as introduced in the previous section.

The second largest family comprise four tRNA-dihydrouridine synthases encoded by *dus1*–4 (Table 1, entry 5). The reduction of uracils to dihydrouridines in tRNA is one of the most common modifications of nucleosides in tRNA in all kingdoms of life [39]. A recent mechanistic study employing Dus2p revealed that reduction of uracil to dihydrouracil (see Scheme 2, top) is promoted by other tRNA modifications suggesting that tRNA maturation may occur in an ordered fashion [40]. Cytoplasmic tRNA in *S. cerevisiae* contains dihydrouridine in the D loop at positions 16, 17, 20, 20A, 20B and at the base of the variable arm at position 47. The four yeast enzymes exclusively reduce uracils in specific positions in tRNA: Dus1p reduces uracils in positions 16 and 17, Dus2p in position 20, Dus3p in position 47 and Dus4p in positions 20a and 20b. Thus these four enzymes are sufficient to generate all dihydrouridine modifications known in yeast [41]. In humans, only one dihydrouridine synthase homologous to yeast Dus2p (42% identity) was identified so far, which reduces uracil in tRNA for phenylalanine [28,42]. The human enzyme appears to be upregulated in malignant tissues resulting in higher levels of dihydrouridine [42]. Despite its putative role in malignancy the specificity and exact role of the human enzyme remains unclear.

In addition to reduction of uracil, the flavoenzyme Mto1p (also termed GidA) is involved in the biosynthesis of modifications at the C5-position of the uracil base in tRNAs [43,44]. Depending on the nitrogen source, ammonia or glycine, this reaction leads to the formation of either 5-aminomethyl- or 5-carboxymethylaminomethyluridine (Scheme 2, bottom). This modification occurs at the wobble position in mitochondrial tRNAs for lysine, glutamate and glutamine [44]. Detailed characterization of the bacterial protein complex of MnmE and MnmG (homolog of Mto1p) led to a mechanistic proposal in which the FAD-dependent MnmG serves a dual function during the reaction [43,45]. In this model,



Scheme 2. Flavoproteins in tRNA-modification. Top, reaction catalyzed by tRNA-dihydrouridine synthase (Dus1-4p); Bottom, reaction catalyzed by Mto1p/Mss1p. Depending on the co-substrate, ammonia or glycine, the side chain in position 5' of the uracil base is aminomethyl or carboxymethylaminomethyl. "R" represents the next 3'-nucleotide in the tRNA molecule.

methylene tetrahydrofolate bound to MnmE reacts with either ammonia or glycine to form a methylene amino group at N-5 of the tetrahydrofolate cofactor. Then, FAD oxidizes the carbon–nitrogen bond to yield an imine, which is then nucleophilically attacked by the uracil base of the tRNA substrate. In the next step the reduced FAD transfers a hydride to the imine to reduce the carbon–nitrogen double bond thus completing the biosynthesis of the C-5 side chain (see Scheme 2). Thus MnmG combines two canonical flavin-dependent reactions – oxidation of amines and reduction of double bonds – to catalyze the biosynthesis of the amino methyl or carboxymethylaminomethyl side chain.

Recently, yet another flavin-dependent enzyme encoded by *tyw1* (Table 1, entry 25) was discovered that catalyzes the second step in the biosynthesis of wybutosine-modified tRNA [46]. This enzyme belongs to the radical SAM superfamily characterized by the presence of a [4Fe–4S] cluster and a S-adenosylmethionine (SAM) domain [47]. Catalytic activity requires reduction of the [4Fe–4S] cluster in order to initiate one-electron transfer for reductive cleavage of SAM to generate the 5'-deoxyadenosyl radical [48]. In vivo, flavodoxins or ferredoxins might act as potential electron donors to convert [4Fe–4S]²⁺ to [4Fe–4S]⁺ and therefore it is conceivable that the N-terminal flavodoxin domain of Tyw1p relays electrons from an external electron donor such as NAD(P)H or an electron transfer protein to the [4Fe–4S] cluster. Such a functional role is supported by the finding that deletion of the flavodoxin domain abolishes TYW1p activity [49].

Interestingly, the yeast genome contains three homologous genes, *pst1*, *rfs1* and *ycp4* encoding three highly similar flavodoxin-like proteins (Table 1, entry 46) [50]. Although none of the proteins was functionally characterized with respect to their electron transfer properties and physiological redox partners they were found to act as transcriptional regulators of *spi1*, a gene responding to various environmental stimuli [51]. The lack of information on yeast flavodoxins is very surprising in view of the abundance of structural (148 structures of wild-type and variants in the pdb) and biochemical studies available for bacterial flavodoxins. Therefore, the current state of affairs for yeast flavodoxin-like proteins is very unsatisfactory and clearly warrants further investigations to define their biochemical and structural properties.

The family of D-lactate dehydrogenases comprising three enzymes, Dld1-3p, will be discussed in the context of redox processes in the next section.

5. Yeast flavoproteins in redox balancing

More than a quarter of yeast flavoproteins listed in Table 1 participate in redox reactions in the mitochondrion. As shown in Scheme 1, transfer of electrons into the ETC can either occur through electron donation to cytochrome c (cyt. c) in the intermembrane space or directly by reduction of ubiquinone to ubiquinol in the inner mitochondrial membrane. The latter route is clearly the dominating process in yeast mitochondria. Electrons transferred to NAD⁺ in the isocitrate, α -ketoglutarate and malate dehydrogenase reactions of the tricarboxylic acid cycle enter the ETC. via the NADH:ubiquinone oxidoreductase Ndi1p ("internal NADH dehydrogenase"). In contrast to complex I of higher eukaryotes this membrane-bound enzyme does not engage in proton translocation resulting in lower phosphorylation efficiency. The oxidation of succinate to fumarate is catalyzed by a canonical membrane-bound succinate dehydrogenase in which the covalently linked FAD becomes reduced by the substrate and the electrons are passed on to ubiquinone via an iron–sulfur cluster and heme relay system. The Sdh1p subunit of yeast succinate dehydrogenase (complex II) is one of only two flavin-dependent proteins exhibiting a covalent linkage (see Table 1, entry 9). Typically, covalent flavinylation is a spontaneous co- or posttranslational process. However, in the case of Sdh1p the assistance of Emi1p (Sdh5p) is required, which is conserved in higher eukaryotes and hence appears to be essential for complex II assembly [52,53]. Yeast also possesses a heterodimeric electron transfer flavoprotein (Aim45p/Cir1p) located in the mitochondrial matrix, which communicates with a membrane-bound electron transferring flavoprotein ubiquinone oxidoreductase (Cir2p). The latter flavoprotein feeds electrons received from Aim45p/Cir1p into the ETC. The clients for Aim45p/Cir1p, however, remain elusive as most electron donor proteins, such as the acyl-Co dehydrogenases involved in β -oxidation or amino acid degradation, are not present in *S. cerevisiae*. A potential candidate, L-proline dehydrogenase (Put1p), evidently feeds electrons from L-proline oxidation directly into the ETC. by reduction of ubiquinone to ubiquinol (see Scheme 1) [54].

Cytosolic NADH generated for example by the glycolytic enzyme glyceraldehyde 3-phosphate dehydrogenase is oxidized by either Nde1p or Nde2p ("external NADH:ubiquinone oxidoreductases") and the electrons serve to reduce ubiquinone (Scheme 1). The

mitochondrial ETC. can also be fuelled by the glycerol 3-phosphate shuttle: glycerol is first phosphorylated by glycerol kinase (Gut1p) in the cytosol and then transported to the intermembrane space to become oxidized by the membrane-bound glycerol 3-phosphate dehydrogenase (Gut2p) [55,56]. Several of the membrane-bound flavoproteins involved in substrate oxidation and electron transfer form a large supramolecular complex containing Nde1p, Nde2p and Gut2p and therefore inter-protein electron transfer may also occur prior to ubiquinone reduction [57].

Yeast possesses three D-lactate dehydrogenases (Dld1p-3, see Table 1), which operate in different compartments of the cell: Dld1p is located in the inner mitochondrial membrane, Dld2p in the matrix and Dld3 in the cytosol [58,59]. D-lactate is produced by the glyoxalase pathway that detoxifies methylglyoxal adventitiously generated by non-enzymatic elimination of hydrogen and phosphate from the enediol intermediate of triose phosphates [60]. Since this detoxification pathway is active in the cytosol and the mitochondrial matrix D-lactate dehydrogenase activity is required in these compartments to oxidize D-lactate to pyruvate (Scheme 1). Oxidation of D-lactate by the D-lactate dehydrogenase (Dld2p) localized in the mitochondrial matrix is coupled to ATP synthesis and therefore Dld2p apparently donates substrate-derived electrons to the ETC [61]. However, it is currently unknown whether electrons are directly used to reduce ubiquinone or transferred to the heterodimeric Aim45p/Cir2p electron transfer complex (Scheme 1).

The involvement of flavoproteins in central mitochondrial redox processes is also reflected by the fact that the flavin oxidation state oscillates in synchronized aerobically grown yeast cultures. During the oxidative phase of the culture the increase of flavin fluorescence indicates that more flavoproteins become oxidized whereas in the reductive phase of the internal rhythm a decrease of flavin fluorescence indicates a shift to the reduced state [62,63].

6. Flavin biosynthesis and transport

The biosynthesis of riboflavin in *S. cerevisiae* utilizes the canonical precursors, GTP and ribulose 5-phosphate. However, riboflavin biosynthesis deviates from the bacterial pathway in that deamination and reduction of the initial metabolite, 2,5-diamino-6-(ribosylamino)-4-(3H)-pyrimidinone 5'-phosphate (DRAP), take place in reverse order (www.kegg.jp). Briefly, in the first step GTP is converted by GTP cyclohydrolase II, encoded by *rib1*, to DRAP, which is reduced by Rib7p to 2,5-diamino-6-(ribitylamino)-4-(3H)-pyrimidinone 5'-phosphate (Table 2 and Scheme 3). This reaction is followed by deamination to 5-amino-6-ribitylamino-2,4-(1H,3H)-pyrimidinedione 5'-phosphate catalyzed by Rib2p [64]. After dephosphorylation by an unidentified

phosphatase condensation with 3,4-dihydroxy-2-butanone-4-phosphate (DHAB) occurs. The latter metabolite is synthesized from ribulose 5-phosphate by DHBP synthase (encoded by *rib3*). The condensation reaction is catalyzed by lumazine synthase (encoded by *rib4*) and yields 6,7-dimethyl-8-(1-D-ribityl)lumazine [65,66]. In the final reaction, riboflavin synthase (encoded by *rib5*) uses two molecules of 6,7-dimethyl-8-(1-D-ribityl)-lumazine where one acts as donor and the other as acceptor of four carbon atoms leading to the generation of the isoalloxazine ring of one molecule of riboflavin [67]. The coenzyme forms of riboflavin, FMN and FAD, are synthesized from riboflavin by riboflavin kinase (Fmn1p) and FAD synthetase (Fad1p), respectively [68,69].

In addition to de novo biosynthesis, yeast is also capable of riboflavin uptake from the medium and it was shown that a plasma membrane flavin transporter, encoded by *mch5*, is regulated by the proline-dependent transcription factor Put3p [70,71]. Since proline utilization depends on the FAD-dependent proline dehydrogenase Put1p (Table 1) upregulation of Mch5p suggests that riboflavin uptake is necessary under these conditions to meet the cellular demand for flavin coenzymes.

Despite the wealth of genetic and biochemical information available on riboflavin biosynthesis in the cytosol, transport to other compartments, in particular the mitochondrion as the dominant organelle for flavoenzyme catalyzed reactions, remains controversial [53]. Based on the finding that yeast mitochondria possess riboflavin kinase but no FAD synthetase activity, Tzagaloff et al. [72] proposed a model according to which the carrier protein Flx1p acts as a "flavin antiporter" by exchanging FMN from the mitochondrial matrix with FAD from the cytosol. In contrast to this model, Barile and co-workers claim that riboflavin is transported into mitochondria where both FMN and FAD can be synthesized and are even exported back to the "extramitochondrial phase" [73,74]. More recent data from Pallotta indicated that mitochondria can also hydrolyze FAD and FMN to riboflavin and are thus capable of balancing the pools of riboflavin, FMN and FAD [75]. Yeast FAD synthetase (Fad1p) is essential and deletion of *fad1* makes yeast unviable. The localization of yeast FAD1p is still unclear, although recent studies on human FAD synthetase isoform 1 (hFADS1) suggest a mitochondrial localization in eukaryotes [76].

In addition to *flx1* and *mch5*, yeast possesses three *flc* genes encoding putative transporters of flavins (Table 2). These transporters are responsible for FAD transport into the endoplasmic reticulum (ER) where several flavoenzymes (e. g. Ero1p, Erv2p and Fmo1p) are involved in the redox balance of thiols and disulfide linkages [77]. However, the exact role and localisation of Flc1-3p in yeast are currently not fully understood.

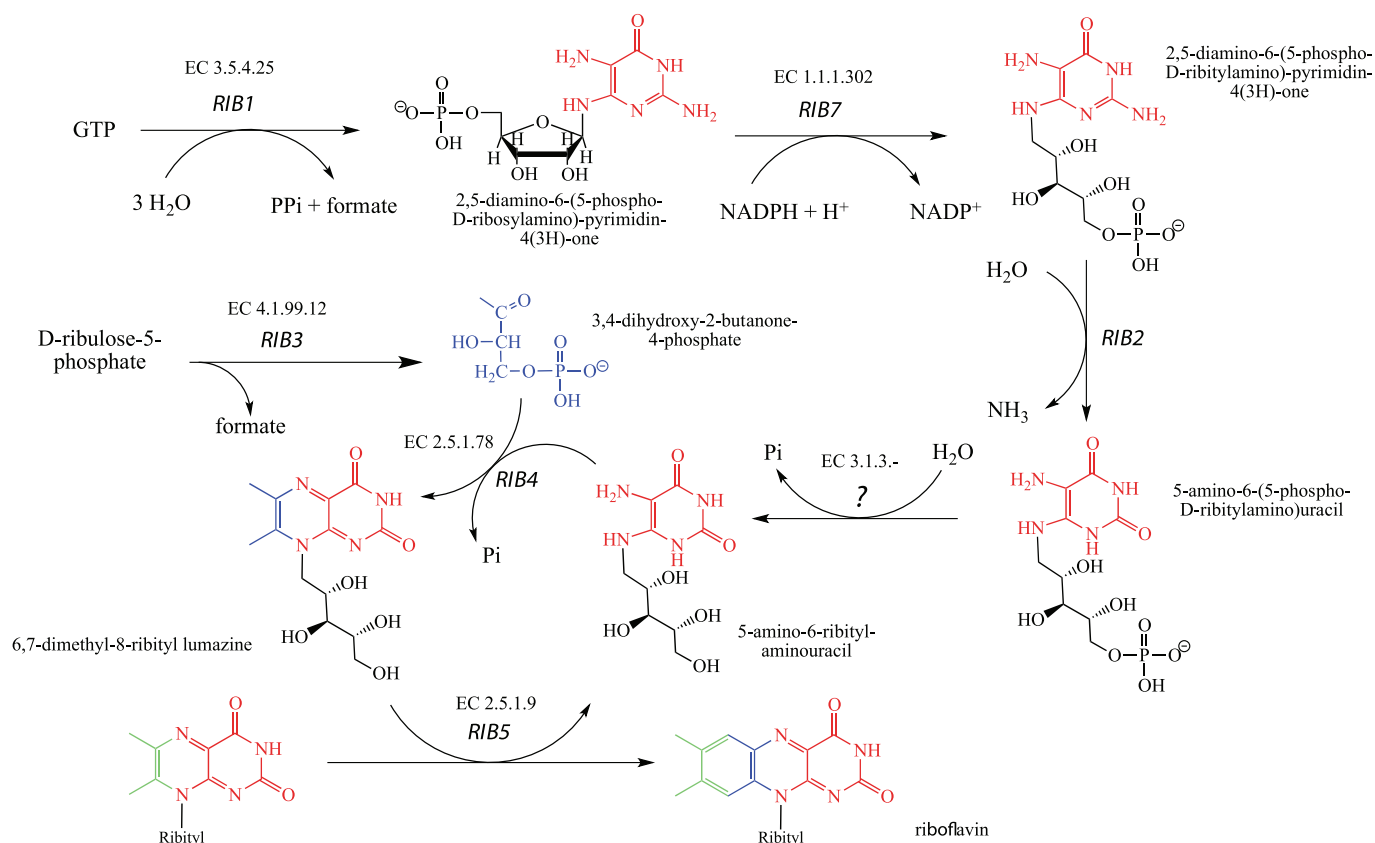
An alternative mechanism for assembling the holo-flavoenzyme is realized for the sole peroxisomal flavoenzyme, acyl-CoA oxidase

Table 2
Yeast flavin transporters and biosynthesis.

No.	E.C.	Protein/enzyme	Substrate/ligand	Structure clan (family) ^a	Abbrev.	Syst. name
<i>Transporters</i>						
1	–	FAD transmembrane transporter	FAD	–	<i>flx1</i>	YIL134W
2	–	FAD transporter (into ER)	FAD	–	<i>flc1</i>	YPL221W
3	–	FAD transporter (into ER)	FAD	–	<i>flc2</i>	YAL053W
4	–	FAD transporter (into ER)	FAD	–	<i>flc3</i>	YGL139W
5	–	Plasma-membrane riboflavin transporter	Riboflavin	–	<i>mch5</i>	YOR306C
<i>Biosynthesis of riboflavin, FMN and FAD</i>						
1	3.5.4.25	GTP cyclohydrolase II (1st step)	–	<i>GTP cyclohydrolase II</i>	<i>rib1</i>	YBL033C
2	1.1.1.302	DRAP reductase (2nd step)	–	DHFPred (RibD_C)	<i>rib7</i>	YBR153W
3	–	Deaminase (3rd step)	–	DHPred (RibD_C)	<i>rib2</i>	YOL066C
4	4.1.99.12	DHBP synthase (4th step)	–	<i>DHBP synthase</i>	<i>rib3</i>	YDR487C
5	2.5.1.78	Lumazine synthase (5th step)	–	DMRL synthase	<i>rib4</i>	YOL143C
6	2.5.1.9	Riboflavin synthase (6th step)	–	<i>FAD_Lum_binding (Lum_binding)</i>	<i>rib5</i>	YBR256C
7	2.7.1.26	Riboflavin kinase	Riboflavin	<i>Flavokinase</i>	<i>fmn1</i>	YDR236C
8	2.7.7.2	FAD-adenylyl transferase (synthetase)	FMN	HUP (PAPS_reduct)	<i>fad1</i>	YDL045C

Abbreviations used in Table 2 are: DHBP, 3,4-dihydroxy-2-butanone-4-phosphate; DRAP, 2,5-diamino-6-ribosylamino-4(3H)-pyrimidinone 5'-phosphate.

^a Pfam classification given in plain text is for yeast proteins and those in italics are for homologs from other species.



Scheme 3. Biosynthesis of riboflavin in *S. cerevisiae*. GTP and D-ribulose-5-phosphate serve as building blocks for the biosynthesis of 5-amino-6-ribityl-aminouracil and 3,4-dihydroxy-2-butanone-4-phosphate, respectively. These two compounds are then used by Rib4p to synthesize 6,7-dimethyl-8-ribityl lumazine. Two molecules 6,7-dimethyl-8-ribityl lumazine are converted by Rib5p to riboflavin and 5-amino-6-ribityl-aminouracil which serves again as substrate for Rib4p. This way all atoms of the dimethylbenzene moiety are derived from 3,4-dihydroxy-2-butanone-4-phosphate (colored in blue and green) while remainder of riboflavin is derived from GTP (colored in red).

(Pox1p). In this case, the holo-enzyme is formed in the cytosol, then binds to the import receptor Pex5p and, following an unknown import pathway, is transported into the peroxisome [78,79].

7. Yeast flavoproteins as models for human diseases

The yeast *S. cerevisiae* has been used as a model organism for studying fundamental biological processes for some time [80]. In 1997, Botstein and colleagues showed that nearly 31% of yeast open reading frames (ORF) have a homologue in mammalian genomes [81]. Since the number of annotated ORFs has almost doubled since 1997 this percentage is likely to have risen significantly. Moreover, an estimated 30% of human genes implicated in human diseases have a yeast homologue [82]. In a recent review, we have documented that fifty human flavoproteins are implicated in human diseases [28]. As shown in Table 3, nearly half of the disease-related human flavoproteins possess a yeast homologue. Interestingly, the majority of disease-related human flavoproteins operate in the mitochondrion [28]. Owing to the similarity of mitochondrial processes in eukaryotes it is conceivable that the yeast homologs located in mitochondria (see Table 3) may be particularly suitable as models for an improved understanding of human mitochondrial diseases.

Functional assignments based on sequence similarity generated ambiguities for several flavoproteins. For example, the yeast D-lactate dehydrogenases (Dld1-3p) show remarkable similarity to human D-2-hydroxyglutarate dehydrogenase and to a much lesser degree to alkyl-dihydroxyacetone phosphate synthase. Similarly, the yeast glutamate synthase, Glt1p, exhibits similarity to human dihydropyrimidine dehydrogenase (see Table 3). On the other hand the yeast NAD(P)H:quinone oxidoreductase Lot6p shows only a very low similarity to the human ortholog ($P = 1$) although it possesses a similar structure and

function [83–86]. These examples illustrate the need for biochemical characterization to provide a solid basis for comparative functional studies.

Yeast deletion strains were also used as convenient models to investigate the impact of mutations discovered in human genes. Examples are deletions of the genes *ura1*, *sdh1*, *ldp1* and *coq6*, leading to auxotrophic yeast strains, which were complemented with the orthologous human gene to investigate the functional impairment of mutations [87–90]. Yeast was also utilized as a host for heterologous expression of the human gene encoding 3 β -hydroxysterol Δ 24-reductase (DHCR24). Desmosterolosis, a rare autosomal recessive disorder is caused by mutations in the gene encoding DHCR24. Heterologous expression of the human *DHCR24* gene bearing different missense mutations confirmed their role in desmosterolosis [91].

A genetic screen in yeast suggested that kynurenine 3-monooxygenase may be a useful therapeutic target for Huntington disease [92]. This has prompted structural studies with the yeast enzyme leading to the elucidation of its X-ray crystal structure, which may serve as a model to investigate the structural basis of inhibitor binding [30]. Similarly, the crystal structure of the yeast flavin-containing monooxygenase Fmo1p proved useful as a model to understand the effect of mutations in human FMO3 that cause trimethylaminuria (“fish-odor” syndrome) [93].

8. Concluding remarks

Our analysis of the yeast flavoproteome has highlighted the importance of flavin-dependent enzymes in mitochondrial redox processes. Many of these mitochondrial enzymes have human homologs involved in diseases and thus genetically manipulated yeast strains (e.g. gene deletions) have potential as convenient model systems. On the other hand,

Table 3
Yeast flavoproteins as human disease models.

No.	E.C.	Human enzyme	Disease	OMIM	Yeast homolog	E value ^a
1	1.1.5.3	Glycerol 3-phosphate dh	<i>Diabetes mellitus</i> , type 2	138430	Gut2p	7.3 e−124
2	1.1.99-	D-2-Hydroxyglutarate dh	D-2-Hydroxyglutaric aciduria	605176	Dld1p Dld2p Dld3p	1.9 e−39 8.7 e−128 3.3 e−112
3	1.3.1.2	Dihydropyrimidine dh	Deficiency	612779	Glt1p	2.7 e−14
4	1.3.5.2	Dihydroorotate dh	Miller syn.	126064	Ura1p	2.0 e−6
5	1.3.3.4	Protoporphyrinogen IX ox.	Variagate porphyria	600923	Hem1p	7.2 e−20
6	1.3.3.6	Acyl-CoA ox.	Deficiency	609751	Pox1p	2.0 e−45
7	1.3.5.1	Succinate dh	Complex II deficiency,	600857	Sdh1p	3.9 e−219
		Flavoprotein subunit A	Leigh syn., paraganglioma 5		Sdh1bp	3.0 e−214
8	1.4.3.4	Monoamine ox	Brunner syn., antisocial behavior, autism	309850	Fms1p	7.8 e−11
9	1.4.3.5	Pyridoxine 5'-phosphate ox.	Encephalopathy	603287	Pdx3p	5.1 e−36
10	1.5.1.20	Methylenetetrahydrofolate red.	Homocystinuria, neural tube Defects, schizophrenia	607093	Met12p Met13p	2.9 e−98 7.5 e−122
11	1.5.5.1	Electron-transferring flavo-protein ubiquinone oxidored.	Glutaric academia IIC	231675	Cir2p	8.0 e−157
12	–	Electron-transferring flavoprot.	Glutaric academia IIA Glutaric academia IIB	608053 130410	Aim45p	8.5 e−66
13	1.5.99.8	Proline dh	Hyperprolinemia type I, schizophrenia	606810	Put1p	8.7 e−12
14	1.6.2.2	Cytochrome-b5 red.	Methemoglobinemia types I & II	613213	Cbr1p	1.9 e−30
15	1.6.2.4	NADPH-hemoprotein red. (cytochrome P450 red.)	Antley-Bixler syn.,	124015	Ncp1p	2.4 e−86
16	1.6.5.2	NAD(P)H:quinone oxidored.	Benzene toxicity, breast cancer	125860	Lot6p	1
17	1.8.1.4	Dihydrolipoyl dh	Leigh syn., maple syrup urine disease	238331	Lpd1p	2.8 e−147
18	1.8.1.7	Glutathione-disulfide red.	Hemolytic anemia	138300	Glr1p	1.4 e−104
19	1.14.13.8	Flavin-containing monooxy.	Trimethylaminuria	136132	Fmo1p	4.8 e−27
20	1.14.13.39	Nitric-oxide synthase	Hypertension	163729 163730	Tah18p	9.6 e−27
21	1.14.99.-	Monooxy. in coenzyme Q	Deficiency, nephrotic syn.	614647	Coq6p	7.0 e−55
22	1.16.1.8	Methionine synthase red.	Homocystinuria, neural tube	602568	Met5p	0.24
23	2.5.1.26	Alkyldihydroxyacetone Phosphate synthase	Rhizomelic chondrodysplasia Punctata type 3	603051	Dld1p Dld2p Dld3p	2.1 e−25 4.4 e−16 1.1 e−15
24	–	Apoptosis inducing protein	Combined oxidative phosphorylation deficiency	300169	Aif1p	8.8 e−4

Abbreviations used in Table 3: dh, dehydrogenase; flavoprot., flavoprotein; monooxy., monooxygenase; ox, oxidase; oxidored., oxidoreductase; red., reductase; syn., syndrome.

^a E value; expect value, was generated by searching of *Saccharomyces* Genome Database (SGD; <http://www.yeastgenome.org>) open reading frames (DNA or protein) against human protein sequences using the SGD WU_Blast2 program.

many yeast flavoenzymes are barely characterized with regard to their biochemical properties, such as substrate specificity, kinetic parameters and reaction partners. This deficit is clearly illustrated by the yeast flavodoxin-like proteins and the electron-transferring flavoprotein, none of which were characterized in any biochemical or structural detail. Similarly, our understanding of riboflavin uptake and trafficking between cellular compartments as well as flavin homeostasis are at an early stage necessitating further studies. Since these processes are also poorly understood in humans, yeast lends itself as a valuable model organism to gain insight into uptake, transport and trafficking of this vital vitamin.

9. Methods

The names and gene abbreviations of yeast flavoproteins were recently compiled for a review article [27]. This list of flavoproteins was updated using the information available in the *Saccharomyces* genome database (<http://www.yeastgenome.org/>). This database was also used to extract information on viability of gene knock-outs and localisation of flavoproteins in the yeast cell. Structural information was obtained from the protein database (<http://www.pdb.org>).

Acknowledgments

We thank the Austrian Research Fund (FWF) for financial support through project P22361 and the PhD program “Molecular Enzymology” (W901).

References

[1] O. Warburg, W. Christian, Über das gelbe Ferment und seine Wirkungen, *Biochem. Z.* 266 (1933) 377–392.

- [2] H. Theorell, O. Warburg, Reindarstellung (Kristallisation) des gelben Atmungsfermentes und die reversible Spaltung desselben, *Biochem. Z.* 272 (1934) 155–156.
- [3] E. Haas, O. Warburg, Isolierung eines neuen gelben Ferments, *Biochem. Z.* 298 (1938) 378–390.
- [4] V. Massey, L.M. Schopfer, Reactivity of Old Yellow Enzyme with alpha-NADPH and other pyridine nucleotide derivatives, *J. Biol. Chem.* 261 (1986) 1215–1222.
- [5] B.K. Haarer, D.C. Amberg, Old Yellow Enzyme protects the actin cytoskeleton from oxidative stress, *Mol. Biol. Cell* 15 (2004) 4522–4531.
- [6] K.M. Fox, P.A. Karplus, Old Yellow Enzyme at 2 Å resolution: overall structure, ligand binding, and comparison with related flavoproteins, *Structure* 2 (1994) 1089–1105.
- [7] Y.S. Niino, S. Chakraborty, B.J. Brown, V. Massey, A new Old Yellow Enzyme of *Saccharomyces cerevisiae*, *J. Biol. Chem.* 270 (1995) 1983–1991.
- [8] K. Stott, K. Saito, D.J. Thiele, V. Massey, Old Yellow Enzyme. The discovery of multiple isozymes and a family of related proteins, *J. Biol. Chem.* 268 (1993) 6097–6106.
- [9] Y. Meah, V. Massey, Old Yellow Enzyme: stepwise reduction of nitro-olefins and catalysis of aci-nitro tautomerization, *Proc. Natl. Acad. Sci. U. S. A.* 97 (2000) 10733–10738.
- [10] A.D. Vaz, S. Chakraborty, V. Massey, Old Yellow Enzyme: aromatization of cyclic enones and the mechanism of a novel dismutation reaction, *Biochemistry* 34 (1995) 4246–4256.
- [11] M. Hall, C. Stueckler, W. Kroutil, P. Macheroux, K. Faber, Asymmetric bioreduction of activated alkenes using cloned 12-oxophytodienoate reductase isoenzymes OPR-1 and OPR-3 from *Lycopersicon esculentum* (tomato): a striking change of stereoselectivity, *Angew. Chem. Int. Ed.* 46 (2007) 3934–3937.
- [12] A. Muller, R. Sturmer, B. Hauer, B. Rosche, Stereospecific alkyne reduction: novel activity of Old Yellow Enzymes, *Angew. Chem. Int. Ed.* 46 (2007) 3316–3318.
- [13] R. Sturmer, B. Hauer, M. Hall, K. Faber, Asymmetric bioreduction of activated C=C bonds using enoate reductases from the Old Yellow Enzyme family, *Curr. Opin. Chem. Biol.* 11 (2007) 203–213.
- [14] R.E. Williams, N.C. Bruce, ‘New uses for an old enzyme’ – the Old Yellow Enzyme family of flavoenzymes, *Microbiology* 148 (2002) 1607–1614.
- [15] R.E. Williams, D.A. Rathbone, N.S. Scrutton, N.C. Bruce, Biotransformation of explosives by the Old Yellow Enzyme family of flavoproteins, *Appl. Environ. Microbiol.* 70 (2004) 3566–3574.
- [16] F. Schaller, E.W. Weiler, Molecular cloning and characterization of 12-oxophytodienoate reductase, an enzyme of the octadecanoid signaling pathway from *Arabidopsis thaliana*. Structural and functional relationship to yeast Old Yellow Enzyme, *J. Biol. Chem.* 272 (1997) 28066–28072.
- [17] J. Strassner, A. Fürholz, P. Macheroux, N. Amrhein, A. Schaller, A homolog of Old Yellow Enzyme in tomato: Spectral properties and substrate specificity of the recombinant protein, *J. Biol. Chem.* 274 (1999) 35067–35073.

- [18] C.E. French, N.C. Bruce, Bacterial morphinone reductase is related to Old Yellow Enzyme, *Biochem. J.* 312 (1995) 671–678.
- [19] T.B. Fitzpatrick, N. Amrhein, P. Macheroux, Characterization of YqjM, an Old Yellow Enzyme homolog from *Bacillus subtilis*, *J. Biol. Chem.* 278 (2003) 19891–19897.
- [20] O. Adachi, K. Matsushita, E. Shinagawa, M. Ameyama, Occurrence of old yellow enzyme in *Gluconobacter suboxydans*, and the cyclic regeneration of NADP, *J. Biochem.* 86 (1979) 699–709.
- [21] C.E. French, S. Nicklin, N.C. Bruce, Sequence and properties of pentaerythritol tetranitrate reductase from *Enterobacter cloacae* PB2, *J. Bacteriol.* 178 (1996) 6623–6627.
- [22] J.R. Snape, N.A. Walkley, A.P. Morby, S. Nicklin, G.F. White, Purification, properties, and sequence of glycerol trinitrate reductase from *Agrobacterium radiobacter*, *J. Bacteriol.* 179 (1997) 7796–7802.
- [23] D.S. Blehert, B.G. Fox, G.H. Chambliss, Cloning and sequence analysis of two *Pseudomonas* flavoprotein xenobiotic reductases, *J. Bacteriol.* 181 (1999) 6254–6263.
- [24] J. Strassner, F. Schaller, U. Frick, G.A. Howe, E.E. Weiler, N. Amrhein, P. Macheroux, A. Schaller, Characterization and cDNA-microarray expression analysis of 12-oxophytodiene reductases reveals differential roles for octadecanoid biosynthesis in the local versus the systemic wound response, *Plant J.* 32 (2002) 585–601.
- [25] A. Stintzi, J. Browse, The *Arabidopsis* male-sterile mutant, opr3, lacks the 12-oxophytodiene acid reductase required for jasmonate synthesis, *Proc. Natl. Acad. Sci. U. S. A.* 97 (2000) 10625–10630.
- [26] A. Goffeau, B.G. Barrell, H. Bussey, R.W. Davis, B. Dujon, H. Feldmann, F. Galibert, J.D. Hoheisel, C. Jacq, M. Johnston, E.J. Louis, H.W. Mewes, Y. Murakami, P. Philippsen, H. Tettelin, S.G. Oliver, Life with 6000 genes, *Science* 274 (1996) 546(563–547).
- [27] P. Macheroux, B. Kappes, S.E. Ealick, Flavogenomics—a genomic and structural view of flavin-dependent proteins, *FEBS J.* 278 (2011) 2625–2634.
- [28] W.D. Lienhart, V. Gudipati, P. Macheroux, The human flavoproteome, *Arch. Biochem. Biophys.* 535 (2013) 150–162.
- [29] K.M. Fox, P.A. Karplus, Crystallization of Old Yellow Enzyme illustrates an effective strategy for increasing protein crystal size, *J. Mol. Biol.* 234 (1993) 502–507.
- [30] M. Amaral, C. Levy, D.J. Heyes, P. Lafite, T.F. Outeiro, F. Giorgini, D. Leys, N.S. Scrutton, Structural basis of kynurenine 3-monooxygenase inhibition, *Nature* 496 (2013) 382–385.
- [31] D.G. Bernard, S. Quevillon-Cheruel, S. Merchant, B. Guiard, P.P. Hamel, Cyc2p, a membrane-bound flavoprotein involved in the maturation of mitochondrial c-type cytochromes, *J. Biol. Chem.* 280 (2005) 39852–39859.
- [32] V. Corvest, D.A. Murrey, M. Hirasawa, D.B. Knaff, B. Guiard, P.P. Hamel, The flavoprotein Cyc2p, a mitochondrial cytochrome c assembly factor, is a NAD(P)H-dependent haem reductase, *Mol. Microbiol.* 83 (2012) 968–980.
- [33] N. Soler, E. Delagoutte, S. Miron, C. Facca, D. Baille, B. d’Autreaux, G. Craescu, Y.M. Frapart, D. Mansuy, G. Baldacci, M.E. Huang, L. Vernis, Interaction between the reductase Tah18 and highly conserved Fe–S containing Dre2 C-terminus is essential for yeast viability, *Mol. Microbiol.* 82 (2011) 54–67.
- [34] A. Nishimura, N. Kawahara, H. Takagi, The flavoprotein Tah18-dependent NO synthesis confers high-temperature stress tolerance on yeast cells, *Biochem. Biophys. Res. Commun.* 430 (2013) 137–143.
- [35] A. Dancis, D.G. Roman, G.J. Anderson, A.G. Hinnebusch, R.D. Klausner, Ferric reductase of *Saccharomyces cerevisiae*: molecular characterization, role in iron uptake, and transcriptional control by iron, *Proc. Natl. Acad. Sci. U. S. A.* 89 (1992) 3869–3873.
- [36] E. Georgatsou, D. Alexandraki, Regulated expression of the *Saccharomyces cerevisiae* Fre1p/Fre2p Fe/Cu reductase related genes, *Yeast* 15 (1999) 573–584.
- [37] L.J. Martins, L.T. Jensen, J.R. Simon, G.L. Keller, D.R. Winge, Metalloregulation of FRE1 and FRE2 homologs in *Saccharomyces cerevisiae*, *J. Biol. Chem.* 273 (1998) 23716–23721.
- [38] M. Rinnerthaler, S. Buttner, P. Laun, G. Heeren, T.K. Felder, H. Klinger, M. Weinberger, K. Stolze, T. Grousl, J. Hasek, O. Benada, I. Frydlova, A. Klockner, B. Simon-Nobbe, B. Jansko, H. Breitenbach-Koller, T. Eisenberg, C.W. Gourlay, F. Madeo, W.C. Burhans, M. Breitenbach, Yno1p/Aim14p, a NADPH-oxidase ortholog, controls extramitochondrial reactive oxygen species generation, apoptosis, and actin cable formation in yeast, *Proc. Natl. Acad. Sci. U. S. A.* 109 (2012) 8658–8663.
- [39] M. Sprinzl, C. Steegborn, F. Hubel, S. Steinberg, Compilation of tRNA sequences and sequences of tRNA genes, *Nucleic Acids Res.* 24 (1996) 68–72.
- [40] L.W. Rider, M.B. Ottosen, S.G. Gattis, B.A. Palffy, Mechanism of dihydrouridine synthase 2 from yeast and the importance of modifications for efficient tRNA reduction, *J. Biol. Chem.* 284 (2009) 10324–10333.
- [41] F. Xing, S.L. Hiley, T.R. Hughes, E.M. Phizicky, The specificities of four yeast dihydrouridine synthases for cytoplasmic tRNAs, *J. Biol. Chem.* 279 (2004) 17850–17860.
- [42] T. Kato, Y. Daigo, S. Hayama, N. Ishikawa, T. Yamabuki, T. Ito, M. Miyamoto, S. Kondo, Y. Nakamura, A novel human tRNA-dihydrouridine synthase involved in pulmonary carcinogenesis, *Cancer Res.* 65 (2005) 5638–5646.
- [43] M.E. Armengod, I. Moukadiri, S. Prado, R. Ruiz-Partida, A. Benitez-Paez, M. Villarroja, R. Lomas, M.J. Garzon, A. Martinez-Zamora, S. Meseguer, C. Navarro-Gonzalez, Enzymology of tRNA modification in the bacterial MnmEG pathway, *Biochimie* 94 (2012) 1510–1520.
- [44] X. Wang, Q. Yan, M.X. Guan, Mutation in MTO1 involved in tRNA modification impairs mitochondrial RNA metabolism in the yeast *Saccharomyces cerevisiae*, *Mitochondrion* 9 (2009) 180–185.
- [45] I. Moukadiri, S. Prado, J. Piera, A. Velazquez-Campoy, G.R. Bjork, M.E. Armengod, Evolutionarily conserved proteins MnmE and GidA catalyze the formation of two methyluridine derivatives at tRNA wobble positions, *Nucleic Acids Res.* 37 (2009) 7177–7193.
- [46] L. Li, X. Jia, D.M. Ward, J. Kaplan, Yap5 protein-regulated transcription of the TYW1 gene protects yeast from high iron toxicity, *J. Biol. Chem.* 286 (2011) 38488–38497.
- [47] H.J. Sofia, G. Chen, B.G. Hetzler, J.F. Reyes-Spindola, N.E. Miller, Radical SAM, a novel protein superfamily linking unresolved steps in familiar biosynthetic pathways with radical mechanisms: functional characterization using new analysis and information visualization methods, *Nucleic Acids Res.* 29 (2001) 1097–1106.
- [48] S.C. Wang, P.A. Frey, S-adenosylmethionine as an oxidant: the radical SAM superfamily, *Trends Biochem. Sci.* 32 (2007) 101–110.
- [49] Y. Suzuki, A. Noma, T. Suzuki, M. Senda, T. Senda, R. Ishitani, O. Nureki, Crystal structure of the radical SAM enzyme catalyzing tricyclic modified base formation in tRNA, *J. Mol. Biol.* 372 (2007) 1204–1214.
- [50] R. Grandori, J. Carey, Six new candidate members of the alpha/beta twisted open-sheet family detected by sequence similarity to flavodoxin, *Protein Sci.* 3 (1994) 2185–2193.
- [51] F. Cardona, H. Orozco, S. Friant, A. Aranda, M. del Olmo, The *Saccharomyces cerevisiae* flavodoxin-like proteins Ycp4 and Rfs1 play a role in stress response and in the regulation of genes related to metabolism, *Arch. Microbiol.* 193 (2011) 515–525.
- [52] H.X. Hao, O. Khalimonchuk, M. Schradars, N. Dephoure, J.P. Bayley, H. Kunst, P. Devilee, C.W. Cremers, J.D. Schiffman, B.G. Bentz, S.P. Gygi, D.R. Winge, H. Kremer, J. Rutter, SDH5, a gene required for flavination of succinate dehydrogenase, is mutated in paraganglioma, *Science* 325 (2009) 1139–1142.
- [53] H.J. Kim, D.R. Winge, Emerging concepts in the flavinylation of succinate dehydrogenase, *Biochim. Biophys. Acta* 1827 (2013) 627–636.
- [54] J. Lopes, M.J. Pinto, A. Rodrigues, F. Vasconcelos, R. Oliveira, The *Saccharomyces cerevisiae* genes, AIM45, YGR207c/CIR1 and YOR356w/CIR2, Are Involved in Cellular Redox State Under Stress Conditions, *Open Microbiol. J.* 4 (2010) 75–82.
- [55] R. Ansell, K. Granath, S. Hohmann, J.M. Thevelein, L. Adler, The two isoenzymes for yeast NAD⁺-dependent glycerol 3-phosphate dehydrogenase encoded by GPD1 and GPD2 have distinct roles in osmoadaptation and redox regulation, *EMBO J.* 16 (1997) 2179–2187.
- [56] M. Grauslund, J.M. Lopes, B. Ronnow, Expression of GUT1, which encodes glycerol kinase in *Saccharomyces cerevisiae*, is controlled by the positive regulators Adr1p, Ino2p and Ino4p and the negative regulator Opi1p in a carbon source-dependent fashion, *Nucleic Acids Res.* 27 (1999) 4391–4398.
- [57] X. Grandier-Vazeille, K. Bathany, S. Chaignepain, N. Camougrand, S. Manon, J.M. Schmitter, Yeast mitochondrial dehydrogenases are associated in a supramolecular complex, *Biochemistry* 40 (2001) 9758–9769.
- [58] A. Chelstowska, Z. Liu, Y. Jia, D. Amberg, R.A. Butow, Signalling between mitochondria and the nucleus regulates the expression of a new D-lactate dehydrogenase activity in yeast, *Yeast* 15 (1999) 1377–1391.
- [59] E.E. Rojo, B. Guiard, W. Neupert, R.A. Stuart, Sorting of D-lactate dehydrogenase to the inner membrane of mitochondria. Analysis of topogenic signal and energetic requirements, *J. Biol. Chem.* 273 (1998) 8040–8047.
- [60] M.J. Penninckx, C.J. Jaspers, M.J. Legrain, The glutathione-dependent glyoxalase pathway in the yeast *Saccharomyces cerevisiae*, *J. Biol. Chem.* 258 (1983) 6030–6036.
- [61] M.L. Pallotta, D. Valenti, M. Iacovino, S. Passarella, Two separate pathways for D-lactate oxidation by *Saccharomyces cerevisiae* mitochondria which differ in energy production and carrier involvement, *Biochim. Biophys. Acta* 1608 (2004) 104–113.
- [62] D.B. Murray, K. Haynes, M. Tomita, Redox regulation in respiring *Saccharomyces cerevisiae*, *Biochim. Biophys. Acta* 1810 (2011) 945–958.
- [63] D.B. Murray, S. Roller, H. Kuriyama, D. Lloyd, Clock control of ultradian respiratory oscillation found during yeast continuous culture, *J. Bacteriol.* 183 (2001) 7253–7259.
- [64] A. Urban, I. Ansmant, Y. Motorin, Optimisation of expression and purification of the recombinant YoI066 (Rib2) protein from *Saccharomyces cerevisiae*, *J. Chromatogr. B Anal. Technol. Biomed. Life Sci.* 786 (2003) 187–195.
- [65] C. Jin, A. Barrientos, A. Tzagoloff, Yeast dihydroxybutanone phosphate synthase, an enzyme of the riboflavin biosynthetic pathway, has a second unrelated function in expression of mitochondrial respiration, *J. Biol. Chem.* 278 (2003) 14698–14703.
- [66] J.J. Garcia-Ramirez, M.A. Santos, J.L. Revuelta, The *Saccharomyces cerevisiae* RIB4 gene codes for 6,7-dimethyl-8-ribityllumazine synthase involved in riboflavin biosynthesis. Molecular characterization of the gene and purification of the encoded protein, *J. Biol. Chem.* 270 (1995) 23801–23807.
- [67] M.A. Santos, J.J. Garcia-Ramirez, J.L. Revuelta, Riboflavin biosynthesis in *Saccharomyces cerevisiae*. Cloning, characterization, and expression of the RIB5 gene encoding riboflavin synthase, *J. Biol. Chem.* 270 (1995) 437–444.
- [68] M.A. Santos, A. Jimenez, J.L. Revuelta, Molecular characterization of FMN1, the structural gene for the monofunctional flavokinase of *Saccharomyces cerevisiae*, *J. Biol. Chem.* 275 (2000) 28618–28624.
- [69] M. Wu, B. Repetto, D.M. Glerum, A. Tzagoloff, Cloning and characterization of FAD1, the structural gene for flavin adenine dinucleotide synthetase of *Saccharomyces cerevisiae*, *Mol. Cell. Biol.* 15 (1995) 264–271.
- [70] P. Reihl, J. Stolz, The monocarboxylate transporter homolog Mch5p catalyzes riboflavin (vitamin B2) uptake in *Saccharomyces cerevisiae*, *J. Biol. Chem.* 280 (2005) 39809–39817.
- [71] A. Spitzner, A.F. Perzlmaier, K.E. Geillinger, P. Reihl, J. Stolz, The proline-dependent transcription factor Put3 regulates the expression of the riboflavin transporter MCH5 in *Saccharomyces cerevisiae*, *Genetics* 180 (2008) 2007–2017.
- [72] A. Tzagoloff, J. Jang, D.M. Glerum, M. Wu, FLX1 codes for a carrier protein involved in maintaining a proper balance of flavin nucleotides in yeast mitochondria, *J. Biol. Chem.* 271 (1996) 7392–7397.

- [73] M.L. Pallotta, C. Brizio, A. Fratianni, C. De Virgilio, M. Barile, S. Passarella, *Saccharomyces cerevisiae* mitochondria can synthesise FMN and FAD from externally added riboflavin and export them to the extramitochondrial phase, *FEBS Lett.* 428 (1998) 245–249.
- [74] V. Bafunno, T.A. Giancaspero, C. Brizio, D. Bufano, S. Passarella, E. Boles, M. Barile, Riboflavin uptake and FAD synthesis in *Saccharomyces cerevisiae* mitochondria: involvement of the Flx1p carrier in FAD export, *J. Biol. Chem.* 279 (2004) 95–102.
- [75] M.L. Pallotta, Evidence for the presence of a FAD pyrophosphatase and a FMN phosphohydrolase in yeast mitochondria: a possible role in flavin homeostasis, *Yeast* 28 (2011) 693–705.
- [76] E.M. Torchetti, C. Brizio, M. Colella, M. Galluccio, T.A. Giancaspero, C. Indiveri, M. Roberti, M. Barile, Mitochondrial localization of human FAD synthetase isoform 1, *Mitochondrion* 10 (2010) 263–273.
- [77] O. Protchenko, R. Rodriguez-Suarez, R. Androphy, H. Bussey, C.C. Philpott, A screen for genes of heme uptake identifies the FLC family required for import of FAD into the endoplasmic reticulum, *J. Biol. Chem.* 281 (2006) 21445–21457.
- [78] A.T. Klein, M. van den Berg, G. Bottger, H.F. Tabak, B. Distel, *Saccharomyces cerevisiae* acyl-CoA oxidase follows a novel, non-PTS1, import pathway into peroxisomes that is dependent on Pex5p, *J. Biol. Chem.* 277 (2002) 25011–25019.
- [79] S. Subramani, Hitchhiking fads en route to peroxisomes, *J. Cell Biol.* 156 (2002) 415–417.
- [80] D. Drubin, The yeast *Saccharomyces cerevisiae* as a model organism for the cytoskeleton and cell biology, *Cell Motil. Cytoskeleton* 14 (1989) 42–49.
- [81] D. Botstein, S.A. Chervitz, J.M. Cherry, Yeast as a model organism, *Science* 277 (1997) 1259–1260.
- [82] F. Foury, Human genetic diseases: a cross-talk between man and yeast, *Gene* 195 (1997) 1–10.
- [83] R. Li, M.A. Bianchet, P. Talalay, L.M. Amzel, The three-dimensional structure of NAD(P)H:quinone reductase, a flavoprotein involved in cancer chemoprotection and chemotherapy: Mechanism of the two-electron reduction, *Proc. Natl. Acad. Sci. U. S. A.* 92 (1995) 8846–8850.
- [84] D. Liger, M. Graille, C.-Z. Zhou, N. Leulliot, S. Quevillon-Cheruel, K. Blondeau, J. Janin, H. van Tilbeurgh, Crystal structure and functional characterization of yeast YLR011wp, an enzyme with NAD(P)H-FMN and ferric iron reductase activities, *J. Biol. Chem.* 279 (2004) 34890–34897.
- [85] S. Sollner, R. Nebauer, H. Ehammer, A. Prem, S. Deller, B.A. Palfey, G. Daum, P. Macheroux, Lot6p from *Saccharomyces cerevisiae* is a FMN-dependent reductase with a potential role in quinone detoxification, *FEBS J.* 274 (2007) 1328–1339.
- [86] S. Sollner, P. Macheroux, New roles of flavoproteins in molecular cell biology: an unexpected role for quinone reductases as regulators of proteasomal degradation, *FEBS J.* 276 (2009) 4313–4324.
- [87] N. Burnichon, J.J. Briere, R. Libe, L. Vescovo, J. Riviere, F. Tissier, E. Jouanno, X. Jeunemaitre, P. Benit, A. Tzagoloff, P. Rustin, J. Bertherat, J. Favier, A.P. Gimenez-Roqueplo, SDHA is a tumor suppressor gene causing paraganglioma, *Hum. Mol. Genet.* 19 (2010) 3011–3020.
- [88] S.F. Heeringa, G. Chernin, M. Chaki, W. Zhou, A.J. Sloan, Z. Ji, L.X. Xie, L. Salvati, T.W. Hurd, V. Vega-Warner, P.D. Killen, Y. Raphael, S. Ashraf, B. Ovunc, D.S. Schoeb, H.M. McLaughlin, R. Airik, C.N. Vlangos, R. Gbadegesin, B. Hinkes, P. Saisawat, E. Trevisson, M. Doimo, A. Casarin, V. Pertegato, G. Giorgi, H. Prokisch, A. Rotig, G. Nurnberg, C. Becker, S. Wang, F. Ozaltin, R. Topaloglu, A. Bakkaloglu, S.A. Bakkaloglu, D. Muller, A. Beissert, S. Mir, A. Berdeli, S. Varpizen, M. Zenker, V. Matejas, C. Santos-Ocana, P. Navas, T. Kusakabe, A. Kispert, S. Akman, N.A. Soliman, S. Krick, P. Mundel, J. Reiser, P. Nurnberg, C.F. Clarke, R.C. Wiggins, C. Faul, F. Hildebrandt, COQ6 mutations in human patients produce nephrotic syndrome with sensorineural deafness, *J. Clin. Invest.* 121 (2011) 2013–2024.
- [89] J. Rainger, H. Bengani, L. Campbell, E. Anderson, K. Sokhi, W. Lam, A. Riess, M. Ansari, S. Smithson, M. Lees, C. Mercer, K. McKenzie, T. Lengfeld, B. Gener Querol, P. Branney, S. McKay, H. Morrison, B. Medina, M. Robertson, J. Kohlhasse, C. Gordon, J. Kirk, D. Wieczorek, D.R. Fitzpatrick, Miller (Genee-Wiedemann) syndrome represents a clinically and biochemically distinct subgroup of postaxial acrofacial dysostosis associated with partial deficiency of DHODH, *Hum. Mol. Genet.* 21 (2012) 3969–3983.
- [90] R.A. Vaubel, P. Rustin, G. Isaya, Mutations in the dimer interface of dihydroliipoamide dehydrogenase promote site-specific oxidative damages in yeast and human cells, *J. Biol. Chem.* 286 (2011) 40232–40245.
- [91] H.R. Waterham, J. Koster, G.J. Romeijn, R.C. Hennekam, P. Vreken, H.C. Andersson, D.R. FitzPatrick, R.I. Kelley, R.J. Wanders, Mutations in the 3beta-hydroxysterol Delta24-reductase gene cause desmosterolosis, an autosomal recessive disorder of cholesterol biosynthesis, *Am. J. Hum. Genet.* 69 (2001) 685–694.
- [92] F. Giorgini, P. Guidetti, Q. Nguyen, S.C. Bennett, P.J. Muchowski, A genomic screen in yeast implicates kynurenine 3-monooxygenase as a therapeutic target for Huntington disease, *Nat. Genet.* 37 (2005) 526–531.
- [93] C.K. Yeung, E.T. Adman, A.E. Rettie, Functional characterization of genetic variants of human FMO3 associated with trimethylaminuria, *Arch. Biochem. Biophys.* 464 (2007) 251–259.

Quinone reductases and their role in regulating 20S proteasome

2.1 Introduction

Quinones are naturally occurring compounds present in all living organisms. Naturally occurring quinones mainly function as electron and proton carriers in photosynthesis (plastoquinone and phylloquinone) and respiratory electron transport chains (ubiquinones) (Figure 1). Ubiquinone (Coenzyme Q₁₀) previously thought to be localized in the inner mitochondrial membrane was later shown to be localized in endoplasmic reticulum, golgi apparatus and lysosomes (1). The functional role of ubiquinone outside the mitochondrial membranes is currently unexplained.

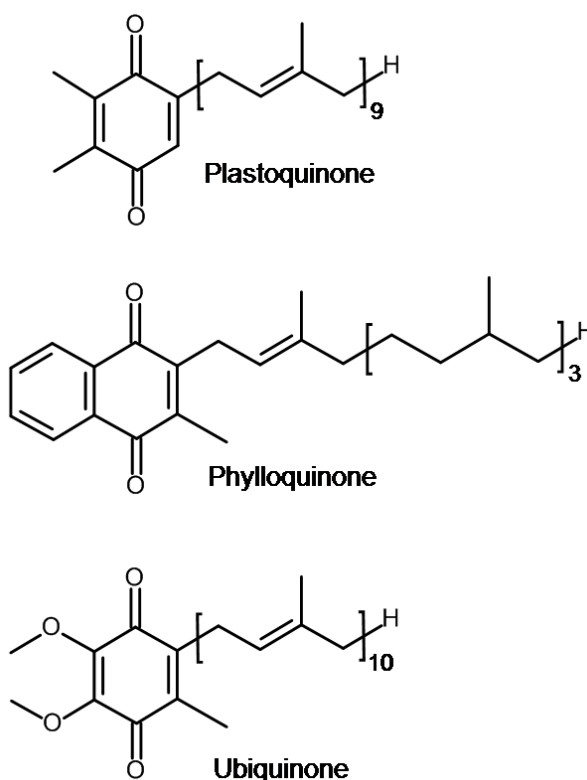


Figure 1: Naturally occurring quinones involved in photosynthesis (plastoquinone and phylloquinone) and electron transport chain (ubiquinone).

Quinones are broadly divided into two structural groups, naphthoquinones (vitamin K) and benzoquinones (ubiquinones and plastoquinones). Higher eukaryotes are only able to synthesize benzoquinones whereas naphthoquinones are mainly obtained through the diet or

obtained from intestinal symbiotic bacteria (2). Quinones generated from polycyclic aromatic hydrocarbons are abundant in all burnt organic material, including urban air particles, automobile exhaust, cigarette smoke and food products (3). Quinones are reduced by one and two electrons to form semiquinone and hydroquinone respectively (figure 2).

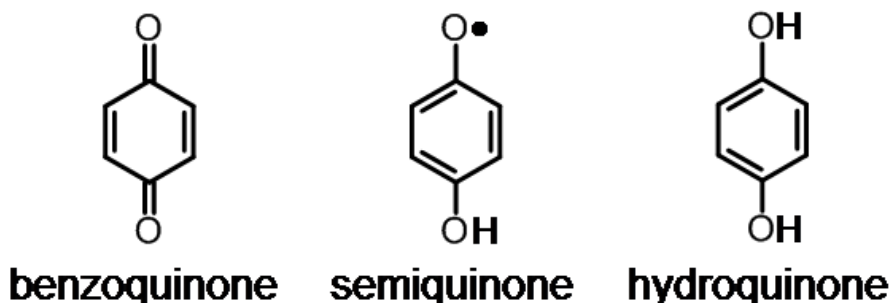


Figure 2: Benzoquinones can be reduced to semiquinones or hydroquinones.

Formation of semiquinones is preferentially avoided both in prokaryotes and eukaryotes since they are prone to react with molecular dioxygen leading to the formation of superoxide radicals. Hydroquinones on the other hand are conjugated with glutathione or glucuronic acid and rapidly excreted.

2.1.1 Quinone reductases are essential for combating oxidative stress

Quinone reductases (QR) are evolutionarily conserved enzymes present in bacteria, fungi, plants and mammals (4). These enzymes utilize a flavin coenzyme (FMN or FAD) for transferring a hydride from the electron donors (e.g. NAD(P)H) to the quinone substrate. Quinone reductases have a unique ability to transfer two electrons to a quinone thereby catalyzing the formation of completely reduced hydroquinone without generation of semiquinone species (5). In contrast to quinone reductases, single electron oxidoreductases such as cytochrome P450 are able to reduce quinones to reactive semiquinone radicals which subsequently undergo redox cycling, leading to the production of highly reactive oxygen species (ROS). This leads to oxidative damage, tissue degeneration, apoptotic cell death, premature aging, cellular transformation and neoplasia (6). Hence quinone reductases are essential for combating oxidative stress by preventing the formation of ROS.

2.1.2 Yeast quinone reductase Lot6p

Yeast quinone reductase *Lot6* (YLR011wp) was identified in a group of genes which are up-regulated in response to low temperature (7). Lot6p was shown to be homologue of *Bacillus subtilis* Yhda protein, whose function was unknown at that time but was later shown to be a quinone reductase (8).

2.1.3 Biochemical and Structural properties of Lot6p

Biochemical studies showed that Lot6p reduces several electron accepting substrates such as ferricyanide and it was proposed that Lot6p is involved in ferric iron assimilation (9). A later study showed that it is also efficient in reducing quinones to hydroquinones, hence establishing Lot6p as the first quinone reductase of *Saccharomyces cerevisiae* (10). Analysis by X-ray crystallography showed that Lot6p exists as a homodimer exhibiting a flavodoxin-like folding (9). A typical flavodoxin fold is characterized by a central five-stranded β -sheet sandwiched in between α helices (11). Quinone reductases show remarkable conservation of flavodoxin-like folding, as shown in figure 3 with a central five stranded β sheet surrounded by α helices.

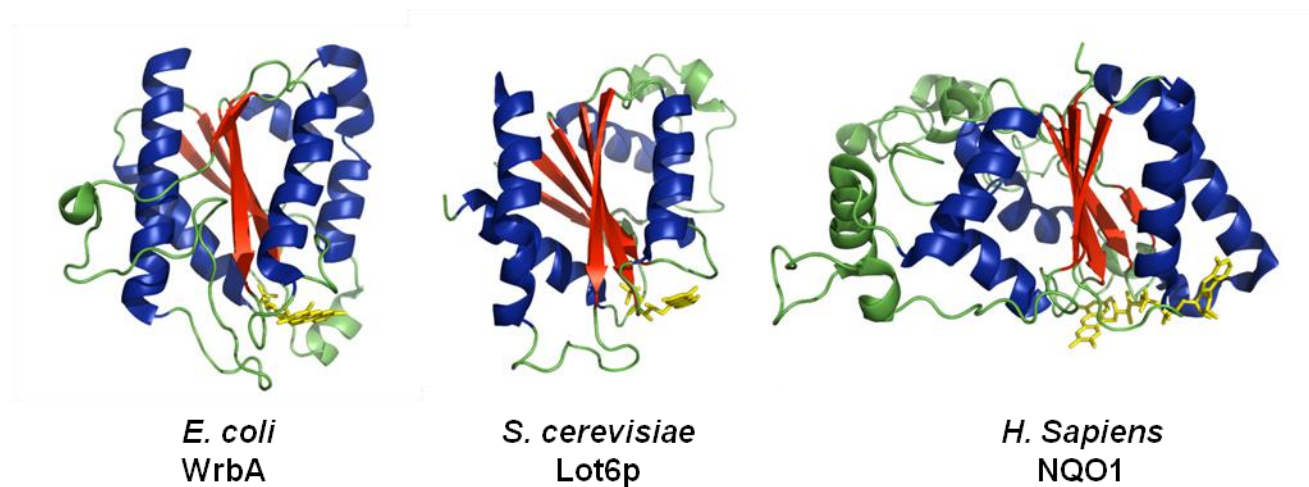


Figure 3: X-ray crystal structures of quinone reductases WrbA from *E.coli*, Lot6p from *S. cerevisiae* and NQO1 from *H. sapiens*.

Flavodoxins are named after small monomeric flavoproteins (15–22 kDa) that non covalently bind a single FMN molecule, function as electron transferases and only found in certain bacteria, algae and yeast (12, 13). Bacterial Flavodoxins served as paradigms for studying various proteins involved in electron-transport systems belonging to higher eukaryotes, many multi domain eukaryotic proteins exhibit striking conservation of the bacterial flavodoxin FMN binding site (14). The folding of quinone reductases is classified as flavodoxin-like due to the absence of the flavodoxin key fingerprint motif ((T/S)XTGXT) usually involved in FMN phosphate binding (15). Quinone reductases exist as a dimers in solution which is also unexpected since most flavodoxin-like proteins are monomeric (16, 17). As shown in figure 4 Lot6p exists as a dimer and each protomer binds to one FMN molecule (9). The phosphoribityl moiety of FMN cofactor is deeply buried in the protein, whereas the isoalloxazine ring remains partially accessible to the solvent. Each FMN is in contact with both subunits, and only 10% of its surface is solvent-accessible. In total, each FMN molecule forms 12 direct hydrogen bonds (Table I) (9).

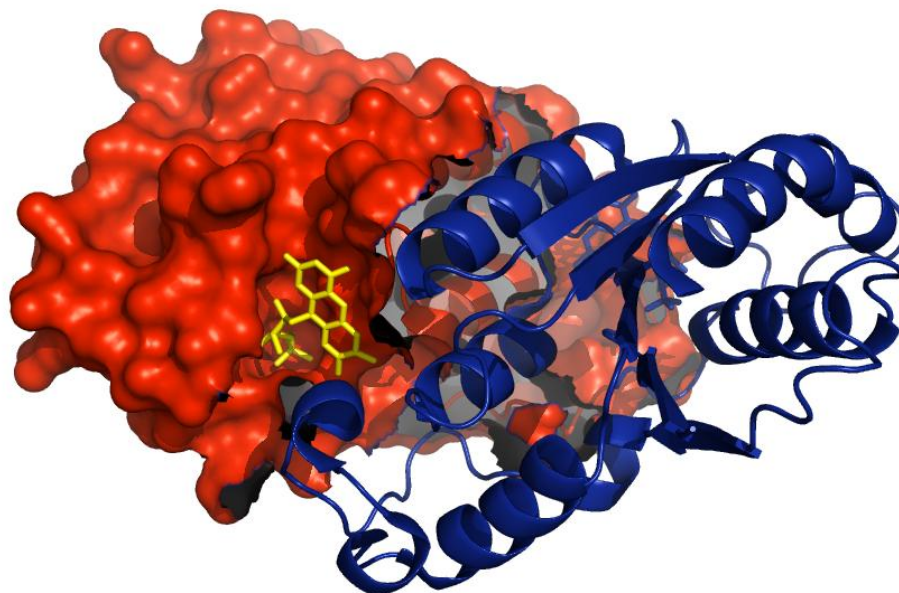


Figure 4: X-ray crystal structure of quinone reductase Lot6p. Both the protomers are colored (blue and red) and represented (surface and cartoon). The FMN cofactor present in the binding pocket is colored in yellow.

Polar contacts involved in FMN binding with Lot6p backbone		
Protein	FMN	Distance
		Å
Ser ⁹ O _{γ[ρ]}	O ₂ P	2.4
Arg ¹¹ N _{ε[ρ]}	O ₂ P	3.2
Arg ¹¹ N _{η[ρ]1}	O ₃ P	3
Val ¹⁵ N	O ₃ P	3
Cys ¹⁶ N	O ₁ P	3.1
Tyr ⁹⁵ O _{η[ρ]}	O ₂ P	2.7
Tyr ¹²⁴ O _{η[ρ]}	O ₁ P	2.5
Gln ⁹⁴ O _{ε1}	N ₃	3
Asn ⁹⁶ N	N ₅	2.8
Asn ⁹⁶ N	O ₄	3
Trp ⁹⁷ N	O ₄	3.2
Gly ¹²⁶ N	O ₂	3

Table 1: Amino acids from Lot6p backbone form 12 hydrogen bonds with the FMN cofactor (9).

All living organisms encounter a variety of quinones both endogenous and exogenous. Quinone reductases exhibit broad substrate specificity, catalyzing the reduction of simple benzo-, naphtho-, and anthra- quinones, as well as complex molecules such as benzimidazolediones (18). Quinones reductases typically reduce a substrate by following ping-pong bi-bi reaction mechanism, where the reducing agent binds first to the active site to deliver the electrons to the active-site cofactor and then dissociates before the electron-accepting substrate binds to the active site to sequester the electrons (19). Generally, the enzymes catalyzing substrates via ping-pong bi-bi reaction mechanism possess only one active site capable of binding two structurally different substrates. It generally implies that binding of one substrate excludes the binding of the other (20). Lot6p alike to quinone reductases follows a ping-pong bi-bi reaction mechanism (10). In the case of Lot6p, NAD(P)H binds to the active site to deliver electrons to the FMN cofactor and then disassociates before the quinone substrate binds to the active site to accept the electrons from the reduced FMN cofactor.

2.1.4 Physiological role of quinone reductase Lot6p

Human DT-diaphorase discovered by Ernster and Navazio was the first quinone reductase to be discovered (21). DT-diaphorase was subsequently renamed as NAD(P)H dehydrogenase [quinone] 1 (NQO1) due to its ability to accept electrons from both NADH and NADPH. The physiological role of quinone reductases is a topic of debate since the discovery of NQO1. Many proteins exhibit multiple biological roles, not only they function as enzymes but also participate in regulatory mechanisms (22). In addition to its function as a quinone reductase, NQO1 also binds to the 20S proteasome and affects the lifetime of several transcription factors (e.g. p53, p33 and p73) by inhibiting their ubiquitin-dependent and independent proteasomal degradation (23).

Lot6p is an orthologue of NQO1, Lot6p exhibits both sequence (23%) and structural similarity to NQO1 (10). Akin to NQO1, Lot6p is shown to physically associate with the 20S proteasome *in vitro* and inhibit the degradation of transcription factor Yap4p by the 20S proteasome (24). Yap4p is a member of the yeast activator protein (Yap) family involved in the oxidative and osmotic stress response (25). The interaction of Yap4p with Lot6p is dependent on the redox state of FMN cofactor, the complex formation between Lot6p-20S proteasome and Yap4p occurs only when the Lot6p bound FMN cofactor is reduced. The localization of Yap4p also depends on its interaction with Lot6p, when the flavin cofactor of Lot6p is oxidized Yap4p dissociates from Lot6p-20S proteasome present in the cytoplasm and migrates into the nucleus to initiate transcription (24). The ability of Lot6p and NQO1 to sense oxidative stress and initiate cellular responses through their interactions with transcription factors and proteasome has led to the proposal that they function as redox sensors of the cell (26).

The flavin binding active site of Lot6p was only studied so far in respect to its enzymatic function but not in respect to its role in protein interactions. As previously mentioned above, Yap4p dissociates from the Lot6p-20S proteasome complex when Lot6p is oxidized, thus it is conceivable that upon oxidation of the flavin cofactor conformational changes occur at the binding site which lead to the dissociation of Yap4p. In recent years mechanistic details have emerged about flavoproteins regulating protein-protein interactions by acting as redox switches. A flavin redox switch has been explained as a change in the conformation of a flavoprotein when the redox state of the protein flavin cofactor is altered (27). The following flavoproteins, Pyruvate oxidase and proline utilization A (PutA) from *E. coli* and the photoreceptor Vivid (28–30) from fungus *Neurospora crassa* are previously shown to exhibit redox switching. In all the

above mentioned proteins it is shown that upon change in the redox state of flavin cofactor, the interactions between the flavin cofactor and protein back bone are altered, presumably leading to peptide plane flipping.

Peptide plane flipping is defined as large scale rotation of the peptide plane that shifts the backbone dihedral angles φ and ψ at amino acid residue i and $i+1$ to different structural (stable) regions with relatively small effect on the orientation of side chains (31). Peptide plane flips are not only expected to play a much more important role during the early stages of protein folding, when the atoms of the peptide plane are not hydrogen-bonded to other parts of the polypeptide chain but also during the protein native state dynamics (31, 32). β -Turns are commonly occurring structural elements in protein structures that exhibit peptide plane flipping (33). A β -turn consists of four consecutive residues defined by positions i , $i+1$, $i+2$, $i+3$ and the distance between i and $i+3$ is usually less than 7\AA (34). β -Turns are stereochemically mobile and are capable of inter conversions between type I and type II turns by means of peptide plane flipping (35).

Lot6p exhibits a typical β -turn near the FMN binding region comprising four amino acids tyrosine, asparagine, tryptophan and glycine at 95, 96, 97 and 98 respectively (Figure 5). The second and third amino acid in the β -turn, asparagine 96 and tryptophan 97 form four hydrogen bonds with the FMN cofactor (9). A β -turn (E104-G107) is also present in NQO1 at a similar position to that of Lot6p (figure 5). In a similar fashion to Lot6p the second and third amino acid tryptophan and phenylalanine of the β -turn form four hydrogen bonds with NQO1 bound FAD cofactor.

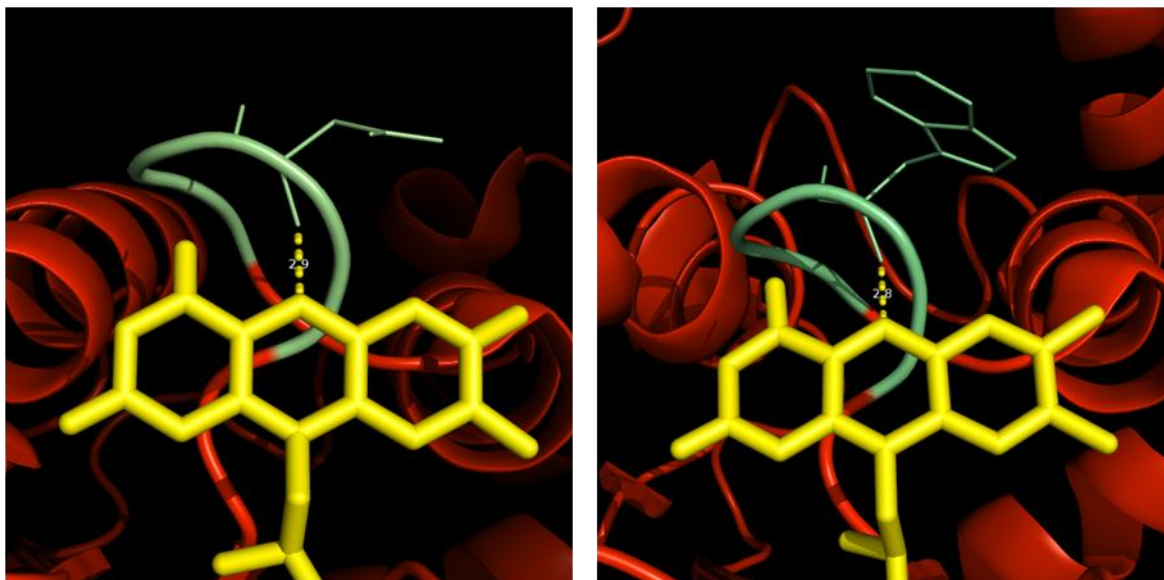


Figure 5: Lot6p (left panel) and NQO1 (right panel) exhibit β -turns near the cofactor binding site. The amino acids forming the β -turn are colored in green. The N5 atom of the isoalloxazine ring forms the crucial hydrogen bond (yellow dashed lines) with Lot6p N96 and NQO1 W105.

It is conceivable that the four amino acids comprising the β -turn exhibit a peptide flip dependent on the redox state of the FMN or FAD cofactor thereby affecting the stability of (Lot6p/NQO1)-20S proteasome or (Lot6p/NQO1)-20S-(Yap4p/p53) complex. In order to assess the role of the amino acids forming the β -turn three Lot6p variants (Lot6p N96C, Lot6p W97A and Lot6p G98L) were generated by directed mutagenesis. The aim of this project is to characterize the Lot6p variants in regard to their biochemical, structural and proteasome interaction properties.

2.2 Materials and methods

Reagents

Unless stated otherwise all chemicals were of highest grade commercially available and were purchased either from Sigma-Aldrich (St. Louis, MO, USA), Fluka (Buchs, Switzerland), or Merck (Darmstadt, Germany). DNA primers were purchased from VBC-Biotech (Vienna, Austria), site-directed mutagenesis Kit was purchased from Stratagene (La Jolla, CA, USA).

Site-directed mutagenesis

A pET21a plasmid encoding for Lot6 C-terminal His6 fusion protein (10) was used as a template for generating Lot6p variants. DNA primer design, experimental recipe, cycling parameters and restriction digestion were performed as per manufacturer's instruction manual. The plasmids obtained after restriction digestion were used to transform *E. coli* TOP10 strain according to standard molecular biology protocols. The transformed *E.coli* were plated on lysogeny broth (LB) agar plates containing 100 µg/ml ampicillin and incubated at 37 °C for 16 hours. A single *E. coli* colony from the transformation plates was used to inoculate 10 ml LB containing 100 µg/ml ampicillin and incubated at 37 °C for 16 hours while shaking at 130 rpm after which the cells were harvested. Plasmid DNA was isolated from the harvested cells and used for sequencing or transforming *E.coli* expression strains.

Recombinant protein expression

Chemically competent *E. coli* BL21(DE3) cells were transformed with pET21a Lot6p or pET21a Lot6p_N96C or pET21a Lot6p_W97A or pET21a Lot6p_G98L plasmids and grown in similar conditions mentioned above. A single *E.coli* colony from the transformation plates was inoculated into LB medium containing 100 µg/ml ampicillin and incubated at 37 °C for 18 hours while shaking at 130 rpm to obtain preculture. The preculture was used for inoculating fresh lysogeny broth containing 100 µg/ml ampicillin to an optical density of 0.1 at 600 nm. The culture flasks were incubated at 37 °C while shaking at 130 rpm until the optical density has increased to 0.6-0.8 (Ca 4-6 hours). In order to induce protein expression isopropyl β-D-1-thiogalactopyranoside (IPTG) was added to the cultures for a final concentration of 0.5 mM. The culture flasks expressing Lot6p G98L protein were shifted to 20 °C. The cultures were further incubated until the optical density has increased to 1.5-2 (ca 3-5 hours for Lot6p, Lot6p W97A,

Lot6p N96C and 15-17 hours for Lot6p G98L). The cells were harvested at 8,000 g for 10 minutes. The cell pellets were resuspended in 0.9% saline and vortexed for 30 sec after which they are pelleted at 4,000 g for 20 minutes in 50 ml falcon tubes. The supernatant was discarded and the pellet was immediately used for protein purification or flash frozen in liquid nitrogen and stored at -70 °C.

Note: The culture volumes were not mentioned since the volumes were variable depending on the expression and solubility level of a given protein. The expression and solubility level of any given protein was determined by performing an initial small scale experiment (ca. 50 ml culture volume).

Protein purification

The cell pellets were resuspended in 50 mM NaH₂PO₄, 300 mM NaCl, 20 mM imidazole pH 8.00 (Buffer A) and lysed by sonication. A pinch of FMN was added to the cell lysate after which the lysate was incubated at 4 °C for 30 minutes. The cell lysate was centrifuged at 30000g for 30 minutes. The supernatant was collected into 50 ml falcon tubes. The soluble protein from the supernatant was purified by using 5 ml HisTrap HP (GE health care) according to the manufacturer's instructions. Buffer A was used as washing buffer, buffer A containing 300 mM imidazole was used as elution buffer. All the purification steps were performed at 4 °C. The eluted protein was dialyzed into 50 mM NaH₂PO₄, 300 mM NaCl pH 8.00 and immediately used or flash frozen in liquid nitrogen and stored at -70 °C.

FMN reductase activity assays

Lot6p and Lot6p W97A were assayed for FMN reductase activity in a reaction mixture (1 ml of final volume) consisting of 150 μM NADPH, 100 μM FMN, and 0.24 μM enzyme in 25 mM Tris-HCl, pH 7.5 at 30 °C. Initially NADPH and buffer was added to both the measurement and reference cuvettes, at this point the enzyme is added to measurement cuvette and the spectrum is recorded for 100 sec. The recording is paused and FMN is added to both the cuvettes and mixed by pipetting and the recording is continued for 500 more sec. NADPH oxidization was followed by measuring the decrease in absorption at 340 nm.

2.3 Results

Three *Lot6* variants (*Lot6_N96C*, *Lot6_W97A* and *Lot6_G98L*) were successfully generated by performing site directed mutagenesis (Figure 6).

	81	90	100	110	120
	-----+	-----+	-----+	-----+	-----
<i>Lot6p</i>	IVNALDIIIVFVTPQYNWGYPAALKNAIDRLYHEWHGKPAL				
<i>Lot6p_N96C</i>	IVNALDIIIVFVTPQY C WGYPAALKNAIDRLYHEWHGKPAL				
<i>Lot6p_W97A</i>	IVNALDIIIVFVTPQYN A GYPALKNALDRLYHEWHGKPAL				
<i>Lot6p_G98L</i>	IVNALDIIIVFVTPQYN L YPAALKNAIDRLYHEWHGKPAL				

Figure 6: Multiple alignment of the *Lot6p* variants. DNA sequence of *Lot6* N96C, *Lot6* W97A and *Lot6* G98L obtained after mutagenesis was translated into protein sequence with ExPASy DNA translate tool. The open reading frames were aligned against the *Lot6p* coding sequence using multiple sequence alignment tool (MultAlin).

E.coli BL21(DE3) expression strain was used for expressing recombinant proteins *Lot6p*, *Lot6p_W97A*, *Lot6p_N96C* and *Lot6p_G98L*. In order to determine appropriate conditions for protein expression, protein solubility screens were performed for *Lot6p* variants. *Lot6p*, *Lot6p_N96C* and *Lot6p_W97A* were expressed in soluble form at 37 °C whereas *Lot6p_G98L* was only soluble at 20 °C (Figure 7).

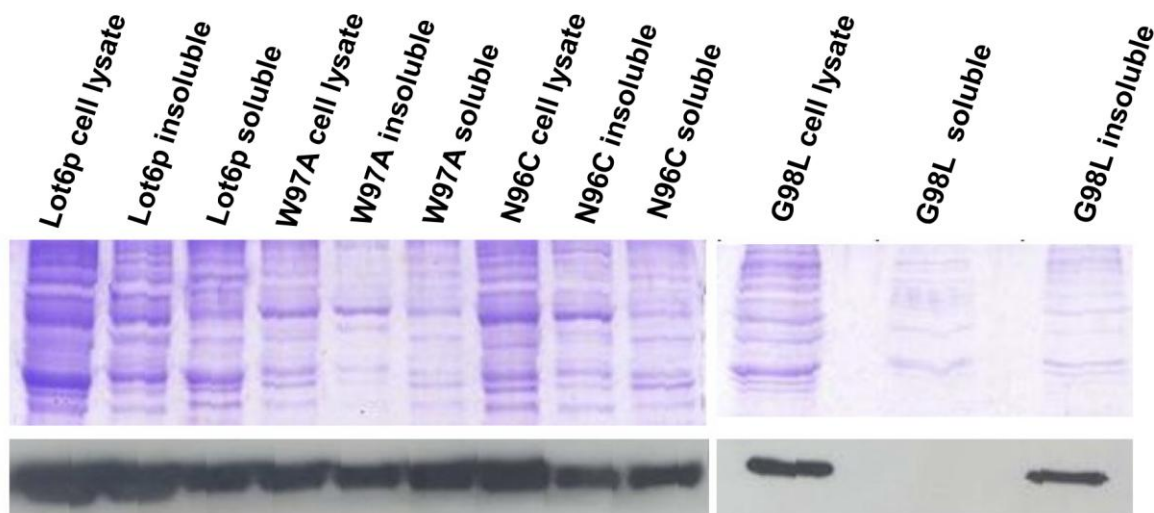


Figure 7: Solubility screen of Lot6p variants. SDS-Page and western blot analysis of *E. coli* BL21(DE3) strains expressing Lot6p variants. The protein expression was below the threshold where it can be visualized by SDS-PAGE, so western blotting was performed with anti-Lot6p antibody. Lot6p, Lot6p_W97A and Lot6p_N96C were expressed in soluble form when expressed at 37 °C where as Lot6p_G98L is completely insoluble.

After determining the appropriate conditions for protein expression, the culture volumes were scaled and Lot6p variants were purified by performing Ni-NTA chromatography. Figure 8 shows SDS-PAGE analysis of NI-NTA purification of Lot6p_N96C and Lot6p_W97A. The same procedure was followed for purifying Lot6p and Lot6_G98L (data not shown).

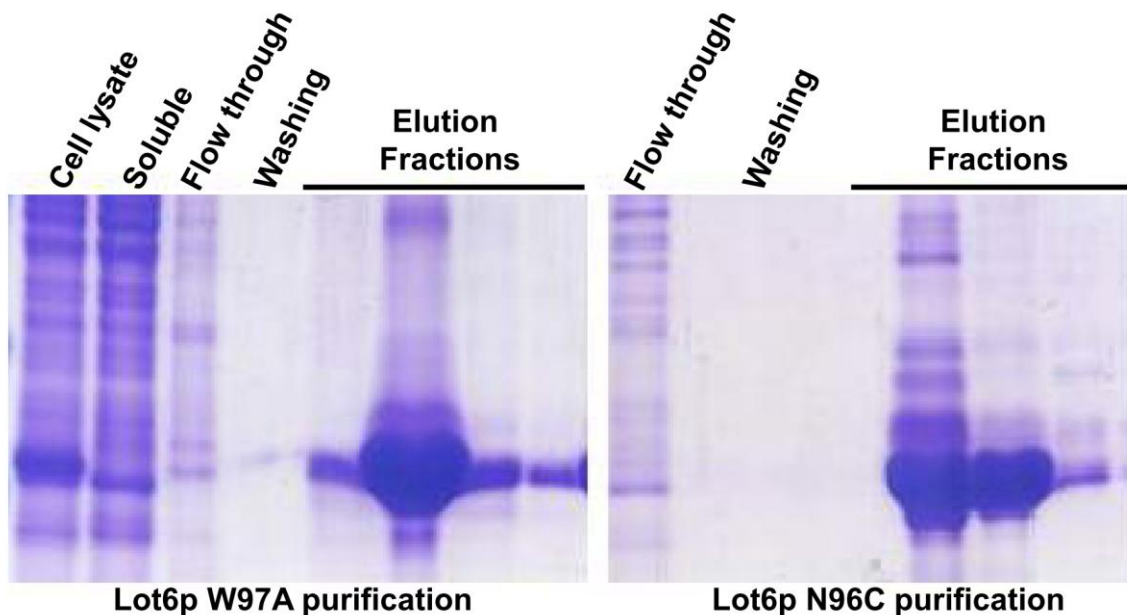


Figure 8: Ni-NTA purification of Lot6p N96C and Lot6p W97A and SDS-PAGE analysis of various fractions collected during Ni-NTA purification. Elution fractions collected during purification showed that recombinant Lot6p_W97A and Lot6p_N96C were stable during the purification procedure.

However, up to 70 % of Lot6p_N96C and Lo6p_G98L precipitated while removing imidazole after NI-NTA purification by dialysis. Experiments that are not described in this thesis indicated that rebuffering with centrifugal filter devices (Amicon) decrease the amount of protein being precipitated and increase the overall yield. The elution fractions from both purifications (Figure 8) indicate that Lot6p-His6 fusion proteins bind to the nickel column very tightly, but unknown proteins also seem to bind to the NI-NTA column with similar affinity. Size exclusion chromatography was performed to purify Lot6p proteins further. The elution fractions were collected every time a peak is detected at 280 nm. The fractions corresponding to the molecular mass of Lot6p-His6 fusion protein (22.88 kDa) analyzed by SDS-PAGE (Figure 9).

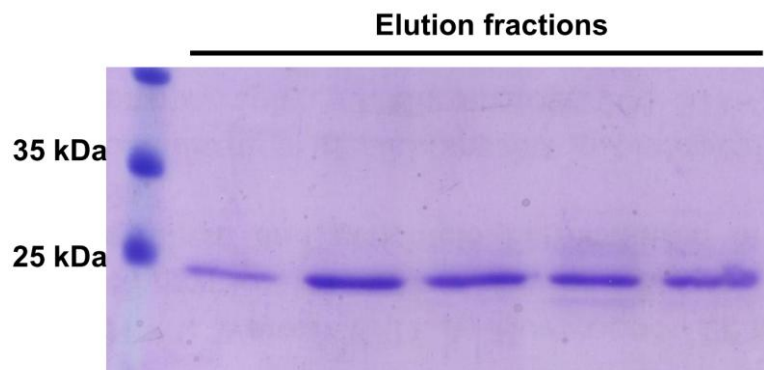


Figure 9: Purification by size exclusion chromatography. SDS-PAGE analysis of elution fractions collected during SEC. Elution fractions corresponding to the molecular mass of Lot6p-His6 fusion protein (22.88 kDa) were collected and analyzed for purity.

The purity of Lot6p proteins was vastly improved by performing size exclusion chromatography. During purification of the recombinant Lot6p proteins by Ni-NTA affinity and size exclusion chromatography it was observed that Lot6p_N96C and Lot6p_G98L were devoid of FMN cofactor (absence of distinctive yellow color), whereas Lot6p_W97A retains the cofactor. In order to confirm the absence of FMN cofactor UV-Vis spectroscopy was performed (Figure 10).

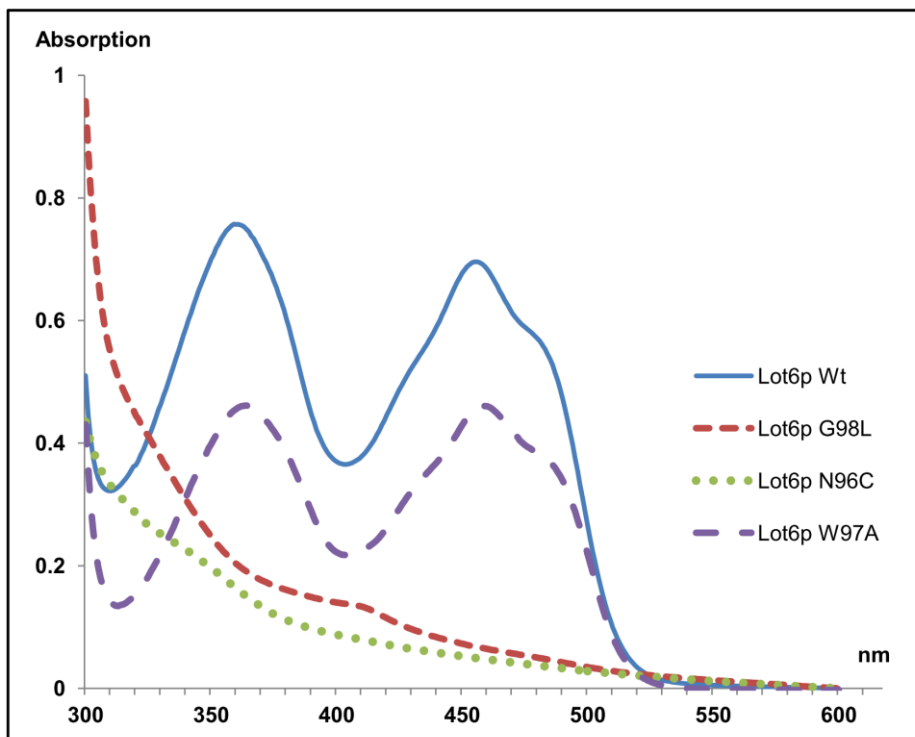


Figure 10: UV-Vis spectroscopy of Lot6p variants. Absorption spectra of purified Lot6p variants between 300-600 nm shows that Lot6p_N96C and Lot6p_G98L are unable to bind the FMN cofactor.

It can be seen from the UV-Vis absorption spectra that Lot6p_N96C and Lot6p_G98L does not exhibit typical flavin absorption peaks. In order to be absolutely sure about the loss of FMN cofactor in Lot6p_N96C and G98L, higher concentrations of these protein were used to measure the spectra compared to Lot6p.

The ability of Lot6p and Lot6p_W97A to reduce NADPH was measure by performing FMN reduction assays. Lot6p_W97A was able to reduce NADPH in presence of free FMN at a slightly faster rate than that of Lot6p (Figure 11).

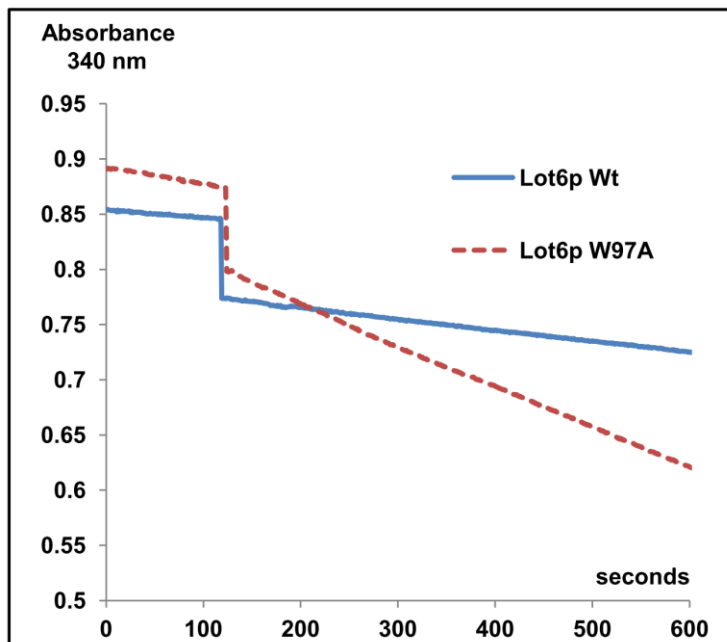


Figure 11: FMN reductase activity assays. The ability of Lot6p and Lot6p_W97A to reduce NADPH was measured by continuously monitoring the absorption at 340 nm.

The FMN reductase activity of Lot6p and Lot6p W97A is strictly dependent on exogenously added oxidized FMN. NADPH oxidation rate is very slow in the absence of exogenous FMN (first 100 seconds), it can be observed that up on addition of FMN the NADPH is rapidly oxidized (only observable as a very steep drop in the spectrum which can be attributed to the lag time in mixing) followed by gradual oxidation of NADPH. The FMN reductase activity observed reflects the reduction of free oxidized FMN, in a physiological condition the electron acceptor would be a substrate, preferably quinones. Loss of FMN in Lot6p_N96C and Lot6p G98L supports the hypothesis that amino acids 96-99 are essential for enzymatic function as well as the stability of holo protein. In order to determine the changes in the structure of Lot6p variants, attempts to solve the three dimensional structure by crystallography were made. The crystallization attempts of Lot6p W97A were successful; the x-ray crystallographic structure of Lot6p W97A is virtually identical to Lot6p (data not shown). Pull-down assays were performed with Lot6p W97A to verify the interaction with 20S proteasome (Figure 12).

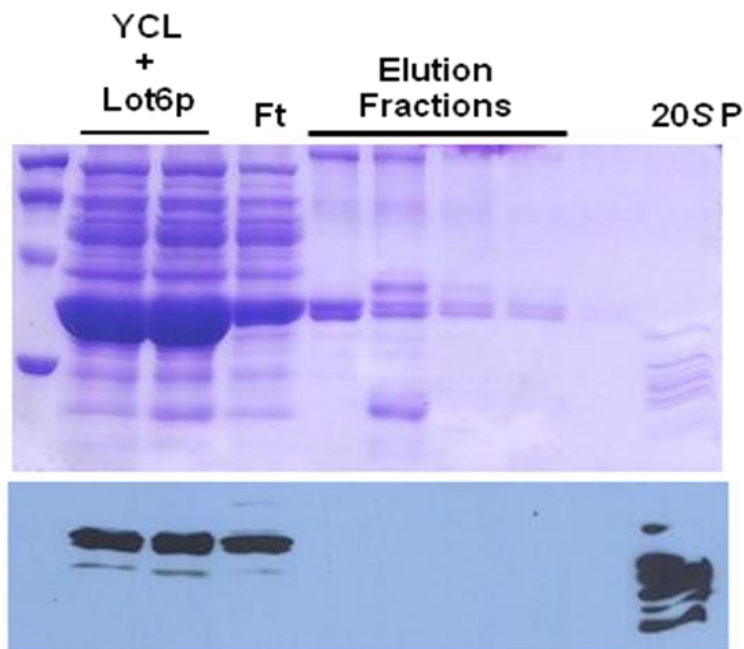


Figure 12: Recombinant Lot6p W97A is incubated with yeast cell lysate (YCL) and applied on Ni-NTA chromatography column. Flow through (FT) was collected and the column was washed to elute unbound proteins. Bound proteins were eluted by competitive elution and analyzed by SDS-PAGE and immunoblotting with antibody against yeast 20S proteasome (20S P).

Lot6p W97A was unable to bind to the proteasome even though its biochemical and structural properties are similar to that of Lot6p. Lot6p was previously shown to bind to the 20S proteasome, while apo-Lot6p was unable to bind to the 20S proteasome indicating that FMN cofactor is essential for this interaction (24). Lot6p N96C and G98L, were unable to bind the FMN cofactor. It is probable that these variants are not able to bind the 20S proteasome, since it was previously shown that apo-Lot6p is unable to bind the 20S proteasome. Crystallization attempts of Lot6p N96C and Lot6p G98L were unsuccessful and the possible reasons are discussed.

2.4 Discussion

Unlike 26S proteasome where a target protein is selectively ubiquitinated by E1, E2 and E3 enzymes for degradation (36), information regarding enzymes that selectively regulate the protein degradation by 20S proteasome is currently unavailable. Ubiquitin independent degradation of intrinsically disordered proteins by the 20S proteasome is a new and emerging area of protein degradation pathways (37). A new physiological role has been attributed to quinone reductases (Lot6p and NQO1) as regulators of 20S proteasome. Quinone reductases Lot6p and NQO1 were shown to regulate the 20S proteasomal degradation of transcription factors Yap4p and p53 respectively. It was shown that quinone reductases bind to the transcription factors only in their reduced form. The general assumption that can be drawn from the experimental evidence available is that a conformational change occurs in quinone reductases upon oxidation leading to the dissociation of transcription factor from the quinone reductase-20S proteasome complex. It is already known that flavoproteins exhibit conformational change upon change in the redox state. The conformational changes studied so far only revealed how the affinity of flavoproteins towards membranes varied depending on the redox state (28–30). On the other hand, no information is available on conformational change effecting protein-protein interactions.

In order to study putative conformational changes in Lot6p, amino acids were exchanged in a conserved β -turn near the FMN binding region of Lot6p. The variants were characterized in regard to their biochemical and interaction properties. The W97A mutant retains the cofactor and behaves similar to Lot6p. The FMN reductase activity assays (figure 11) show that Lot6p_W97A is able to reduce free FMN at a slightly faster rate than Lot6p. This observation indicates that the exchange of bulky tryptophan to alanine provides more space for the FMN cofactor or substrate to fit into the active site. Contrastingly, Lot6p N96C and Lot6p G98L were shown to lose the cofactor. It is probable that both these amino acid exchanges lead to changes in the local structures at the FMN binding site thereby affecting the binding of FMN cofactor. Numerous crystallization attempts with both Lot6p N96C and Lot6p G98L were unsuccessful indicating that the three dimensional structure of these variants is probably different to that of Lot6p W97A whose crystallization was successful.

The variants studied in this chapter confirm that the amino acids forming the β -turn are essential for the biochemical and interaction properties of Lot6p. However, it is still unclear if a peptide flip occurs during the change of redox state and if the peptide flip brings about

conformational changes in the protein. Crystallization of reduced Lot6p under hypoxic conditions or NMR spectroscopy might provide insights to whether a peptide flip occurs or not.

Experiments were also carried out to isolate and crystallize Lot6p-20S proteasome complex. Most of the experiments were unsuccessful owing to the complexity of purifying proteasome as well as isolating Lot6p-20S proteasome complex. Purification of 20S proteasome is a long and tedious process and it is hard to reproduce similar experimental conditions for each batch of purification. The proteasome has been traditionally viewed as a very stable complex able to withstand stringent purification methods. This notion has since changed owing to knowledge gained from studying affinity tag-purified proteasome by high throughput proteomics. Elevated salt conditions employed during conventional purification protocols lead to dissociation of proteasome associated proteins (38, 39). A new strain of yeast engineered to carry a Flag- polyhistidine tag on the Pre1p subunit (Flag-His6 Pre1 strain) of the 20S proteasome was donated by Prof. Dr. Jürgen Dohmen. This strain allows for rapid purification of proteasome without employing elevated salt conditions. Flag-His6 Pre1 strain was transformed with a centromeric vector encoding for Lot6p and Yap4p. It might be possible to isolate Lot6p-20S proteasome complex from this strain since the purification is rapid and the conditions are not very stringent. It is not surprising that not even a single structure of proteasome in complex with proteins other than those involved in proteasome assembly is available. It would be interesting to further develop the technology for isolating and crystallizing Lot6p-20S proteasome complex and investigate if they act as redox switches.

References

1. ElMBERGER, P. G., Kalén, A., Brunk, U. T., and Dallner, G. (1989) Discharge of newly-synthesized dolichol and ubiquinone with lipoproteins to rat liver perfusate and to the bile. *Lipids* **24**, 919–30
2. Nowicka, B., and Kruk, J. (2010) Occurrence, biosynthesis and function of isoprenoid quinones. *Biochim. Biophys. Acta* **1797**, 1587–605
3. Chesis, P. L., Levin, D. E., Smith, M. T., Ernster, L., and Ames, B. N. (1984) Mutagenicity of quinones: pathways of metabolic activation and detoxification. *Proc. Natl. Acad. Sci. U. S. A.* **81**, 1696–700
4. Deller, S., Macheroux, P., and Sollner, S. (2008) Flavin-dependent quinone reductases. *Cell. Mol. Life Sci.* **65**, 141–60
5. Iyanagi, T., and Yamazaki, I. (1970) One-electron-transfer reactions in biochemical systems. V. Difference in the mechanism of quinone reduction by the NADH dehydrogenase and the NAD(P)H dehydrogenase (DT-diaphorase). *Biochim. Biophys. Acta* **216**, 282–94
6. Brunmark, A., and Cadenas, E. (1989) Redox and addition chemistry of quinoid compounds and its biological implications. *Free Radic. Biol. Med.* **7**, 435–77
7. Zhang, L., Ohta, A., Horiuchi, H., Takagi, M., and Imai, R. (2001) Multiple mechanisms regulate expression of low temperature responsive (LOT) genes in *Saccharomyces cerevisiae*. *Biochem. Biophys. Res. Commun.* **283**, 531–5
8. Binter, A., Staunig, N., Jelesarov, I., Lohner, K., Palfey, B. A., Deller, S., Gruber, K., and Macheroux, P. (2009) A single intersubunit salt bridge affects oligomerization and catalytic activity in a bacterial quinone reductase. *FEBS J.* **276**, 5263–74
9. Liger, D., Graille, M., Zhou, C.-Z., Leulliot, N., Quevillon-Cheruel, S., Blondeau, K., Janin, J., and van Tilbeurgh, H. (2004) Crystal structure and functional characterization of yeast YLR011wp, an enzyme with NAD(P)H-FMN and ferric iron reductase activities. *J. Biol. Chem.* **279**, 34890–7
10. Sollner, S., Nebauer, R., Ehammer, H., Prem, A., Deller, S., Palfey, B. a, Daum, G., and Macheroux, P. (2007) Lot6p from *Saccharomyces cerevisiae* is a FMN-dependent reductase with a potential role in quinone detoxification. *FEBS J.* **274**, 1328–39
11. Sancho, J. (2006) Flavodoxins: sequence, folding, binding, function and beyond. *Cell. Mol. Life Sci.* **63**, 855–64
12. Wakabayashi, S., Kimura, T., Fukuyama, K., Matsubara, H., and Rogers, L. J. (1989) The amino acid sequence of a flavodoxin from the eukaryotic red alga *Chondrus crispus*. *Biochem. J.* **263**, 981–4
13. Simonsen, R. P., and Tollin, G. (1980) Structure-function relations in flavodoxins. *Mol. Cell. Biochem.* **33**, 13–24
14. Zhao, Q., Modi, S., Smith, G., Paine, M., McDonagh, P. D., Wolf, C. R., Tew, D., Lian, L. Y., Roberts, G. C., and Driessen, H. P. (1999) Crystal structure of the FMN-binding domain of human cytochrome P450 reductase at 1.93 Å resolution. *Protein Sci.* **8**, 298–306

15. Drennan, C. L., Pattridge, K. A., Weber, C. H., Metzger, A. L., Hoover, D. M., and Ludwig, M. L. (1999) Refined structures of oxidized flavodoxin from *Anacystis nidulans*. *J. Mol. Biol.* **294**, 711–24
16. Watenpaugh, K. D., Sieker, L. C., and Jensen, L. H. (1973) The binding of riboflavin-5'-phosphate in a flavoprotein: flavodoxin at 2.0-Angstrom resolution. *Proc. Natl. Acad. Sci. U. S. A.* **70**, 3857–60
17. Hoover, D. M., and Ludwig, M. L. (1997) A flavodoxin that is required for enzyme activation: the structure of oxidized flavodoxin from *Escherichia coli* at 1.8 Å resolution. *Protein Sci.* **6**, 2525–37
18. Suleman, A., and Skibo, E. B. (2002) A comprehensive study of the active site residues of DT-diaphorase: rational design of benzimidazolediones as DT-diaphorase substrates. *J. Med. Chem.* **45**, 1211–20
19. Titovets, E. P., and Petrovskii, G. G. (1976) Properties and reaction mechanism of mitochondrial menadione reductase. *Biokhimiia* **41**, 1522–30
20. Matthews, R. (1999) *BI Bi ping pong: is there really such a mechanism?*, Enzymatic Mechanisms, IOS Press
21. Ernster, L., and Navazio, f (1958) Soluble Diaphorase in Animal Tissues. *Acta Chem. Scand.* **12**, 595
22. Ross, D., and Siegel, D. (2004) NAD(P)H:quinone oxidoreductase 1 (NQO1, DT-diaphorase), functions and pharmacogenetics. *Methods Enzymol.* **382**, 115–44
23. Dicoumarol, P. I., Asher, G., Dym, O., Tsvetkov, P., Adler, J., and Shaul, Y. (2006) The Crystal Structure of NAD (P) H Quinone Oxidoreductase 1 in Complex with Its. , 6372–6378
24. Sollner, S., Schober, M., Wagner, A., Prem, A., Lorkova, L., Palfey, B. a, Groll, M., and Macheroux, P. (2009) Quinone reductase acts as a redox switch of the 20S yeast proteasome. *EMBO Rep.* **10**, 65–70
25. Nevitt, T., Pereira, J., and Rodrigues-Pousada, C. (2004) YAP4 gene expression is induced in response to several forms of stress in *Saccharomyces cerevisiae*. *Yeast* **21**, 1365–74
26. Sollner, S., Deller, S., Macheroux, P., and Palfey, B. A. (2009) Mechanism of flavin reduction and oxidation in the redox-sensing quinone reductase Lot6p from *Saccharomyces cerevisiae*. *Biochemistry* **48**, 8636–43
27. Becker, D. F., Zhu, W., and Moxley, M. a (2011) Flavin redox switching of protein functions. *Antioxid. Redox Signal.* **14**, 1079–91
28. Zoltowski, B. D., Schwerdtfeger, C., Widom, J., Loros, J. J., Bilwes, A. M., Dunlap, J. C., and Crane, B. R. (2007) Conformational switching in the fungal light sensor Vivid. *Science* **316**, 1054–1057
29. Srivastava, D., Zhu, W., Johnson, W. H., Whitman, C. P., Becker, D. F., and Tanner, J. J. (2010) The structure of the proline utilization a proline dehydrogenase domain inactivated by N-propargylglycine provides insight into conformational changes induced by substrate binding and flavin reduction. *Biochemistry* **49**, 560–569

30. Neumann, P., Weidner, A., Pech, A., Stubbs, M. T., and Tittmann, K. (2008) Structural basis for membrane binding and catalytic activation of the peripheral membrane enzyme pyruvate oxidase from *Escherichia coli*. *Proc. Natl. Acad. Sci. U. S. A.* **105**, 17390–17395
31. Hayward, S. (2001) Peptide-plane flipping in proteins. *Protein Sci.* **10**, 2219–2227
32. Kitao, A., Hayward, S., and Go, N. (1998) Energy landscape of a native protein: jumping-among-minima model. *Proteins* **33**, 496–517
33. Richardson, J. S. (1981) The anatomy and taxonomy of protein structure. *Adv. Protein Chem.* **34**, 167–339
34. Rose, G. D., Gierasch, L. M., and Smith, J. A. (1985) Turns in peptides and proteins. *Adv. Protein Chem.* **37**, 1–109
35. Gunasekaran, K., Gomathi, L., Ramakrishnan, C., Chandrasekhar, J., and Balaram, P. (1998) Conformational interconversions in peptide beta-turns: analysis of turns in proteins and computational estimates of barriers. *J. Mol. Biol.* **284**, 1505–16
36. Glickman, M. H., and Ciechanover, A. (2002) The ubiquitin-proteasome proteolytic pathway: destruction for the sake of construction. *Physiol. Rev.* **82**, 373–428
37. Jariel-Encontre, I., Bossis, G., and Piechaczyk, M. (2008) Ubiquitin-independent degradation of proteins by the proteasome. *Biochim. Biophys. Acta* **1786**, 153–77
38. Stadtmueller, B. M., Kish-Trier, E., Ferrell, K., Petersen, C. N., Robinson, H., Myszka, D. G., Eckert, D. M., Formosa, T., and Hill, C. P. (2012) Structure of a proteasome Pba1-Pba2 complex: implications for proteasome assembly, activation, and biological function. *J. Biol. Chem.* **287**, 37371–82
39. Leggett, D. S., Hanna, J., Borodovsky, A., Crosas, B., Schmidt, M., Baker, R. T., Walz, T., Ploegh, H., and Finley, D. (2002) Multiple associated proteins regulate proteasome structure and function. *Mol. Cell* **10**, 495–507

***In vivo* role of Lot6p in the regulation of transcription factor Yap4p**

3.1 Introduction

The ability of an organism to sense internal and external stimuli and regulate gene expression is crucial for survival and reproduction. The regulation of gene expression is mostly achieved at the level of transcription and to a lesser extent by post translation modifications. Heat shock elements (HSE) are short DNA sequences located upstream of genes which are induced by exposure to elevated temperatures. The discovery of HSE proved that these sequences are crucial for regulating gene transcription (1, 2). It was later discovered that specific regulatory proteins known as transcription factors bind to these short DNA sequences and regulate the transcription of a downstream gene either positively or negatively (3). Transcription factors comprise a large group of proteins which generally exhibit a modular structure. A transcription factor is made up of different structural domains, a DNA binding, activating and ligand binding domain (4–6). Transcription factors are commonly classified based on the structure of the DNA binding domain e.g. helix-turn-helix domain, Zn-binding domains, β -ribbon domain and leucine-zipper coiled-coil domain (7). The leucine-zipper coiled-coil domain is discussed in detail below.

3.1.1 The leucine-zipper coiled-coil domain

The leucine-zipper coiled-coil domain is defined by its dimerization motif, a motif exhibiting periodic repetition of leucine residues in α -helices. Leucines of one α -helix interdigitate with leucines of another α -helix belonging to a different subunit and form a stable noncovalent linkage in the dimer interface (8). The interdigitating leucines of two subunits give rise to a zipper like appearance, hence the name leucine zipper. The leucine zipper region is either preceding or following a positively charged DNA binding domain (basic region) (figure 1). For this reason these proteins were renamed as basic leucine zipper (bZIP) transcription factors (9). Generally, crucial amino acids of bZIP transcription factors that bind to the DNA are conserved. Additionally, the distance between these amino acids and the start of leucine zipper domain is invariant. Conservation of amino acids at the same positions has led to the discovery of "scissors-grip" model for DNA binding (10).

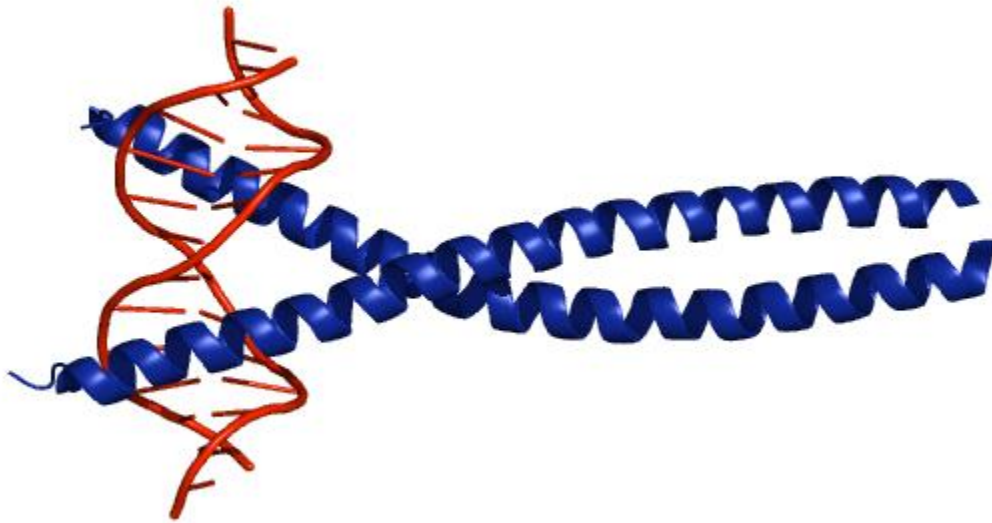


Figure 1: Crystal structure of yeast bZIP transcription factor PAP1 dimer (blue) showing the scissors-grip model for binding DNA (red) binding (11).

The leucine zipper segments of some bZIP transcription factors preferentially form heterodimers with other bZIP transcription factors (12). The formation of hetero dimers allows bZIP transcription factors to be involved in complex regulatory circuits (7).

3.1.2 Yeast activator protein family

The budding yeast *Saccharomyces cerevisiae* exhibits a complex pattern of gene expression due to rapid changes in growth conditions. Yeast cells maintain their homeostasis through coordinated transcription regulated by several transcription factors (13). The majority of transcriptional regulation in response to changes in growth conditions is dedicated towards stress response mechanisms. Two yeast transcription factors, Msn2p and Msn4p, regulate the majority of genes involved in a plethora of stress responses and have been extensively studied (14,15). In addition, the Yap (yeast activator protein) family consists of eight bZIP transcription factors involved in various forms of stress responses (16). The Yap family of transcription factors is classified as a separate family since all the family members differ from conventional yeast bZIP transcription factors (Gcn4p) at the crucial DNA binding amino acids. Six Yap transcription factors are involved in different kinds of stress response. Yap1p in oxidative stress,

Yap2p in cadmium stress, Yap4p & Yap6p in osmotic stress, Yap5p & Yap1p in iron metabolism and Yap1p & Yap8p in detoxification of arsenic compounds (13). The overlapping functionality of Yap family members led to the proposal that this family operates as an independent network and that different members of the family form heterodimers (17–19). The Yap transcription factors Yap3p and Yap7p are still uncharacterized with regard to their function. The Yap family member Yap4p is of particular interest in the context of this chapter.

3.1.3 Yeast activator protein Yap4p

Yap4p is a 33 kDa bZIP transcription factor belonging to the Yap family. Yap4p was shown to be involved in various stress responses, including oxidative, osmotic and heat induced stress (20–22). The regulation of Yap4p under osmotic stress condition was shown to be mediated by Msn2p, whilst under oxidative stress it was shown to be co-regulated by Yap1p and Msn2p (23, 24). A novel pathway involving the regulation of Yap4p by the quinone reductase Lot6p under oxidative stress was recently discovered (25). Quinone reductase Lot6p was shown to regulate the ubiquitin independent degradation and localization of bZIP transcription factor Yap4p. Similarly, the human quinone reductase NQO1 which is a homolog of Lot6p was shown to regulate the degradation of p53 and p73 by ubiquitin independent degradation (26).

The number of documented ubiquitin-independent protein degradation pathways is relatively small compared to ubiquitin dependent or lysosomal degradation pathways, but accumulating evidence suggests that this pathway also plays a major role in protein degradation (27, 28). The majority of proteins shown to be degraded by the 20S proteasome are either completely disordered or partially disordered (29, 30). In recent years, a large number of proteins which are completely disordered or partially disordered were discovered (31, 32). Especially, transcription factors contain a large portion of intrinsically disordered regions which are essential for transcriptional regulation (33). *Ab initio* protein modeling of Yap4p by using the Robetta server revealed that large parts of the protein are unstructured (figure 2), with the exception of an α -helix which probably is the DNA binding region (34, 35).

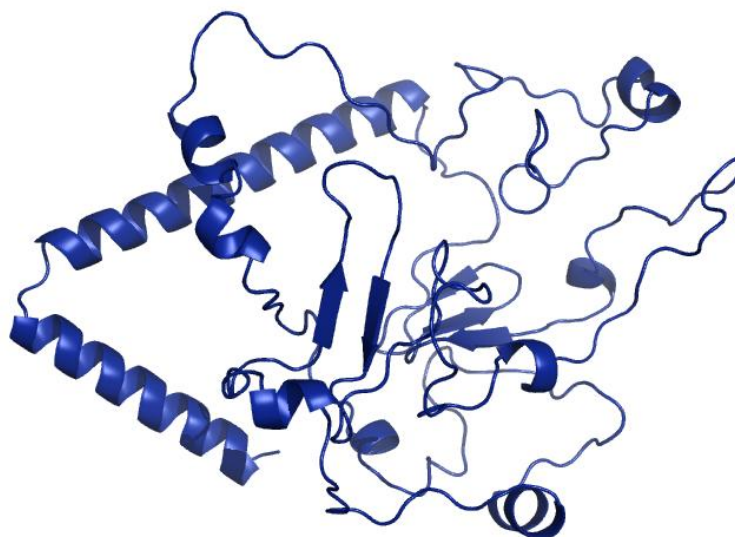


Figure 2: *Ab initio* modeled structure of Yap4p predicted by the Robetta server. The DNA binding region forms a distinct α -helix, whereas the rest of the protein appears to be poorly structured.

Transcriptional profiling of $\Delta yap4$ yeast strain revealed that mRNA levels of more than 100 genes decreased by at least two-fold in this strains (13). The analysis of these genes revealed that they belong to several functional classes (13). Hence, it was proposed that Yap4p plays a general role in yeast stress response. It is very likely that Yap4p itself is regulated by various other transcription factors or proteins, since the promoter region of Yap4p is rich in regulatory stress-associated cis-elements (13). However, information regarding the *in vivo* regulation of Yap4p itself is sparse or inconclusive. Sollner *et al.*, (25) showed that Yap4p migration into the nucleus upon induction of oxidative stress is regulated by the redox state of Lot6p. On the other hand, Pereira *et al.*, (36) showed that Yap4p is always localized in the nucleus. These authors also showed that Yap4p is phosphorylated under various stress conditions and that phosphorylation does not affect the localization of Yap4p.

Essentially, the *in vivo* role of Lot6p in the regulation of Yap4p remains unclear. The aim of the work described is to determine whether the intracellular levels of Yap4p are dependent on Lot6p and if ubiquitination is essential for degradation of Yap4p.

3.2 Materials and methods

Reagents

Unless stated otherwise all chemicals were of highest grade commercially available and were purchased either from Sigma-Aldrich (St. Louis, MO, USA), Fluka (Buchs, Switzerland), or Merck (Darmstadt, Germany). DNA primers were purchased from VBC-Biotech (Vienna, Austria). $\Delta lot6$ strain was from euroscarf strain collection.

$\Delta lot6$ Strain verification

Genomic DNA was extracted from BY4741 and $\Delta lot6$ strains obtained from Euroscarf strain collection by following manufacturer's instructions (E.Z.N.A.® Yeast DNA Kit, OMEGA bio-tek). The primers mentioned below were used to amplify either the open reading frame (ORF) of *LOT6* or a part of the *kanMX4* cassette substituted for *LOT6*. A standard Taq polymerase protocol was used to amplify the DNA. The amplified DNA products were resolved on a 1% Et-Br agarose gel and visualized under ultraviolet light.

Primers used to amplify *LOT6* ORF:

5' CGA AGA TCT ATG AAA GTG GGT ATT ATA ATG GGT TC 3'

5' TAT GGT ACC C TTT ATT CCT CGT TGT TTC GAT GC '3

Primers used to amplify part of *kanMX4* cassette:

5'-GAT GAT TAC AGT CTC GTC TTG GTC-3'

5'-GAT TGT CGC ACC TGA TTG C-3'

Molecular cloning:

The coding sequence of *YAP4* was amplified and isolated by using primers overlapping with the first and last 20-30 base pairs of the ORF in the genomic DNA. The forward and reverse primers are appended with DNA sequences for restriction enzymes, EcoRI and KpnI, respectively, for cloning *YAP4* into ppm323 and ppm96 vectors. The plasmids were originally designed by modifying yeast centromeric plasmid YCplac111. The plasmids ppm323 and ppm96 were obtained from Prof. Dr. Jürgen Dohmen. The *E. coli* and yeast selection markers for both the plasmids were ampicillin and leucine respectively and both the plasmids also possessed a copper inducible promoter (CUP1). The plasmid ppm323 appends an N-terminal Myc tag, while ppm96 appends a C-terminal Ha tag to encode for a Yap4p fusion protein.

Yeast transformation and cell culture

Log phase yeast cells were transformed with plasmids by following standard LiAc/SS Carrier DNA/PEG method (37). A single colony from the transformation plate was further propagated and stored at 4 °C for future use.

Cell culture and preparation of total cellular protein extracts

A single colony with desired plasmid was inoculated into liquid minimal media and incubated at 30 °C for 12-14 hours while shaking at 130 rpm for preparing a preculture. Fresh media were inoculated with the preculture to an OD₆₀₀ of 0.1 and propagated at 30 °C, 130 rpm. The OD₆₀₀ of cultures was measured again and 1 OD₆₀₀ unit of cells were harvested when the optical density had reached to 0.8-1. In some cases the cultures were supplemented with CuSO₄ at an OD₆₀₀ of 0.6-0.8 to a final concentration of 1mM and further propagated for one more hour before harvesting. In the experiment where the proteasomes are inhibited, bortezomib was added to cultures to a final concentration of 30 μM at an OD₆₀₀ of 0.6-0.8, and 1 OD unit of cells were harvested at required time points. Cell cultures of *uba1-ts26* strain were propagated at 25 °C until the OD₆₀₀ had reached to 0.8-1 and then shifted to a restrictive temperature of 37 °C. 1 OD₆₀₀unit of cells were further harvested at required time points.

The cell pellets were resuspended in urea buffer to a final concentration of 6 M urea. Appropriate amount of SDS-PAGE loading buffer was added to the resuspended cells and immediately boiled at 95 °C for 5 min to prepare total cellular protein extracts. The total protein extract was briefly centrifuged at 13,000g and then frozen at -20 °C until further use.

SDS-PAGE and immunoblotting

To determine the steady state intra cellular levels (SSL) of Yap4p, total cellular protein extract from 1 OD₆₀₀ unit of cells was loaded per lane of a 12.5% linear hand cast polyacrylamide gel. After gel electrophoresis the proteins were transferred onto an immunoblotting membrane using a semi-dry blotting unit. The membranes were blocked with 3% milk powder in PBST for 60 min after the transfer was completed. The membranes were further incubated in appropriate antibodies and visualized by the enhanced chemiluminescence (ECL) method or Odyssey Infrared Imaging System (LI-COR Biosciences). Yap4p antibodies used in this study were generated in collaboration with Prof. Günther Daum. The other

antibodies used in this study were, anti-HA tag antibody (16B12) from Covance anti-Myc tag antibody (9B11) from NEB and anti-rabbit secondary antibodies (NA9340) from GE healthcare.

3.3 Results and discussion:

In order to verify the steady state intercellular levels (SSL) of Yap4p two yeast strains, BY4741 (Wild type) and $\Delta lot6$ from the Euroscarf *strain collection* were used throughout this study (38). In order to verify the deletion of *LOT6*, PCR was performed to amplify the open reading frame (ORF) of *LOT6* or a part of the *kanMX4* cassette which substituted *LOT6* (Figure 3).

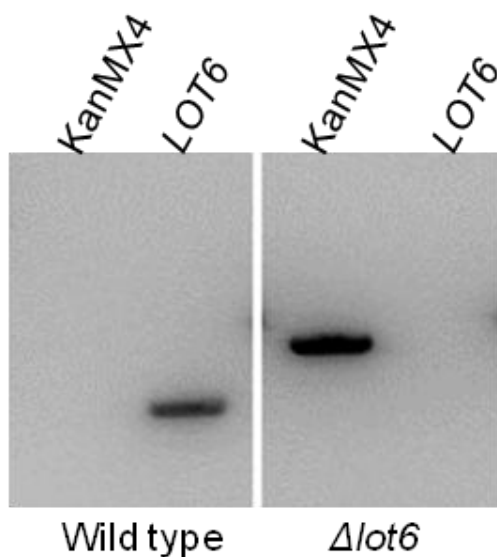


Figure 3: Agarose gel electrophoresis showing $\Delta lot6$ strain verification. Genomic DNA isolated from wild type and $\Delta lot6$ strains was used in an PCR performed to amplify either the ORF of $\Delta lot6$ or a part of the *kanMX4* gene. As can be seen in the above figure *LOT6* is present in the wild type strain, whereas in the $\Delta lot6$ strain it is replaced by *kanMX4*.

The modular nature of transcription factors is ideal for complexes involved in gene regulation (39). For example, interactions mediated by the C-terminal domain of lambda repressor lead to cooperative changes in DNA binding and gene expression (40). On the other hand, the N-terminal region of intrinsically disordered transcription factors is essential for their degradation by the proteasome (41). In order to determine the role of N-terminal and C-terminal domains of Yap4p, the *YAP4* gene was cloned into centromeric plasmids (ppm323 or ppm96) to encode for an N-terminal Myc tag Yap4p or C-terminal HA tag Yap4p. The experiments shown

in the rest of the study were at least repeated twice, and the SSL were also quantified by using imagej software (42)

The SSL of N-terminal Myc Yap4p were measured in wild type and $\Delta lot6$ strain in presence of spermidine and H_2O_2 (Figure 4). The media was supplemented with spermidine and H_2O_2 to simulate polyamine and oxidative stress respectively. The SSL of N-terminal Myc Yap4p were unchanged in $\Delta lot6$ strain compared to wild type strain indicating that Yap4p was not regulated by Lot6p when the N-terminal region was blocked by a tag. In the presence of H_2O_2 an incremental shift in the mobility of Yap4p was observed independent of Lot6p. The pattern of this mobility shift is similar to that of phosphorylation reported by Pereira et al (36). The phosphorylation of Yap4p due to addition of H_2O_2 indicates that Yap4p is involved in oxidative stress response.

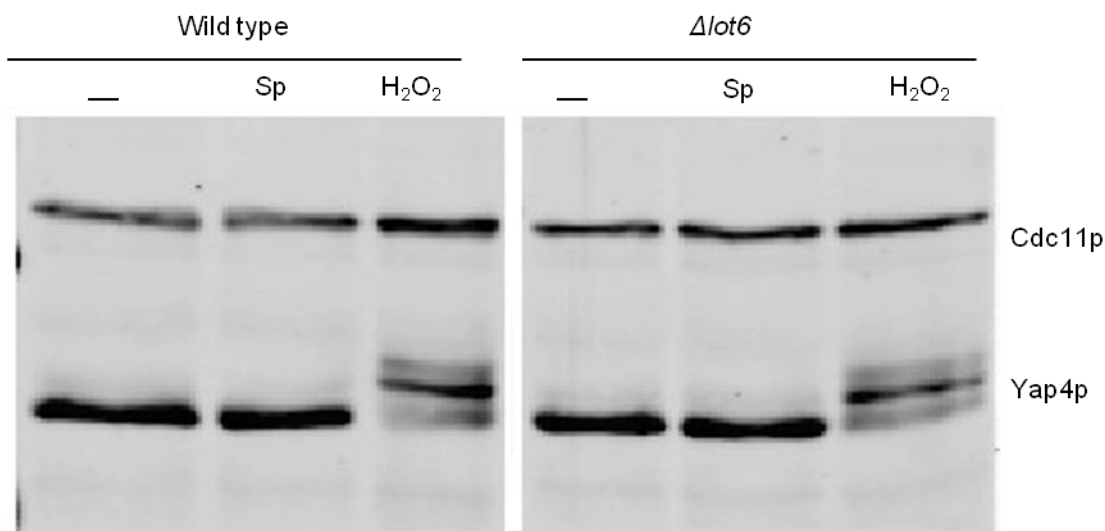


Figure 4: Determination of N-terminal Myc Yap4p SSL. Western blot analysis of total protein extracts from Wild type and $\Delta lot6$ cells by anti- Myc antibodies and Cdc11p (loading control) antibodies.

Along similar lines the SSL of C-terminal HA Yap4p were determined (Figure 5). Initial experiments indicated that Yap4p levels were depleted in $\Delta lot6$ strain. The experiment was repeated with six colonies for each strain and the same effect was not observed with statistical significance. Difference in the levels of protein expression could be due to variation in the copy number of the plasmids. Since centromeric plasmids were used in this study it could be

assumed that the copy number was constant. No explanation could be found why the Yap4p levels were depleted in the cells used for the experiment shown in figure 5.

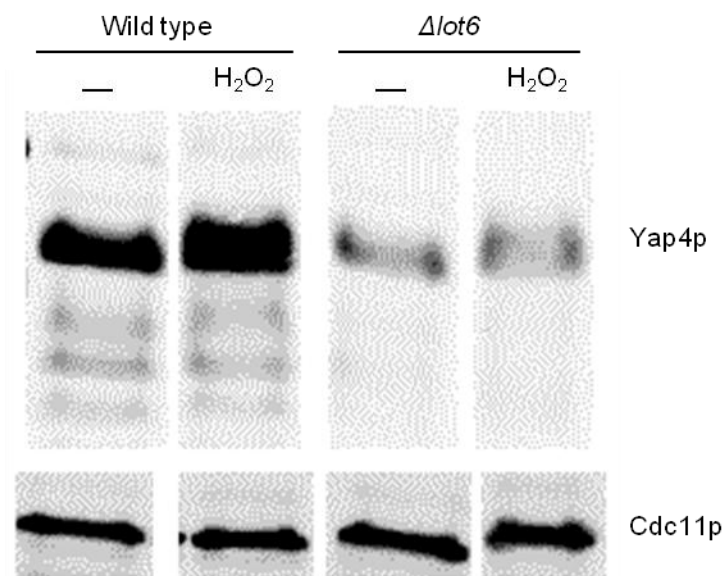


Figure 5: Determination of C-terminal Ha Yap4p SSL. Western blot analysis of total protein extracts from Wild type and $\Delta lot6$ cells by anti- Ha antibodies and Cdc11p (loading control) antibodies.

SSL of endogenous Yap4p were measured to determine if regulation by Lot6p is still retained when both the N-terminus and C-terminus are untagged (Figure 6). It is clearly observable that Yap4p is strongly induced and phosphorylated under both osmotic or oxidative stress conditions as indicated by Pereira et al., (36). Most importantly, the levels of Yap4p were unchanged in $\Delta lot6$ strain compared to of wild type strain.

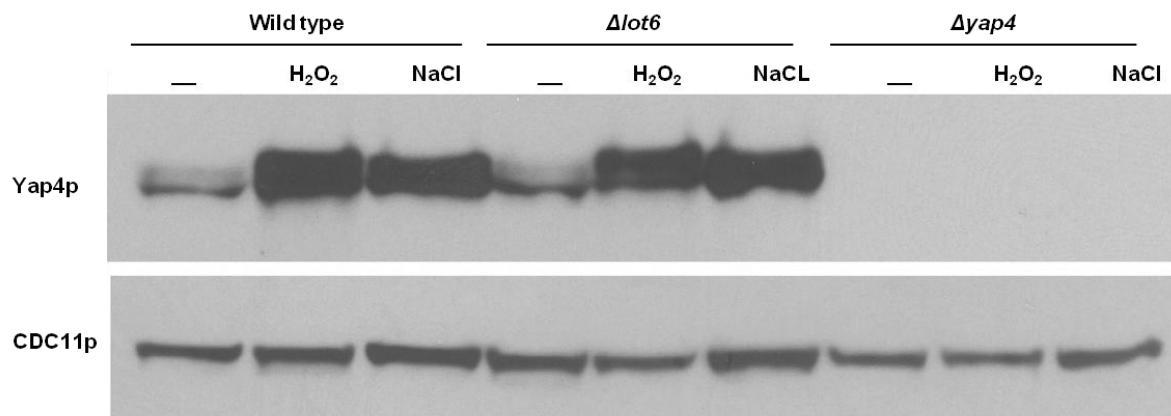


Figure 6: Determination of endogenous Yap4p SSL. Western blot analysis of total protein extracts from Wild type, $\Delta lot6$ and $\Delta yap4$ cells by anti-Yap4p antibodies and Cdc11p (loading control) antibodies. $\Delta yap4$ cell extracts were used as a control to show that anti-Yap4p antibodies are only specific against Yap4p.

Since Lot6p is a quinone reductase, similar experiments were repeated in the presence of quinones. Yap4p is also induced strongly due to quinone stress but no change in the SSL was observed in the absence of Lot6p (data not shown). Significantly, the endogenous levels of Yap4p remained unchanged under various stress conditions (oxidative, osmotic and quinone) despite the absence of Lot6p.

In order to verify if Lot6p is essential for the degradation of Yap4p, SSL of Yap4p was measured in cell cultures where the intracellular proteasome was inhibited by addition of bortezomib (Figure 7). Inhibition of proteasome by bortezomib led to the accumulation of Yap4p over time indicating that Yap4p is indeed degraded by the proteasome.

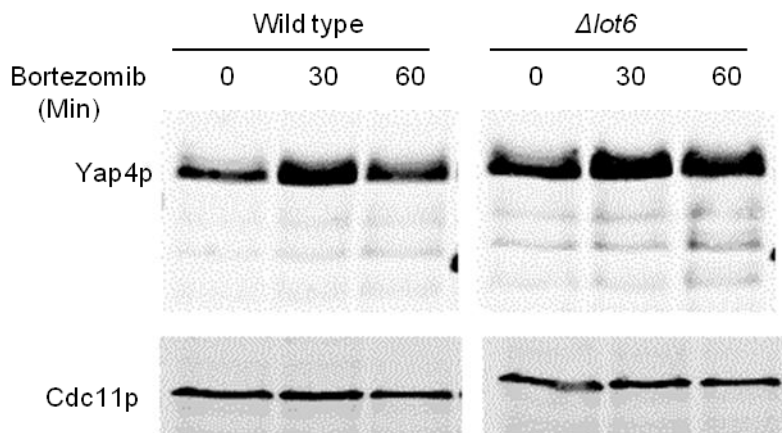


Figure 7: Inhibition of proteasome stabilizes C-Terminal Ha Yap4p. Western blot analysis of total protein extracts from wild type and $\Delta lot6$ with anti-HA and Cdc11p (loading control) antibodies.

To verify if ubiquitination was essential for the degradation of Yap4p (Figure 8), SSL of Yap4p was measured in a temperature-sensitive *uba1-ts26* strain.

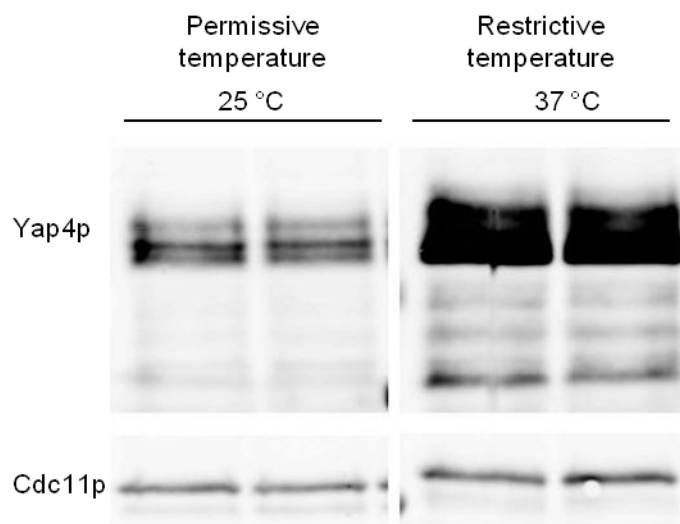


Figure 8: Inhibition of UBA1 stabilizes C-Terminal Ha Yap4p. Western blot analysis of total protein extracts from Wild type and $\Delta lot6$ with anti-Ha and Cdc11p (loading control) antibodies.

The *uba1-ts26* strain was engineered in such a way that the Uba1 (ubiquitin-activating enzyme) is inhibited upon shifting the cell cultures to the restrictive temperature 37 °C, thus effecting the total ubiquitination status of all proteins. In the case of Yap4p the SSL drastically increased upon shifting the cell cultures to 37 °C indicating that ubiquitination was essential for the degradation of Yap4p.

The ability of quinone reductases to interact with the proteasome and regulate the degradation of transcription factors is still a matter of debate. Sollner *et al.*, (25) showed that degradation of Yap4p is regulated by Lot6p, the authors arrived at the conclusion predominantly based on *in vitro* experiments where Yap4p co-elutes with the Lot6p-20S proteasome complex. The *in vivo* experimental evidence shown in this report indicates that Yap4p is regulated through an unknown pathway that is independent of Lot6p. It is highly probable that at some point in its life cycle Yap4p interacts with the proteasome since Yap4p is ubiquitinated and degraded by the proteasome, but this interaction is not mediated by Lot6p. In conclusion, the evidence present in this study does not support a role for quinone reductase Lot6p in the regulation of Yap4p *in vivo*.

References

1. Davidson, E. H., Jacobs, H. T., and Britten, R. J. (1983) Very short repeats and coordinate induction of genes. *Nature* **301**, 468–70
2. Pelham, H. R. (1982) A regulatory upstream promoter element in the *Drosophila* hsp 70 heat-shock gene. *Cell* **30**, 517–28
3. Latchman, D. S. (1997) Transcription factors: an overview. *Int. J. Biochem. Cell Biol.* **29**, 1305–12
4. Brent, R., and Ptashne, M. (1985) A eukaryotic transcriptional activator bearing the DNA specificity of a prokaryotic repressor. *Cell* **43**, 729–36
5. Hope, I. A., and Struhl, K. (1986) Functional dissection of a eukaryotic transcriptional activator protein, GCN4 of yeast. *Cell* **46**, 885–94
6. Hollenberg, S. M., and Evans, R. M. (1988) Multiple and cooperative trans-activation domains of the human glucocorticoid receptor. *Cell* **55**, 899–906
7. Harrison, S. C. (1991) A structural taxonomy of DNA-binding domains. *Nature* **353**, 715–9
8. Landschulz, W. H., Johnson, P. F., and McKnight, S. L. (1988) The leucine zipper: a hypothetical structure common to a new class of DNA binding proteins. *Science* **240**, 1759–64
9. Shuman, J. D., Vinson, C. R., and McKnight, S. L. (1990) Evidence of changes in protease sensitivity and subunit exchange rate on DNA binding by C/EBP. *Science* **249**, 771–4
10. Vinson, C. R., Sigler, P. B., and McKnight, S. L. (1989) Scissors-grip model for DNA recognition by a family of leucine zipper proteins. *Science* **246**, 911–6
11. Fujii, Y., Shimizu, T., Toda, T., Yanagida, M., and Hakoshima, T. (2000) Structural basis for the diversity of DNA recognition by bZIP transcription factors. *Nat. Struct. Biol.* **7**, 889–93
12. O'Shea, E. K., Rutkowski, R., Stafford, W. F., and Kim, P. S. (1989) Preferential heterodimer formation by isolated leucine zippers from *fos* and *jun*. *Science* **245**, 646–8
13. Rodrigues-pousada, C., Menezes, R. A., and Pimentel, C. (2010) The Yap family and its role in stress response. , 245–258
14. Marchler, G., Schüller, C., Adam, G., and Ruis, H. (1993) A *Saccharomyces cerevisiae* UAS element controlled by protein kinase A activates transcription in response to a variety of stress conditions. *EMBO J.* **12**, 1997–2003

15. Belazzi, T., Wagner, A., Wieser, R., Schanz, M., Adam, G., Hartig, A., and Ruis, H. (1991) Negative regulation of transcription of the *Saccharomyces cerevisiae* catalase T (CTT1) gene by cAMP is mediated by a positive control element. *EMBO J.* **10**, 585–92
16. Rodrigues-Pousada, C. A., Nevitt, T., Menezes, R., Azevedo, D., Pereira, J., and Amaral, C. (2004) Yeast activator proteins and stress response: an overview. *FEBS Lett.* **567**, 80–5
17. Cohen, B. A., Pilpel, Y., Mitra, R. D., and Church, G. M. (2002) Discrimination between paralogs using microarray analysis: application to the Yap1p and Yap2p transcriptional networks. *Mol. Biol. Cell* **13**, 1608–14
18. Menezes, R. A., Amaral, C., Delaunay, A., Toledano, M., and Rodrigues-Pousada, C. (2004) Yap8p activation in *Saccharomyces cerevisiae* under arsenic conditions. *FEBS Lett.* **566**, 141–6
19. Tan, K., Feizi, H., Luo, C., Fan, S. H., Ravasi, T., and Ideker, T. G. (2008) A systems approach to delineate functions of paralogous transcription factors: role of the Yap family in the DNA damage response. *Proc. Natl. Acad. Sci. U. S. A.* **105**, 2934–9
20. Gasch, A. P., Spellman, P. T., Kao, C. M., Carmel-Harel, O., Eisen, M. B., Storz, G., Botstein, D., and Brown, P. O. (2000) Genomic expression programs in the response of yeast cells to environmental changes. *Mol. Biol. Cell* **11**, 4241–57
21. Posas, F., Chambers, J. R., Heyman, J. A., Hoeffler, J. P., de Nadal, E., and Ariño, J. (2000) The transcriptional response of yeast to saline stress. *J. Biol. Chem.* **275**, 17249–55
22. Rep, M., Krantz, M., Thevelein, J. M., and Hohmann, S. (2000) The transcriptional response of *Saccharomyces cerevisiae* to osmotic shock. Hot1p and Msn2p/Msn4p are required for the induction of subsets of high osmolarity glycerol pathway-dependent genes. *J. Biol. Chem.* **275**, 8290–300
23. Nevitt, T., Pereira, J., and Rodrigues-Pousada, C. (2004) YAP4 gene expression is induced in response to several forms of stress in *Saccharomyces cerevisiae*. *Yeast* **21**, 1365–74
24. Nevitt, T., Pereira, J., Azevedo, D., Guerreiro, P., and Rodrigues-Pousada, C. (2004) Expression of YAP4 in *Saccharomyces cerevisiae* under osmotic stress. *Biochem. J.* **379**, 367–74
25. Sollner, S., Schober, M., Wagner, A., Prem, A., Lorkova, L., Palfey, B. a, Groll, M., and Macheroux, P. (2009) Quinone reductase acts as a redox switch of the 20S yeast proteasome. *EMBO Rep.* **10**, 65–70
26. Asher, G., Tsvetkov, P., Kahana, C., and Shaul, Y. (2005) A mechanism of ubiquitin-independent proteasomal degradation of the tumor suppressors p53 and p73. *Genes Dev.* **19**, 316–21

27. Hwang, J., Winkler, L., and Kalejta, R. F. (2011) Ubiquitin-independent proteasomal degradation during oncogenic viral infections. *Biochim. Biophys. Acta* **1816**, 147–57
28. Baugh, J. M., Viktorova, E. G., and Pilipenko, E. V (2009) Proteasomes can degrade a significant proportion of cellular proteins independent of ubiquitination. *J. Mol. Biol.* **386**, 814–27
29. Asher, G., Reuven, N., and Shaul, Y. (2006) 20S proteasomes and protein degradation “by default”. *Bioessays* **28**, 844–9
30. Dyson, H. J., and Wright, P. E. (2005) Intrinsically unstructured proteins and their functions. *Nat. Rev. Mol. Cell Biol.* **6**, 197–208
31. Tompa, P. (2002) Intrinsically unstructured proteins. *Trends Biochem. Sci.* **27**, 527–33
32. Radivojac, P., Obradovic, Z., Smith, D. K., Zhu, G., Vucetic, S., Brown, C. J., Lawson, J. D., and Dunker, A. K. (2004) Protein flexibility and intrinsic disorder. *Protein Sci.* **13**, 71–80
33. Minezaki, Y., Homma, K., Kinjo, A. R., and Nishikawa, K. (2006) Human transcription factors contain a high fraction of intrinsically disordered regions essential for transcriptional regulation. *J. Mol. Biol.* **359**, 1137–49
34. Bradley, P., Chivian, D., Meiler, J., Misura, K. M. S., Rohl, C. A., Schief, W. R., Wedemeyer, W. J., Schueler-Furman, O., Murphy, P., Schonbrun, J., Strauss, C. E. M., and Baker, D. (2003) Rosetta predictions in CASP5: successes, failures, and prospects for complete automation. *Proteins* **53 Suppl 6**, 457–68
35. Simons, K. T., Ruczinski, I., Kooperberg, C., Fox, B. A., Bystroff, C., and Baker, D. (1999) Improved recognition of native-like protein structures using a combination of sequence-dependent and sequence-independent features of proteins. *Proteins* **34**, 82–95
36. Pereira, J., Pimentel, C., Amaral, C., Menezes, R. A., and Rodrigues-Pousada, C. (2009) Yap4 PKA- and GSK3-dependent phosphorylation affects its stability but not its nuclear localization. *Yeast* **26**, 641–53
37. Gietz, R. D., and Woods, R. A. (2006) Yeast transformation by the LiAc/SS Carrier DNA/PEG method. *Methods Mol. Biol.* **313**, 107–20
38. Brachmann, C. B., Davies, A., Cost, G. J., Caputo, E., Li, J., Hieter, P., and Boeke, J. D. (1998) Designer deletion strains derived from *Saccharomyces cerevisiae* S288C: a useful set of strains and plasmids for PCR-mediated gene disruption and other applications. *Yeast* **14**, 115–32
39. Frankel, A. D., and Kim, P. S. (1991) Modular structure of transcription factors: implications for gene regulation. *Cell* **65**, 717–9

40. Sauer, R. T., Jordan, S. R., and Pabo, C. O. (1990) Lambda repressor: a model system for understanding protein-DNA interactions and protein stability. *Adv. Protein Chem.* **40**, 1–61
41. Gödderz, D., Schäfer, E., Palanimurugan, R., and Dohmen, R. J. (2011) The N-terminal unstructured domain of yeast ODC functions as a transplantable and replaceable ubiquitin-independent degron. *J. Mol. Biol.* **407**, 354–67
42. Schneider, C. A., Rasband, W. S., and Eliceiri, K. W. (2012) NIH Image to ImageJ: 25 years of image analysis. *Nat. Methods* **9**, 671–5

The human flavoproteome

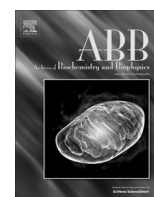
Author contributions

The idea to write this review article was conceived by Peter Macheroux. Wolf-Dieter Lienhart and me compiled the list of human flavoproteins and disease-related human flavoproteins. All the authors contributed equally to the remaining sections of manuscript.



Contents lists available at SciVerse ScienceDirect

Archives of Biochemistry and Biophysics

journal homepage: www.elsevier.com/locate/yabbi

Review

The human flavoproteome

Wolf-Dieter Lienhart, Venugopal Gudipati, Peter Macheroux*

Graz University of Technology, Institute of Biochemistry, Petersgasse 12, A-8010 Graz, Austria

ARTICLE INFO

Article history:

Received 17 December 2012
and in revised form 21 February 2013
Available online 15 March 2013

Keywords:

Coenzyme A
Coenzyme Q
Folate
Heme
Pyridoxal 5'-phosphate
Steroids
Thyroxine
Vitamins

ABSTRACT

Vitamin B₂ (riboflavin) is an essential dietary compound used for the enzymatic biosynthesis of FMN and FAD. The human genome contains 90 genes encoding for flavin-dependent proteins, six for riboflavin uptake and transformation into the active coenzymes FMN and FAD as well as two for the reduction to the dihydroflavin form. Flavoproteins utilize either FMN (16%) or FAD (84%) while five human flavoenzymes have a requirement for both FMN and FAD. The majority of flavin-dependent enzymes catalyze oxidation–reduction processes in primary metabolic pathways such as the citric acid cycle, β -oxidation and degradation of amino acids. Ten flavoproteins occur as isozymes and assume special functions in the human organism. Two thirds of flavin-dependent proteins are associated with disorders caused by allelic variants affecting protein function. Flavin-dependent proteins also play an important role in the biosynthesis of other essential cofactors and hormones such as coenzyme A, coenzyme Q, heme, pyridoxal 5'-phosphate, steroids and thyroxine. Moreover, they are important for the regulation of folate metabolites by using tetrahydrofolate as cosubstrate in choline degradation, reduction of *N*-5,10-methylenetetrahydrofolate to *N*-5-methyltetrahydrofolate and maintenance of the catalytically competent form of methionine synthase. These flavoenzymes are discussed in detail to highlight their role in health and disease.

© 2013 Elsevier Inc. All rights reserved.

Introduction

Vitamin B₂ (or riboflavin) is an essential dietary requirement for humans (*Homo sapiens sapiens*) because the biosynthesis of this compound is absent. The daily requirement for vitamin B₂ was estimated to be 1.1 mg and 1.3 mg for adult females and males, respectively, but may vary depending on metabolic challenges and the efficiency of riboflavin uptake. Dietary riboflavin is taken up in the human gastrointestinal tract by poorly characterized

transporters (Table 1, entry #74). Vitamin B₂ is not used in any human enzyme *per se* but is chemically modified to the flavin mononucleotide (FMN)¹ and flavin adenine dinucleotide form by riboflavin kinase (EC 2.7.1.26) and FAD synthetase (EC 2.7.7.2), respectively. FMN and FAD as well as excess riboflavin are excreted in the urine. Chastain and McCormick have also detected trace amounts of 7-hydroxy- and 8-hydroxy-flavins in human urine which are generated through as yet unknown catabolic reactions [1]. In addition, they have also found 8-sulfonyl-flavin which is supposedly released from enzymes bearing a covalent thioester linkage, e.g. monoamine oxidase A and B (MAOA and MAOB, Table 1).

FMN and FAD possess a tricyclic heteroaromatic isoalloxazine ring that can reversibly accept and donate one or two electrons. Thus the majority of the enzymes utilizing FMN or FAD catalyze reduction–oxidation (“redox”) reactions in metabolic transformations. In fact, the majority of human flavoenzymes belongs to the oxidoreductases with only two example each for a transferase and lyase, respectively (Table 1, entries #65–68). Flavoenzymes may either use FMN or FAD as cofactor and most are specific for one or the other. In the case of human flavoproteins only twelve use FMN and 64 FAD as cofactor amounting to ca. 16% and 84% of the flavoenzymes, respectively (note that five enzymes utilize both FMN and FAD). In a global analysis of FMN and FAD usage in flavoproteins it was noted that 25% of flavoenzymes utilize FMN [2], hence the human flavoproteome has a clear bias towards FAD-dependent enzymes.

* Corresponding author. Address: Graz University of Technology, Institute of Biochemistry, Petersgasse 12, A-8010 Graz, Austria. Fax: +43 316 873 6952.

E-mail address: peter.macheroux@tugraz.at (P. Macheroux).

¹ Abbreviations used: ACAD9acyl-CoA dehydrogenase isoform 9; ACADS, short-chain acyl-CoA dehydrogenase; ACADL, long-chain acyl-CoA dehydrogenase; ACADM, medium-chain acyl-CoA dehydrogenase; DHCR24, 3 β -hydroxysterol Δ^{24} -reductase; DMGDH, dimethylglycine dehydrogenase; ETF, electron transferring flavoprotein; ETFDH, electron-transferring flavoprotein ubiquinone oxidoreductase; FMO3, flavin-containing monooxygenase isoform 3; FOXRED1, FAD-dependent oxidoreductase; MSmethionine synthase; MTHFR, *N*-5,10-methylene-tetrahydrofolate reductase; MTRR, methionine synthase reductase; OMIM, Online Mendelian Inheritance in Man; MAOA, monoamine oxidase isozyme A; MAOB, monoamine oxidase isozyme B; MS, methionine synthase; MSR, methionine synthase reductase; MTHFR, *N*-5,10-methylenetetrahydrofolate reductase; NQO1, NAD(P):quinone oxidoreductase; PANK, pantothenate kinase; PDB, protein data base; PLP, pyridoxal 5'-phosphate; PNPO, pyridoxal 5'-phosphate oxidase; PPOX, protoporphyrinogen IX oxidase; PPCD, 4'-phosphopantothienoylcysteine decarboxylase; PPCS, phosphopantothienoylcysteine synthase; SARDH, sarcosine dehydrogenase; SQLE, squalene monooxygenase; THF, tetrahydrofolate; VP, variegate porphyria.

Table 1
Human flavoproteins.

No.	E.C.	Enzyme	Cofactor	Structure clan (family) ^a	Gene symbol	Gene location
1	1.1.1.28	D-lactate dehydrogenase	FAD	FAD_PCMH (FAD_binding_4)	LDHD	16q23.1
2	1.1.1.204	Xanthine dehydrogenase	FAD	FAD_PCMH (FAD_binding_5)	XDH	2p23.1
3	1.1.3.15	(S)-2-hydroxy-acid oxidase	FMN	TIM_barrel (FMN_dh)	HAO1 HAO2	20p12.3 1p12
4	1.1.5.3	Glycerol 3-phosphate dehydrogenase	FAD	NADP_Rossmann (DAO)	GP2	2q24.1
5	1.1.99.1	Choline dehydrogenase	FAD	GMC_oxred	CHDH	3p21.1
6	1.1.99.2	L-2-Hydroxyglutarate dehydrogenase	FAD	---	L2HGDH	14q21.3
7	1.1.99.-	D-2-Hydroxyglutarate dehydrogenase	FAD	---	D2HGDH	2q37.3
8	1.2.3.1	Aldehyde oxidase	FAD	---	AOX1	2q33.1
9	1.3.1.2	Dihydropyrimidine dehydrogenase	FMN	TIM_barrel (DHO_dh)	DPYD	1p21.3
10	1.3.1.72	3 β -Hydroxysterol Δ^2 -reductase	FAD	NADP_Rossmann (Pyr_redox_2)	---	---
11	1.3.3.1	Dihydroorotate dehydrogenase	FMN	TIM_barrel (DHO_dh)	DHCR24	1p32.3
12	1.3.3.4	Protoporphyrinogen IX oxidase	FAD	NADP_Rossmann (Amino_oxidase)	DHODH	16q22.2
13	1.3.3.6	Acyl-CoA oxidase	FAD	Acyl-CoA_dh (ACOX, acyl-CoA_dh_1)	PPOX ACOX1 ACOX2 ACOX3	1q23.3 17q25.1 3p14.3 4p16.1
14	1.3.3.-	Glutaryl-CoA oxidase	FAD	---	C7orf10	7p14.1
15	1.3.5.1	Succinate dehydrogenase Flavoprotein subunit A	8 α -(N3-His)- -FAD	NAPH_Rossmann (FAD_binding_2)	SDHA	5p15.33 (3q29) ^a
16	1.3.99.2	Short-chain- (butyryl)- acyl CoA dehydrogenase	FAD	Acyl-CoA_dh (Acyl-CoA_dh_1)	ACADS	12q24.31
17	1.3.99.3	Medium-chain acyl-CoA dehydrogenase	FAD	Acyl-CoA_dh (Acyl-CoA_dh_1)	ACADM	1p31.1
18	1.3.99.7	Glutaryl-CoA dehydrogenase	FAD	Acyl-CoA_dh (acyl-CoA_dh_1)	GCDH	19p13.2
19	1.3.99.10	Isovaleryl-CoA dehydrogenase	FAD	Acyl-CoA_dh (acyl-CoA_dh_1)	IWD	15q15.1
20	1.3.99.12	2-Methylbutyryl-CoA dehydrogenase	FAD	Acyl-CoA_dh (acyl-CoA_dh_1)	ACADSB	10q26.13
21	1.3.99.13	Long-chain-acyl-CoA dehydrogenase	FAD	Acyl-CoA_dh (acyl-CoA_dh_1)	ACADL	2q34
22	1.3.99.-	Very long-chain acyl-CoA dh	FAD	Acyl-CoA_dh (acyl-CoA_dh_1)	ACADVL	17p13.1
23	1.3.99.-	Isobutyryl-CoA dehydrogenase	FAD	Acyl-CoA_dh (acyl-CoA_dh_1)	ACAD8	11q25
24	1.3.99.-	Long-chain-unsaturated-acyl-CoA dh (molecular chaperone of complex I)	FAD	Acyl-CoA_dh (acyl-CoA_dh_1)	ACAD9	3q21.3
25	1.3.99.-	Long- and branched-chain-acyl-CoA dh	FAD	Acyl-CoA_dh (acyl-CoA_dh_1)	ACAD10	12q24.1
26	1.3.99.-	C22-long-chain-acyl-CoA dehydrogenase	FAD	Acyl-CoA_dh (acyl-CoA_dh_1)	ACAD11	3q22.1
27	1.4.3.1	D-aspartate oxidase	FAD	NADP_Rossmann (DAO)	DDO	6q21
28	1.4.3.2	L-amino acid oxidase	FAD	NADP_Rossmann (Amino_oxidase)	LAO	19q13.3-q13.4
29	1.4.3.3	D-amino acid oxidase	FAD	NADP_Rossmann (DAO)	DAO	12q24.11
30	1.4.3.4	Monoamine oxidase	8 α -(Cys)-FAD	NADP_Rossmann (Amino_oxidase)	MAOA MAOB	Xp11.3 Xp11.3 ^b
31	1.4.3.5	Pyridoxal 5'-phosphate oxidase	FMN	FMN-binding (Pyridox_oxidase)	PNPO	17q21.32
32	1.4.3.-	Pyridoxine 5'-phosphate oxidase	FAD	NADP_Rossmann (Amino_oxidase)	RNLS	10q23.31
33	1.5.1.20	Catecholamine oxidase (renalase)	FAD	FAD_oxidored (MTHFR)	MTHFR	1p36.22
34	1.5.3.7	Methylenetetrahydrofolate reductase	8 α -(Cys)-FAD	NADP_Rossmann (DAO)	PIPOX	17q11.2
35	1.5.3.16	Spermine oxidase	FAD	NADP_Rossmann (Amino_oxidase)	SMO	20p13
36	1.5.5.1	Electron-transferring flavoprotein-ubiquinone oxidoreductase	FAD	4Fe-4S (ETF_QO)	ETFDH	4q32.1
37	---	Electron transferring flavoprotein	FAD	FAD_DHS (ETF_alpha) HUB (ETF)	ETFFA ETFB	15q24.2-q24.3 19q13.41
38	1.5.99.1	Sarcosine dehydrogenase	8 α -(N3-His)- -FAD	NADP_Rossmann (DAO)	SARDH	9q34.2
39	1.5.99.2	Dimethylglycine dehydrogenase	8 α -(N3-His) -FAD	NADP_Rossmann (DAO)	DMGDH	5q14.1
40	1.5.99.-	Lysine-specific histone demethylase	FAD	NADP_Rossmann	KDM1A	1p36.12
41	1.5.99.8	Proline dehydrogenase	FAD	FAD_oxidored (Pro_dh)	PRODH	22q11.21

(continued on next page)

Table 1 (continued)

No.	E.C.	Enzyme	Cofactor	Structure clan (family) ^a	Gene symbol	Gene location
42	1.6.2.2	Cytochrome-b5 reductase	FAD	FAD_Lum_binding (FAD_binding_6)	CYB5R3	22q13.2
43	1.6.2.4	NADPH-hemoprotein reductase (cytochrome P450 reductase)	FMN	Flavoprotein (flavodoxin_1)	POR	7q11.23
44	1.6.5.2	NAD(P)H dehydrogenase (quinone)	FAD	FAD_Lum_binding (FAD_binding_1)	NQO1	16q22.1
45	1.6.5.3	NADH-ubiquinone oxidoreductase of complex I, subunit UQOR1	FMN	Flavoprotein (Flavodoxin_2)	NDUFB1	11q13.2
46	1.6.-.-	NADPH-dep. diflavin oxidoreductase 1	FMN	complex I_51K	NDOR1	9q34.3
47	1.6.-.-	tRNA dihydrouridine synthase	FAD	FAD_Lum_binding (FAD_binding_1)	DUSZL	16q22.1
48	1.8.1.4	Dihydropyridine synthase	FMN	TIM_barrel (Dus)	DLID	7q31.1
49	1.8.1.7	Dihydropyridinyl dehydrogenase	FAD	NADP_Rossmann (Pyr_redox_2)	GSR	8p12
50	1.8.1.9	Glutathione-disulfide reductase	FAD	NADP_Rossmann (Pyr_redox_2)	TXNR1	12q23.3
		Thioredoxin-disulfide reductase	FAD	NADP_Rossmann (Pyr_redox_2)	TXNR2	22q11.21
51	1.8.1.-	ER flavoprotein associated with degr.	FAD	---	FOXRED2	3q21.3
52	1.8.3.2	Sulfhydryl oxidase	FAD	---	GFER	22q12.3
53	1.8.3.5	Prénylcysteine oxidase	FAD	ErV1_Alr	PCYOX1	16p13.3
54	1.10.99.2	Ribosylidihydrocotinamide dehydrogenase	FAD	Flavoprotein (Flavodoxin_2)	NQO2	6p25.2
55	1.14.13.8	Flavin-containing monoxygenases	FAD	---	FMO1	1q24.3
				---	FMO2	1q24.3
				---	FMO3	1q24.3
				---	FMO4	1q24.3
				---	FMO5	1q21.1
56	1.14.13.9	Kynurenine 3-monoxygenase	FAD	---	KMO	1q43
57	1.14.13.39	Nitric-oxide synthase	FMN	Flavoprotein (Flavodoxin_1)	NOS1	12q24.22
			FAD	FAD_Lum_binding (FAD_binding_1)	NOS2	17q11.2
				---	NOS3	7q36.1
58	1.14.13.132	Squalene monoxygenase	FAD	---	SQLE	8q24.13
59	1.14.99.-	Monoxygenase in coenzyme Q biosyn.	FAD?	---	COQ6	14q24.3
60	1.16.1.2	Ferrereductase (biliverdin IX beta red.)	FMN?	N-terminal domain (1-215)	STEAP3	2q14.2
61	1.16.1.8	Methionine synthase reductase	FMN	Flavoprotein (Flavodoxin_1)	MTRR	5p15.31
62	1.18.1.2	Ferredoxin-NADP ⁺ reductase	FAD	FAD_Lum_binding (FAD_binding_1)	FDXR	17q25.1
63	1.-.-.-	NAD(P)H oxidase cytochrome b(558), beta subunit	FAD	FAD_Lum_binding (FAD_binding_6)	CYBB	Xp11.4
64	1.-.-.-	Thyroid oxidase / dual oxidase	FAD	---	DUOX1	15q21.1
				---	DUOX2	15q21.1
65	2.2.1.6	Acetolactate synthase-like protein	FAD?	---	-	19p13.12
66	2.5.1.26	Alkyldihydroacetone phosphate synthase	FAD	FAD_PCMH (FAD_binding_4)	AGPS	2q31.2
67	4.1.1.36	4-Phosphopantothonylcysteine decarboxylase	FMN	Flavoprotein	PPCDC	15q24.2
68	4.1.99.3	Cryptochrome	FAD	FAD-binding of DNA-photolyase (FAD_binding_7)	CRY1	12q23.3
				---	CRY2	11p11.2
69	---	Apoptosis inducing protein	FAD	NADP_Rossmann (Pyr_redox_2)	AIFM1	Xq26.1
70	---	Apoptosis inducing protein	6-OH-FAD	NADP_Rossmann (Pyr_redox_2)	AIFM2	10q22.1
71	---	Iodotyrosine deiodinase	FMN	Nitroreductase	IYD	6q25.1
72	---	Axon guidance protein	FAD	NADP_Rossmann (FAD_binding_3)	MICAL1	6q21
				---	MICAL2	11p15.3
				---	MICAL3	22q11.21
73	---	FAD-dependent oxidoreductase (molecular chaperone of complex 1)	FAD	---	FOXRED1	11q24.2
74	---	Riboflavin transporter	Riboflavin ^c	---	SIC52A1	17p13.2
				---	SIC52A2	8q24.3
				---	SIC52A3	20p13
75	1.5.1.30	Riboflavin / FMN reductase	FMN ^c	NADP_Rossmann (NmrA-like)	BLVRB	19q13.2
76	2.7.1.26	Riboflavin Kinase	riboflavin ^c	Flavokinase	RFK	9q21.13
77	2.7.7.2	FAD-adenylyl transferase (synthetase)	FMN ^c	HUP (PAPS_reduct)	FLAD1	1q21.3

Abbreviations used: biosyn., biosynthesis; dh, dehydrogenase; degr., degradation; dep., dependent; ER, endoplasmic reticulum; red., reductase.

^a Pfam classification given in plain text is for the structure of human proteins and those in italics for structures of homologs.^b Duplicated pseudogene.^c Opposite orientation on chromosome.^d Substrate of transporter, modifying enzyme or reductase (entries 74–77).

Table 2
Disease-related human flavoproteins.

No.	E.C.	Enzyme	Disease	Metabolic function	Localisation	OMIM
1	1.1.1.204	Xanthine dehydrogenase	Xanthinuria type I	Purine degr.	Cytosol	607633
2	1.1.5.3	Glycerol 3-phosphate dehydrogenase	<i>Diabetes mellitus</i> type II	Electron transport	mito. i. membr.	138430
3	1.1.99.1	Choline dehydrogenase	tooth agenesis, cleft lip sperm motility	Choline degr.	mito. i. membr.	[78– 82]
4	1.1.99.2	L-2-Hydroxyglutarate dehydrogenase	L-2-Hydroxyglutaric aciduria	“Metabolite repair”	mito. membr.	609584
5	1.1.99.-	D-2-Hydroxyglutarate dehydrogenase	D-2-Hydroxyglutaric aciduria	“Metabolite repair”	Mitochondria	605176
6	1.3.1.2	Dihydropyrimidine dehydrogenase	Deficiency	Pyrimidine catab.	Cytosol	612779
7	1.3.1.72	3 β -Hydroxysterol Δ^{24} -reductase	Desmosterolosis	Sterol biosyn.	ER membr.	606418
8	1.3.3.1	Dihydroorotate dehydrogenase	Miller syn.	Please specify the significance of footnote “a” cited in the Table 2, as a corresponding footnote text has not been provided.	mito. i. membr.	126064
9	1.3.3.4	Protoporphyrinogen IX oxidase	Variegate porphyria	Heme biosyn.	Mito. i. membr.	600923
10	1.3.3.6	Acyl-CoA oxidase	Deficiency	Lipid degr.	Peroxisomes	609751
11	1.3.3.-	Glutaryl-CoA oxidase	Glutaric aciduria III	Glutaryl degr.	Peroxisomes	231690
12	1.3.5.1	Succinate dehydrogenase	Complex II deficiency	Citric acid cycle	mito. i. membr.	600857
		Flavoprotein subunit A	Leigh syn. paraganglioma 5			
13	1.3.99.2	Short-chain- (butyryl-) acyl CoA dehydrogenase	Deficiency	β -Oxidation	mito. matrix	201470
14	1.3.99.3	Medium-chain acyl-CoA dehydrogenase	Deficiency	β -Oxidation	mito. matrix	607008
15	1.3.99.7	Glutaryl-CoA dehydrogenase	Glutaric acidemia	Lysine degr.	mito. matrix	608801
16	1.3.99.10	Isovaleryl-CoA dehydrogenase	Isovaleric acidemia	Leucine degr.	mito. matrix	607036
17	1.3.99.12	2-Methylbutyryl-CoA dehydrogenase	Deficiency	Isoleucine degr.	mito. matrix	600301
18	1.3.99.13	Long-chain-acyl-CoA dehydrogenase	Deficiency	β -Oxidation	mito. matrix	609576
19	1.3.99.-	Isobutyryl-CoA dehydrogenase	Deficiency	Valine degr.	mito. matrix	611283
20	1.3.99.-	Long-chain-unsaturated-acyl-CoA dehydrogenase	Deficiency	β -Oxidation	mito. matrix	611126
21	1.3.99.-	very long-chain acyl-CoA dehydrogenase	Deficiency	β -oxidation	mito. matrix	201475
22	1.4.3.3	D-amino acid oxidase	Schizophrenia? amyotrophic lateral sclerosis	Oxidation of D-serine	Peroxisomes	124050
23	1.4.3.4	Monoamine oxidase	Brunner syn. antisocial behaviour autism	Oxidation of neuro-transmitter	mito. o. membr.	309850
24	1.4.3.5	Pyridoxal 5'-phosphate oxidase Pyridoxine 5'-phosphate oxidase	Encephalopathy	Vitamin B ₆ metab.	Cytosol	603287
25	1.4.3.-	Catecholamine oxidase (renalase)	Hypertension?	Oxidation	Secreted (Blood)	609360
26	1.5.1.20	Methylenetetrahydrofolate reductase	Homocystinuria neural tube defects schizophrenia	Folate metab.	Cytosol	607093
27	1.5.5.1	Electron-transferring flavoprotein-ubiquinone oxidoreductase	Glutaric acidemia IIC	Electron transport	mito. i. membr.	231675
28	-----	Electron transferring flavoprotein	Glutaric acidemia IIA	Electron transport	mito. matrix	608053
29	1.5.99.1	Sarcosine dehydrogenase	Glutaric acidemia IIB Sarcosinemia	Electron transport Choline degr.	mito. matrix	130410 604455
30	1.5.99.2	Dimethylglycine dehydrogenase	DMGDH-deficiency	Choline degr.	mito. matrix	605850
31	1.5.99.8	Proline dehydrogenase	Hyperprolinemia type I schizophrenia	Amino acid metab.		606810
32	1.6.2.2	Cytochrome-b5 reductase	Methemoglobinemia type I and II	Heme metab.	membr. soluble (erythro.)	613213
33	1.6.2.4	NADPH-hemoprotein reductase (cytochrome P450 reductase)	Antley-Bixler syn. Disordered steroidogenesis	Electron donor to P450 enzymes	Microsomes (ER)	124015
34	1.6.5.2	NAD(P)H dehydrogenase (quinone)	Benzene toxicity breast cancer	Quinone detox p53 degr.	Cytosol	125860

(continued on next page)

Table 2 (continued)

No.	E.C.	Enzyme	Disease	Metabolic function	Localisation	OMIM
35	1.6.5.3	NADH-ubiquinone oxidoreductase	Complex I deficiency	Electron transport	mito. i. membr.	161015
36	1.8.1.4	Dihydrolipoyl dehydrogenase	Leigh syn. Maple syrup urine dis., III	Energy metab.	mito. matrix	238331
37	1.8.1.7	Glutathione-disulfide reductase	Hemolytic anemia	detox.	Cytosol (erythro.)	138300
38	1.8.3.2	Sulfhydryl oxidase	Myopathy	Disulfide redox balance	mito. im. space	600924
39	1.10.99.2	Ribosylidihydroxynicotinamide dehydrogenase	Breast cancer susceptibility	Quinone detox.	Cytosol	160998
40	1.14.13.8	flavin-containing monooxygenases	trimethylaminuria	detox.	microsomes (ER)	136132
41	1.14.13.39	Nitric-oxide synthase	Hypertension	Vasodilation	Cytosol	163729 163730
42	1.14.99.-	Monooxygenase in coenzyme Q biosyn.	Deficiency/nephrotic syn.	Coenzyme Q biosyn.	Golgi/mito.	614647
43	1.16.1.8	Methionine synthase reductase	Homocystinuria neural tube defects	Methionine biosyn.	Cytosol	602568
44	1.-.-.	NAD(P)H oxidase	Chronic granulomatous dis.	Generation of superoxide	Phagocytes	300481
		Cytochrome b(558), beta subunit	Atypical mycobacteriosis		(membr.)	
45	1.-.-.	Thyroid oxidase/dual oxidase	Thyroid dishormonogenesis 6	Thyroid biosyn.	membr.	606759
46	2.5.1.26	Alkylidihydroxyacetone phosphate synthase	Rhizomelic chondrodysplasia punctata, type 3	Lipid biosyn.	Peroxisomes	603051
47	-----	Apoptosis inducing protein	Combined oxidative phosphorylation deficiency	Redox control	mito./nucleus	300169
48	-----	Iodotyrosine deiodinase	Thyroid dishormonogenesis type 4	Iodide salvage	Cytosol	612025
49	-----	FAD-dependent oxidoreductase	complex I deficiency Leigh syn.	Molecular chaperone	mito. matrix	613622
50	-----	Riboflavin transporter (member 3)	Brown-Vialetto-Van Laere syn. Fazio-Londe dis.	Riboflavin uptake	membr.	613350

Abbreviations used: biosyn., biosynthesis; catab., catabolism; degr., degradation; detox., detoxification; dim., diminished; dis., disease; metabol., metabolism; mito., mitochondrium; mito. i. membr., inner membrane of mitochondria; mito. o. membr., outer membrane of mitochondria; mito. im. space, mitochondrial intermembrane space; ER, endoplasmic reticulum; membr., membrane; syn., syndrome; erythro., erythrocytes.

Most flavoenzymes bind FMN or FAD non-covalently (90%). In six human flavoenzymes the FAD cofactor is covalently linked via the 8- α -methyl group to either the nitrogen (N-3) of a histidine (succinate, sarcosine and dimethylglycine dehydrogenase) or the sulfur of a cysteine residue (MAOA, MAOB and L-pipecolate oxidase). Interestingly, monocovalent attachment to the 6-position of the isoalloxazine ring system as well as bicovalent attachment to the 8- α and 6-position observed in several bacterial, fungal and plant flavoenzymes are absent in human flavoproteins. This is also reflected by the scarcity of flavoenzymes adopting a topology similar to the *p*-cresolmethylhydroxylase (clan FAD_PCMH, family FAD_binding_4) with D-lactate dehydrogenase (EC 1.1.1.28) and alkalidihydroxyacetone phosphate synthase (EC 2.5.1.26) as sole examples for this type of structure. Interestingly, these two enzymes represent a subset of flavoenzymes in this clan that does not engage in covalent linkage of the FAD cofactor, which in fact appears to be the rule rather than the exception in this structure family [2]. Overall, it is encouraging that the structure of more than half of the human flavoproteins was solved by X-ray crystallography (Table 1). In addition, in 23 cases the structure of the human protein can be inferred from the known structure of a homologous flavoprotein. This leaves only fifteen flavoproteins where currently no structural information is available (Table 1). The prevalence of the Rossmann-fold in FAD-dependent flavoenzymes previously noted [2] is also seen in the human FAD-dependent proteins (see Fig. S1). In contrast to the global fold distribution the structural clan Acyl-CoA_dh takes second place

and switches place with the clan FAD_PCMH. This is due to the relatively large number of acyl-CoA dehydrogenases (eleven) and acyl-CoA oxidases (three) compared to only three members in the FAD_PCMH clan. Flavoenzymes in the latter clan appear to be rare in mammals but are very prominent in metabolically active and diverse organisms such as bacteria, fungi and plants [2]. The most common structural clan found for human FMN-dependent proteins is Flavoprotein and TIM_barrel (five and four members, respectively, see Fig. S1) and reflects the general prevalence of these two clans in FMN-dependent flavoproteins [2].

The chromosomal location of the genes encoding flavoproteins is known for all flavoproteins (Table 1 and Fig. S2). They are uniformly distributed over the chromosomes with only chromosome 13, 18, 21 and Y lacking genes encoding flavoproteins (Table 1 and Fig. S2). Eleven flavoenzymes occur as isoforms encoded by multiple genes (2–5). In three cases (DUOX1–2, FMO1–5 and MAOA + B) the genes are on the same chromosome (15, 1 and X, respectively) whereas in all other cases (ACOX1–3, CRY1–2, HAO1–2, MICAL1–3, NOS1–3 and SLC52A1–3) the genes are on different chromosomes (Fig. S2).

Flavoenzymes in human diseases

A surprisingly large number of flavoproteins (ca. 60%) is associated with human disorders caused by mutations in the pertinent gene. Table 2 provides an overview of the 50 flavoproteins along

with their corresponding record number in OMIM. Since most flavoproteins are localized in the mitochondria the diseases are connected with deficiencies in mitochondrial processes. Other compartments, most notably peroxisomes and the endoplasmic reticulum, are also affected by some flavoprotein deficiencies or dysfunctions. In several cases flavoprotein deficiencies occur in connected metabolic pathways and therefore give rise to similar clinical manifestations. For example, glutaric acidemia (OMIM 608801) can be caused by a deficiency of glutaryl-CoA dehydrogenase (type I), electron transferring flavoprotein (type IIA and IIB) or electron-transferring flavoprotein-ubiquinone oxidoreductase (type IIC). Similarly, Leigh syndrome (OMIM 256000) may arise from a defect in any of the respiratory electron transfer complexes in the inner mitochondrial membrane and thus deficiency of complex I (containing the FMN-dependent NDUFV1) or complex II (containing the FAD-dependent subunit A) as well as FOXRED1, an FAD-containing molecular chaperone of complex I, may constitute the molecular cause of the disease.

Since mutations are generally irreversible, adverse effects on the biological function of an encoded protein are untreatable and therapeutic interventions rely on protein substitution or, in the future, gene therapy. For several flavoproteins it was found that the mutation led to an amino acid exchange affecting the binding affinity of the flavin cofactor. In these cases it is conceivable that high-dose riboflavin supplementation may increase the concentration of flavin cofactors and this in turn may increase the fraction of active holo-enzyme. Ames and coworkers have compiled a list of flavoenzymes with decreased cofactor affinity where this strategy may be exploited successfully [3]. Among the flavoenzymes discussed are *N*-5,10-methylenetetrahydrofolate reductase (EC 1.5.1.20, MTHFR), NAD(P):quinone oxidoreductase (EC 1.6.5.2, NQO1), protoporphyrinogen IX oxidase (EC 1.3.3.4, PPOX), electron transferring flavoprotein (ETF), electron-transferring flavoprotein ubiquinone oxidoreductase (EC 1.5.5.1, ETFDH), glutaryl-CoA oxidase (EC 1.3.3.-, C7orf10), short-, medium-, long-chain acyl-CoA dehydrogenases (EC 1.3.99.2, ACADS; EC 1.3.99.3, ACADM; EC 1.3.99.13, ACADL) and complex I (EC 1.6.5.3, NDUFV1) [3]. More recently, it was shown that the neurological disorders Brown-Vialetto-Van Laere and Fazio-Londe syndrome were caused by mutations in the gene encoding an intestinal riboflavin transporter [4,5]. Since this transporter is largely unexplored, the effect of the mutation on riboflavin transport efficiency is currently unknown. However, it appears that at least in some patients riboflavin supplementation ameliorates the symptoms and positively affects disease progression [4,6,7]. Apart from a few flavoproteins with decreased affinity for cofactor mentioned by Ames and coworkers [3] it is largely unknown how mutations in genes encoding flavoproteins impact cofactor binding. In view of the large number of flavoproteins involved in human diseases it is worthwhile investigating the mutational effects on cofactor binding to thoroughly evaluate the benefits of high-dose riboflavin supplementation therapy (see also discussion below).

Flavoenzymes in cofactor biogenesis and metabolism

FMN and FAD are synthesized in the human organism from riboflavin (vitamin B₂) by riboflavin kinase (EC 2.7.1.26) and FAD-adenylyl transferase (EC 2.7.7.2). Riboflavin is absorbed from nutrients as is the case for many other vitamins required to supply vitamin-derived coenzymes to the apo-forms of hundreds of enzymes in the human body. In this context, we were intrigued by the number of flavoenzymes that are involved in the biosynthesis of other cofactors such as coenzyme A, coenzyme Q (ubiquinone), heme and pyridoxal 5'-phosphate. Equally, flavoenzymes participate in the interconversion of various folate metabolites and hence

play an important role in one-carbon (C1-unit) metabolism. Moreover, flavoenzymes catalyze essential reactions in biosynthetic pathways leading to cell signaling molecules such as the steroid and thyroid hormones. These topics are discussed in more depths in the next sections.

Flavoenzymes in folate and cobalamin metabolism

Tetrahydrofolate (THF) is a 6-methylpterin derivative that is widely used to shuttle C1-units in metabolic reactions. THF loaded with a C1-unit occurs in various oxidation states such as *N*-5,10-methylene-THF and *N*-5-methyl-THF. Two FAD-dependent enzymes, dimethylglycine dehydrogenase (EC 1.5.99.2, DMGDH) and sarcosine dehydrogenase (EC 1.5.99.1, SARDH), generate *N*-5,10-methylene-THF from THF which is then converted to *N*-5-methyl-THF by *N*-5,10-methylene-THF reductase (EC 1.5.1.20, MTHFR) at the expense of NADPH (Fig. 1). *N*-5-methyl-THF in turn is utilized by methionine synthase (EC 2.1.1.13, MS) yielding THF and methionine by transferring the methyl group to homocysteine. The cobalamin cofactor of MS is susceptible to oxidation and hence methionine synthase reductase (EC 1.16.1.8, MSR) is required to regenerate methylcob(I)alamin from cob(II)alamin. Hence, these four flavin-dependent enzymes play a role in the inter conversion of THF, *N*-5,10-methylene-THF and *N*-5-methyl-THF and are thus important to balance the pools of folate metabolites (Fig. 1).

DMGDH and SARDH also catalyze two consecutive reactions in choline catabolism (Fig. 1). DMGDH oxidizes dimethylglycine to sarcosine, which is further oxidized to glycine. Both enzymes use THF to capture the C-1 fragment released by the oxidative demethylation of substrates yielding *N*-5,10-methylene-THF [8]. Since these reactions occur in the mitochondrial matrix, electrons extracted from the substrate are delivered to the mitochondrial electron transport chain via electron transferring flavoprotein (ETF) and electron transferring flavoprotein ubiquinone oxidoreductase (EC 1.5.5.1). DMGDH and SARDH were reported to contain a covalently linked 8 α -(N3-His)-FAD cofactor [9,10] and hence belong to the small group of flavoproteins that bind the cofactor covalently (see Table 1). Unfortunately, the structure of these proteins is not known and therefore neither the mode of FAD binding nor the interaction with THF can be firmly established. Interestingly, a recently discovered lysine-specific histone demethylase (EC 1.5.99.-, KDM1A) related to flavin-dependent amine oxidases apparently does not utilize THF to capture the formyl group and hence the demethylation results in the generation of formaldehyde [11]. Since the lysine demethylation occurs in the nucleus and not in mitochondria, the enzyme donates the electrons to oxygen generating hydrogen peroxide as a by-product of the demethylation reaction. The fate of these two potentially harmful compounds in the nucleus is currently not known. A recent study showed that inhibitors of KDM1A selectively target cancer cells with pluripotent stem cell properties [12]. In light of these recent findings it can be concluded that aberrations in KDM1A regulation might lead to development of cancer.

Deficiency of DMGDH is apparently very rare and only a single case was reported so far (OMIM 605850, [13,14]). Binzak et al. identified a homozygous point mutation in a patient (326 A-G) resulting in a histidine to arginine exchange (H109R) in the encoded DMGDH [13]. It is noteworthy that the covalent linkage of the FAD cofactor is to H91 and hence the inactivity of the altered enzyme is probably not due to the inability to form the covalent linkage with the FAD cofactor. Detailed studies with the recombinant DMGDH H109R variant showed effects on both the specific activity (27 times lower) and *K_m* (65 times higher) [15]. Interestingly, fish odor was reported as a salient symptom of DMGDH deficiency which is typically ascribed to impaired *N*-oxygenation of

xenobiotics due to deficiency of flavin-containing monooxygenase isoform 3 (EC 1.14.13.8, FMO3) [16].

Sarcosinemia caused by a deficiency of SARDH [17] is also a rare metabolic disorder characterized by elevated levels of sarcosine in plasma and urine. The mutational frequency in the human SARDH gene apparently varies from 1:350000 to 1:3414. The clinical symptoms reported to be associated with SARDH deficiency include mental retardation and loss of speech (OMIM 268900). Recently, sarcosine was suggested to be a marker for the invasiveness of prostate cancer cell lines [18]. In the same study, it was also noted that reduced levels of SARDH activity led to the induction of an invasive phenotype in benign prostate epithelial cells. The connection of SARDH to cancer development and progression indicated by this study and the usefulness of sarcosine as a tumor marker is currently the subject of an intense scientific debate [19–21].

MTHFR connects the pool of *N*-5,10-methylene-THF, mainly derived from the glycine cleavage system (EC 2.1.2.10) and serine hydroxymethyltransferase (EC 2.1.2.1), with that of *N*-5-methyl-THF, which is used by MS to generate methionine from homocysteine (Fig. 1). This reaction not only provides an important building block for protein biosynthesis but also a substrate for the synthesis of *S*-adenosyl-methionine (SAM), an ubiquitous and powerful reagent in many biological methylation reactions. The MS reaction also regenerates THF, which then re-enters the reactions mentioned above capturing C1-units from glycine, serine, dimethylglycine and sarcosine. More than thirty deleterious mutations of the *MTHFR* gene are known as well as several common variants, like the 677C>T point mutation. *MTHFR* deficiency is connected to several serious diseases, such as neural tube defects, coronary heart disease and schizophrenia (OMIM 607093). Depending on the severity of the mutation hyperhomocysteinemia with homocystinuria or mild hyperhomocysteinemia is observed. The 677C>T polymorphism is of particular interest as it is recognized as the

most frequent genetic cause of homocysteinemia [22,23]. This common C to T mutation gives rise to a conservative amino acid replacement in position 222 of *MTHFR* (A222V). Surprisingly, the A222V variant possesses reduced thermostability and weaker affinity to the FAD cofactor. In the same study it was also reported that folate (and adenosylmethionine) increases the affinity of FAD, which in turn increases the thermostability of the A222V variant [24]. This positive interplay suggests that the status of folate and riboflavin may be critical in cases where cofactor affinity is compromised by the amino acid exchange (see discussion above).

Mechanistically, MS uses *N*-5-methyl-THF to methylate its cob(I)alamin cofactor which in turn transfers the methyl group to the thiol group of homocysteine (Fig. 1). The cob(I)alamin state is highly sensitive to oxidation rendering the enzyme inactive [25]. In order to restore the reduced active form of the cofactor, cob(II)alamin is reductively methylated by MSR using NADPH as electron source and SAM as methyl group donor [26,27]. Since MSR is required to maintain MS activity, it is not surprising that allelic variants resulting in MSR deficiency present similar symptoms, such as homocystinuria, as seen in MS and *MTHFR* deficiency. Accordingly, megaloblastic anemia, an increased risk for neural tube defect and Down syndrome are among the disorders caused by inherited MSR deficiency (OMIM 602568). A common polymorphism found in the MSR gene (allele frequency 0.51) results in a single amino acid replacement, I23M, and increases the risk for neural tube defects [25,28].

Recently, Matthews and coworkers suggested that MSR also plays a role as a chaperone for MS and also acts as an aquacobalamin reductase [29]. They reported that MSR stabilizes the apoform of MS and promotes the association with methylcobalamin. In addition, MSR catalyzes the NADPH-dependent reduction of aquacobalamin to cob(II)alamin and thereby accelerates the formation of holo-MS. Hence, MSR exhibits multiple beneficial effects on MS. In this context, it is interesting to note that MSR was also

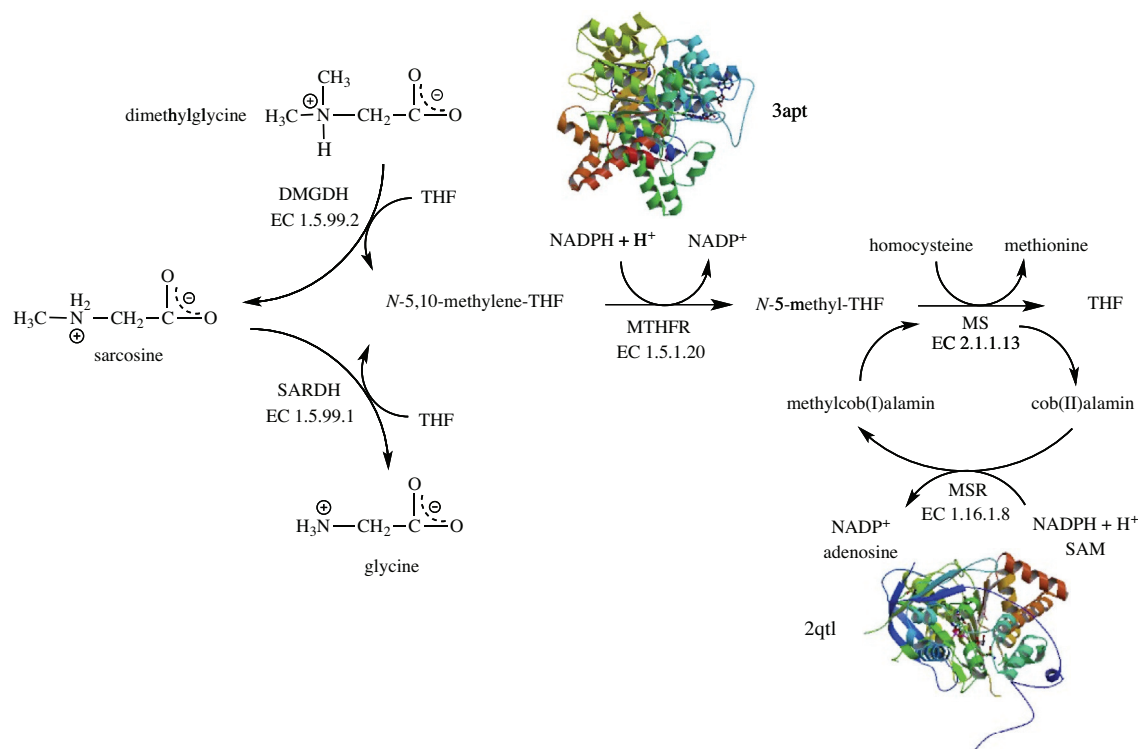


Fig. 1. Flavin-catalyzed reactions connected to folate metabolism: dimethylglycine dehydrogenase (EC 1.5.99.1, DMGDH), sarcosine dehydrogenase (EC 1.5.99.2, SARDH), *N*-5,10-methylene-tetrahydrofolate reductase (EC 1.5.1.20, MTHFR) and methionine synthase reductase (EC 1.16.1.8, MSR). Structures depicted are from the human methionine synthase reductase (2qtl) as well as the *N*-5,10-methylene-tetrahydrofolate reductase from *Thermus thermophilus* HB8 (3apt).

invoked as catalyst for the formation of adenosylcobalamin [25,30]. Recent evidence, however, suggests that reduction of Co^{2+} to Co^+ occurs by free dihydroflavins when cob(II)alamin is bound to human adenosyltransferase [31]. It is currently unknown whether this process is driven solely by free dihydroflavins or involves a specialized flavoprotein reductase *in vivo*.

Heme biosynthesis

The biosynthesis of heme from succinyl-CoA and glycine is initiated in the mitochondria and then proceeds in the cytosol to generate coproporphyrinogen III. This intermediate is transported back into mitochondria to complete the oxidation of the macrocycle by the FAD-dependent protoporphyrinogen IX oxidase (EC 1.3.3.4, PPOX). This reaction involves the six-electron oxidation of the methylene groups linking the pyrrole rings to methenyl groups thereby generating an extensively conjugated π -electron system (Fig. 2). As the isoalloxazine ring system can only handle two electrons at a time, the cofactor needs to run three times through the catalytic cycle of flavin reduction and reoxidation to complete the oxidation of protoporphyrinogen IX to protoporphyrin IX. This catalytic cycling was suggested to proceed by substrate oxidation and release of the dihydro- and tetrahydro-intermediates rather than continuous processing of a constantly bound substrate [32]. PPOX is located in the inner mitochondrial membrane and anchored by acylation to the leaflet oriented towards the intermembrane space [33,34]. Diminished PPOX activity results in variegate porphyria (VP), which belongs to a group of metabolic disturbances caused by genetic defects affecting heme biosynthesis (collectively called as *porphyrias*). Symptoms of autosomal dominant VP include acute abdominal pain, neurological manifestations and/or cutaneous photosensitivity [35]. Apparently, the disease is characterized by severe, sometimes life-threatening, crisis triggered by external factors (*e.g.* medication, toxins) [36]. Perhaps the most controversial case of VP was postulated for King George III (1738–1820) who suffered long episodes of mental and physical illness culminating in the Regency crisis (1788–1789). According to Macalpine & Hunter, King George III was afflicted by VP, a claim supported by several pieces of evidence collected on ancestors and descendants [37,38]. More recently, Cox et al. suggested that high concentrations of arsenic in the medication administered to the king may have triggered the episodes of VP [39].

The structure of the human enzyme was solved to 1.9 Å resolution (pdb code 3nks). Forty-seven variants of PPOX that were found to cause VP in humans were heterologously expressed in *Escherichia coli* and the properties of the variants studied *in vitro* [40]. Based on the observed effects and the locus of the amino acid in the structure of the enzyme the authors of that study classified

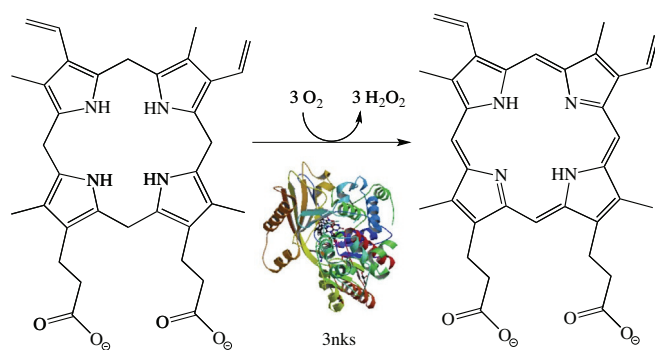


Fig. 2. The penultimate reaction in heme biosynthesis involves the six-electron oxidation of protoporphyrinogen-IX to protoporphyrin-IX by the FAD-dependent protoporphyrinogen-IX oxidase (EC 1.3.3.4, PPOX) (human structure: 3nks).

the variants according to their proposed effect on either FAD- or substrate binding or structural alterations of the protein. Interestingly, the Human Gene Mutation Database (www.hgmd.cf.ac.uk) lists more than 130 mutations, which appear to be uniformly distributed over the entire length of the gene and concern invariant amino acids as well as regions of variability.

Pyridoxal 5'-phosphate biosynthesis

Pyridoxal 5'-phosphate (PLP) serves as a cofactor in more than 140 distinct enzymatic activities and is arguably one of the most utilized vitamin in nature. According to a recent analysis, the human genome contains 68 genes encoding proteins with a structural fold typical for PLP-dependent enzymes [41]. Although functional assignment of these enzymes was not possible in all cases (14 remained unassigned) this result indicates that the supply of PLP is critical for the maintenance of numerous metabolic activities especially in pathways involving biochemical transformations of amino acids, *e.g.* PLP-dependent decarboxylations of amino acids to generate active amines and neurotransmitters. In humans, PLP is mainly generated by enzymatic phosphorylation and oxidation of pyridoxine and pyridoxamine. These two vitamers are available either from nutritional sources or are produced in the course of the degradation of PLP-containing enzymes. In the first step, they are phosphorylated by pyridoxal kinase and then oxidized by pyridoxine 5'-phosphate oxidase (EC 1.4.3.5, PNPO) to the active cofactor PLP (Fig. 3). The three-dimensional structures of the enzyme from several bacteria as well as the recombinant human enzyme were determined by X-ray crystallography ([42], pdb code 1nrg). Interestingly, the structure of the *E. coli* enzyme features two PLP binding sites, one in the active site near the flavin's isoalloxazine ring and a second closer to the surface of the dimeric protein ([43], pdb code 1g79). It is currently unclear whether the latter binding site is identical to the tight binding site identified by functional studies [43]. The human enzyme (261 amino acids) presumably also features a second tight binding site for PLP, however its exact location is currently not known [44]. Di Salvo et al. suggested that this second tight binding site might serve as transient storage for PLP, which is channeled to the apo-forms of PLP-dependent enzymes [44]. In support of this hypothesis, these authors reported that PNPO from *E. coli* interacts with several apo-forms of PLP-dependent enzymes with dissociation constants in the micromolar range (0.3–56 μM ; [44]). Although this appears to be an attractive process for the delivery of PLP to its target enzymes, it is unlikely that this is applicable to all human PLP-dependent enzymes because it would require a common docking site between the single PNPO and the 68 predicted enzymes. On the other hand, PNPO's cytosolic localization would enable the enzyme to deliver PLP directly to the apo-form of PLP-dependent enzymes *in statu nascendi*.

Several allelic variants of the PNPO gene were described (OMIM 603287). The reported mutations either lead to premature termination of protein biosynthesis (at position 174 [45]), extension of the protein by 28 amino acids (X262N) or splicing errors due to a mutation in intron 3 [46]. In addition, Mills et al., reported a point mutation in the PNPO gene resulting in the substitution of arginine in position 229 with tryptophan [46]. This R229W variant was recombinantly expressed and characterized by Musayev et al. [47]. They found that this variant is substantially compromised in its catalytic efficiency (*ca.* 850-fold) due to weaker binding of the substrate and decreased catalytic activity. Moreover, FMN possessed a 50-fold reduced affinity to the variant (see discussion above). These effects could be rationalized based on the involvement of the arginine residue in organizing important interactions in the active site of the enzyme. All of the reported mutations caused severe deficiency of PNPO activity resulting in neonatal epileptic encephalopathy. This disorder has a very poor prognosis

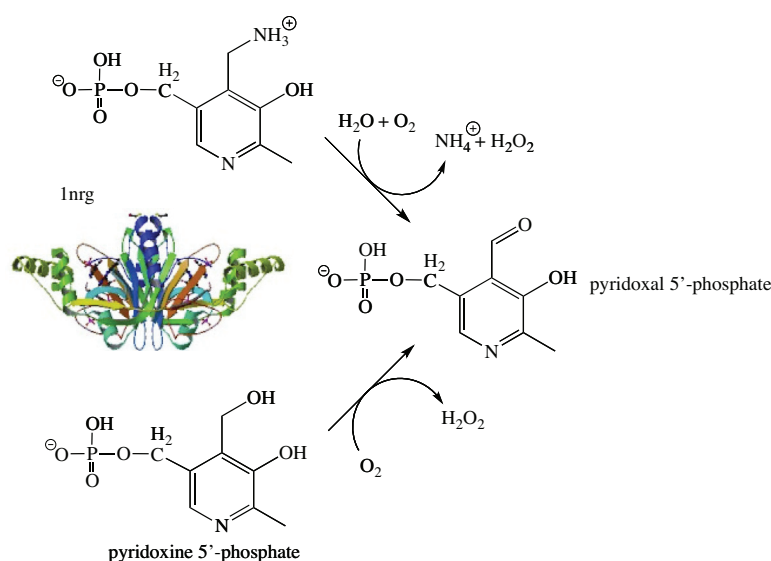


Fig. 3. Oxidation of pyridoxamine and pyridoxine 5'-phosphate to pyridoxal 5'-phosphate by the FMN-dependent pyridoxamine/pyridoxine 5'-phosphate oxidase (EC 1.4.3.5, PNPO), the last step of the PLP-biosynthesis. The structure shown is that of the human enzyme (1nrg).

postnatally and surviving children typically suffer from mental retardation.

PNPO expression in humans is prevalent in liver and kidney with most other tissues (brain, heart, muscle) having clearly reduced levels of mRNA [48]. Interestingly, abnormally low levels of PNPO activity were reported for some neoplastic cell lines, e.g. liver and neurally-derived tumors [49]. Whether and how these low PNPO activities are connected to tumorigenesis remains to be investigated.

Coenzyme A biosynthesis

Coenzyme A (CoA) biosynthesis from pantothenic acid (vitamin B₅) is a five-step enzymatic process. The third reaction in this universal reaction sequence is the decarboxylation of phosphopantothienylcysteine to 4'-phosphopantetheine by phosphopantothienylcysteine decarboxylase (EC 4.1.1.36; PPCD) as shown in Fig. 4 [50]. The structure of the human enzyme shows a non-covalently bound FMN per protomer of the trimeric protein [51]. In eukaryotes PPCD occurs as a monofunctional enzyme whereas in most bacteria – with the exception of streptococci and enterococci – PPCD is fused with phosphopantothienylcysteine synthase (PPCS) the second enzyme of CoA biosynthesis [50]. In contrast to the reactions described above, the decarboxylation does not involve a net redox change. PPCD is one of the few examples where the flavin is not used for a reduction–oxidation reaction in a human flavoprotein (Table 1, entry #67). However, the flavin apparently plays a role as a transient electron acceptor during the reaction involving the transfer of charge from the substrate thiolate group to the isoalloxazine ring [52]. Currently, the OMIM database does not list any diseases related to a deficiency of PPCD. This may be partly due to the fact that approximately 4% of all enzymes utilize substrates linked to coenzyme A (e.g. acyl-CoAs) [53] and hence a deficiency in coenzyme A seriously compromises the viability of cells. This notion is supported by the fact that only the initial enzyme of coenzyme A biosynthesis, pantothenate kinase (EC 2.7.1.33, PANK), is linked to inherited diseases (OMIM 606157) but none of the other enzymes required. Interestingly, four isoforms of PANK were discovered in the human genome and therefore it appears likely that a deficiency of one isoform may be compensated at least partially by the others [54].

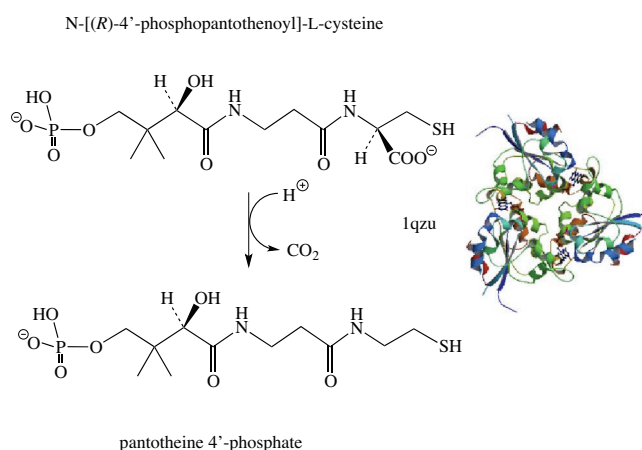


Fig. 4. Decarboxylation of N-[(R)-4'-phosphopantothienyl]-L-cysteine to pantotheine 4'-phosphate by the FMN-dependent 4'-phosphopantothienylcysteine decarboxylase (EC 4.1.1.36, PPCDC). The structure shown is that of the human enzyme (1qzu).

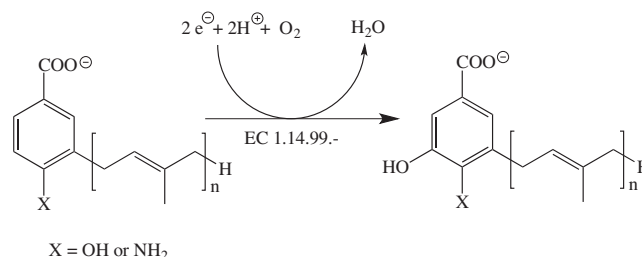


Fig. 5. Hydroxylation of the ubiquinone precursors in 5-position of the aromatic system by COQ6 (EC 1.14.99.-). In yeast, the electrons required for reduction of dioxygen are supplied by an NADPH-dependent ferredoxin reductase-ferredoxin system.

Coenzyme Q biosynthesis

Coenzyme Q or ubiquinone is an essential electron carrier in the mitochondrial electron transport chain shuttling electrons from complex I and II to complex III (see also section below). In contrast

to vitamin-derived coenzymes, ubiquinone is synthesized *de novo* from aromatic precursors such as *p*-hydroxybenzoic acid. In 2011, Pierrel and coworkers identified a FAD-dependent monooxygenase encoded by *coq6*, for the required hydroxylation in 5-position of a ubiquinone precursor in the yeast *Saccharomyces cerevisiae* (Fig. 5) [55]. A human homolog of *coq6* was recently discovered, which apparently catalyzes the hydroxylation in human ubiquinone biosynthesis (Table 1, entry #59) [56]. Flavin-dependent monooxygenases (hydroxylases) require a source of electrons for reduction of the flavin's isoalloxazine ring in order to enable the generation of hydroxylating 4a-hydroperoxy intermediates. Based on the mode of flavin reduction, internal and external monooxygenases are distinguished which either use NAD(P)H or NADH directly for reduction or rely on the activity of an external NAD(P)H/NADH:FAD reductase to supply the reduced flavin cofactor [57]. In the case of yeast Coq6p, reduction of FAD is accomplished by ferredoxin reductase (termed Arh1) and ferredoxin (termed Yah1) at the expense of NADPH and thus has the character of an external reduction mode. It is currently unknown whether the human enzyme is reduced by the same mechanism. The human ortholog of *coq6* was discovered in search of the genetic cause of nephrotic syndrome [56] and several reports of coenzyme Q deficiency are compiled in the OMIM (614647).

Steroid biosynthesis

Steroid hormones play fundamental roles in developmental programs and homeostatic processes. Cholesterol, a central precursor for the biosynthesis of steroid hormones, bile acids and vitamin D, is synthesized from acetyl-CoA via the mevalonate pathway in a multistep pathway [58]. A crucial step in the biosynthesis is the cyclisation of the linear 2,3-oxidosqualene to the first tetracyclic ring system, lanosterol. The preceding reaction, catalyzed by squalene monooxygenase (EC 1.14.13.132, SQLE), enables this cyclisation by epoxidation of the 2,3-carbon-carbon double bond (Fig. 6, top) [59]. The oxygen atom introduced by SQLE remains in the molecule during processing to the steroid target structures and is important for the physical (amphiphilic character) and chemical properties (formation of esters). Although SQLE does not appear to be linked to an inherited disease, it was suggested earlier that the gene encoding SQLE is a candidate for Langer-Giedion syndrome, which is associated with mental retardation and microcephaly [60]. Interestingly, SQLE became a focus as a

drug target for antimycotic compounds in the 1980s [61]. More recently it is also discussed as a potentially useful target in hypercholesterolemic therapy [62,63]. Currently, treatment of hypercholesterolemia is dominated by statins, which inhibit 3-hydroxy-3-methylglutaryl CoA (HMG-CoA) reductase (EC 1.1.1.34), a central and rate-limiting enzyme in the mevalonate pathway. A major drawback of HMG-reductase inhibition results from the adverse effects on the biosynthesis of non-steroidal isoprenoids (e.g. ubiquinone) since the enzyme catalyzes an “early” step in the pathway. To alleviate this problem steps occurring after the committing reaction of steroid biosynthesis, *i.e.* the synthesis of squalene from farnesylpyrophosphate catalyzed by squalene synthase (EC 2.5.1.21) might be potentially useful targets for the design of new cholesterol lowering compounds. Because SQLE is the next enzyme of this metabolic branch point it is a suitable point of intervention to reduce the biosynthesis of cholesterol [62,63].

The ultimate reaction in cholesterol biosynthesis, the reduction of desmosterol, is catalyzed by 3 β -hydroxysterol Δ^{24} -reductase (EC 1.3.1.72, DHCR24). In contrast to SQLE, DHCR24 does not activate dioxygen for insertion into the substrate, but simply reduces the side-chain double bond at the expense of NADPH (Fig. 6, bottom). The gene encoding DHCR24 is a human homolog (also termed seldadin-1) of the *DIMINUTO/DWARF1* gene found in plants and *Caenorhabditis elegans* [64]. Several mutations in the human gene are known which result in reduced enzyme activity leading to desmosterolosis (OMIM 606418). Some of the mutations discovered are in or near the FAD binding site and hence may affect FAD binding. In other cases, however, the mutation is in less conserved areas and their effect on protein structure, folding or stability is unclear. Symptoms of the disease present at or shortly after birth and show a diverse range of developmental anomalies, such as failure to thrive, micro- or macrocephaly, psychomotor retardation, spasticity and seizures. The observed developmental and neurological defects correspond to the high expression of the gene in neuronal cells [64]. More recently it was also shown that DHCR24 is important for long bone growth in mice indicating that the enzyme's activity is also critical for the development of other tissues [65].

Thyroxine biosynthesis and iodine salvage

The thyroid gland produces two iodinated tyrosine-derived hormones, triiodothyronine (T₃) and thyroxine (T₄), which stimulate metabolism in most tissues. The initial biosynthetic reaction

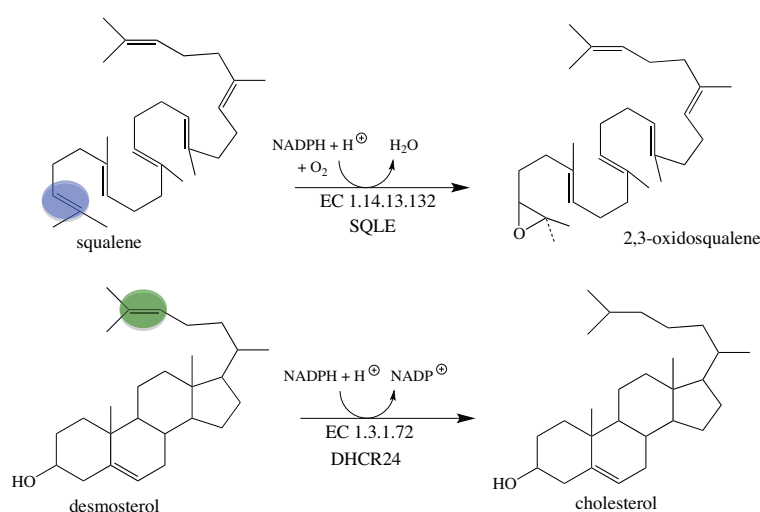


Fig. 6. Reactions of the two FAD-dependent enzymes in cholesterol biosynthesis. The reaction shown on top involves the insertion of an oxygen atom (blue circle) by SQLE (EC 1.14.13.132) and the reaction shown on the bottom the reduction of the side chain double bond (green circle) by DHCR24 (EC 1.3.1.72).

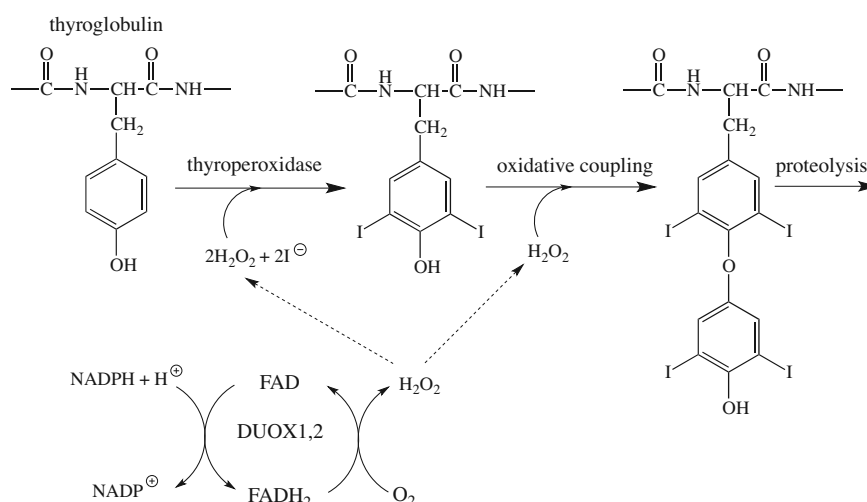


Fig. 7. Role of DUOX1 and 2 in the biosynthesis of thyroxine. The iodination of tyrosine residues and the coupling of two iodinated tyrosines require hydrogen peroxide, which is provided by the oxidation of reduced FAD with molecular dioxygen.

involves incorporation of iodine into tyrosine residues of thyroglobulin. In the next step, two neighboring iodotyrosine residues are oxidatively coupled and the active hormones, T_3 and T_4 , are released by proteolytic cleavage of the precursor protein. The iodination and coupling reaction both require hydrogen peroxide, which is provided by two FAD-dependent thyroid oxidases (termed DUOX1 and 2) [66,67]. During turnover, FAD is reduced at the expense of NADPH and then reoxidized by dioxygen yielding hydrogen peroxide (Fig. 7). Several allelic variants were reported for *DUOX2* leading to thyroid dysmorphogenesis 6 (OMIM 606759). How the resulting single amino acid exchange in the observed variants affect enzyme function is currently not known.

During the production of T_3 and T_4 substantial amounts of mono- and diiodotyrosine are released [68]. Because iodine is a precious trace element, it is recycled in a single reductive step catalyzed by an FMN-dependent dehalogenase (IYD, Fig. 8 [69]). The released iodine can then be reused by thyroperoxidase for incorporation into thyroglobulin (see above). Several allelic variants were reported for IYD, which severely compromise the dehalogenase activity of the enzyme leading to hypothyroidism (dysmorphogenesis 4, OMIM 612025) [70,71].

Flavoproteins providing assistance to other flavoproteins: Assembly of complex I

The human respiratory electron transport chain relies on complex I for electron transfer from NADH to ubiquinone coupled with proton translocation across the inner mitochondrial membrane. In the initial reaction NADH reduces the FMN cofactor in the NDUVF1 subunit (EC 1.6.5.3) of complex I, which in turn passes the electrons to iron-sulfur clusters. The formation of complex I, which

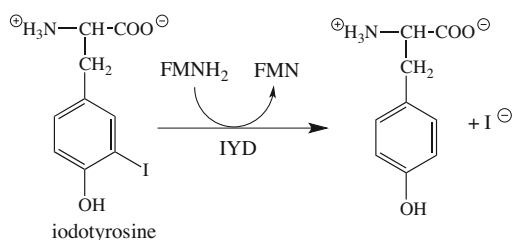


Fig. 8. Dehalogenation of iodotyrosine catalyzed by IYD. The mono- and diiodotyrosine residues released from thyroglobulin are substrates of the enzyme. Reductively released iodine is then reused by thyroperoxidase for incorporation into tyrosine residues of thyroglobulin.

consists of at least 36 nuclear- and seven mitochondrial-encoded subunits (OMIM 252010), requires several assembly factors, such as NDUFAF1 and NUBPL [72,73]. In addition, two FAD-dependent proteins recently emerged as critical factors for complex I assembly, ACAD9 and FOXRED1 (Table 1, entries #24 and #73, respectively). The exact role of the FAD-dependent OXidoREDuctase (FOXRED1) in assembly of complex I is not fully understood at the moment but it was clearly shown that it is essential for complex I activity in the inner mitochondrial membrane [72,74]. A BLASTp search identified two human FAD-dependent flavoproteins, SARDH and DMGDH, as related (22% and 21% identity, respectively) enzymes to FOXRED1. FOXRED1 comprises 486 amino acids and thus is much shorter than SARDH and DMGDH with 918 and 866 amino acids, respectively. The similarity of FOXRED1 to SARDH and DMGDH is found in the N-terminal part of the two dehydrogenases where FAD is covalently bound to a histidine. This amino acid residue is not conserved in FOXRED1 indicating that the FAD cofactor may not be covalently bound.

The discovery of FOXRED1 was closely associated with the search to identify the mechanism of complex I deficiency, leading for example to mitochondrial encephalopathy. Fassone et al. demonstrated that a point mutation in the FOXRED1 gene led to an amino acid exchange (R352W) in the putative FAD binding site [74]. According to their molecular model of the protein this amino acid exchange could prevent FAD binding and hence compromises the assumed chaperone activity of the protein.

ACAD9 (EC 1.3.99.-) was first described as an acyl-CoA dehydrogenase specific for long-chain unsaturated fatty acids [75,76]. Recent evidence however questions the involvement of ACAD9 in the degradation of long-chain fatty acids in the mitochondrial matrix and suggests a role in biogenesis of complex I instead [77]. Although recombinant ACAD9 possesses dehydrogenase activity *in vitro*, mutations in *ACAD9* result in complex I deficiency rather than a disturbance of long-chain fatty acid metabolism [77].

Concluding remarks

Our analysis of the human flavoproteome has led to the identification of several areas where further research is required. Because riboflavin must be supplied by the diet uptake in the human intestine is an important process to make the vitamin available for the synthesis of FMN and FAD. Three poorly characterized transporters seem to be responsible for riboflavin uptake in the human intestine. The relative contribution and role of these

transporters is currently unclear and warrants further investigations. A better understanding of the uptake processes may also have therapeutic benefits as some inherited diseases feature reduced flavin affinity to the affected flavoproteins and thus are potentially treatable by riboflavin supplementation. Equally, little is known about flavin homeostasis and the processes leading to degradation and excretion of flavins.

Although many human flavoprotein structures were solved experimentally by X-ray crystallography or modeled using homologous structures several flavoproteins still elude structural characterisation. Many of these are associated with cellular membranes and are therefore more difficult to obtain by recombinant expression in heterologous hosts. Moreover, membrane integral or associated proteins are challenging for structure elucidation by X-ray crystallography due to their lipophilic character. In view of the important roles of membrane-associated flavoproteins in humans, the potential as drug targets (e.g. SQLE) and the involvement in diseases (e.g. DUOX1/2, IYD) determination of the “missing” structures are certainly rewarding goals.

We found that many genes encoding flavoproteins occur as allelic variants with the potential to cause severe human diseases (Table 2). The number of allelic variants covers a wide range from only a few to more than one hundred. With the exception of a few systematic studies our knowledge of the effect of the mutation on stability, structure and activity of the flavoprotein is incomplete. This lack of insight should be improved by detailed analyses of mutational effects on flavoprotein properties. In light of many indications that flavoprotein variants suffer from a reduced affinity to their cognate flavin cofactor this seems to be of particular importance because riboflavin supplementation may help to remedy symptoms in affected individuals.

Methods

The names and gene abbreviations of human flavoproteins, compiled for a previously published review article [2], were used to search for inherited diseases in the Online Mendelian Inheritance in Man data base (OMIM; <http://www.ncbi.nlm.nih.gov/omim>). This search constituted the basis for Table 2 where the most relevant entry in OMIM is provided as a six-digit number (right column). The reader is referred to these entries for a complete list of references pertaining to the diseases mentioned in this article.

Acknowledgments

We thank the Austrian Research Fund (FWF) for financial support through project P22361 and the PhD program “Molecular Enzymology” (W901).

Appendix A. Supplementary data

Supplementary data associated with this article can be found, in the online version, at <http://dx.doi.org/10.1016/j.abb.2013.02.015>.

References

- [1] J.L. Chastain, D.B. McCormick, *Am. J. Clin. Nutr.* 46 (1987) 830–834.
- [2] P. Macheroux, B. Kappes, S.E. Ealick, *FEBS J.* 278 (2011) 2625–2634.
- [3] B.N. Ames, I. Elson-Schwab, E.A. Silver, *Am. J. Clin. Nutr.* 75 (2002) 616–658.
- [4] A.M. Bosch, N.G. Abeling, L. Ijlst, H. Knoester, W.L. van der Pol, A.E. Stroemer, R.J. Wanders, G. Visser, F.A. Wijburg, M. Duran, et al., *J. Inherit. Metab. Dis.* 34 (2011) 159–164.
- [5] P. Green, M. Wiseman, Y.J. Crow, H. Houlden, S. Riphagen, J.P. Lin, F.L. Raymond, A.M. Childs, E. Sheridan, S. Edwards, et al., *Am. J. Hum. Gen.* 86 (2010) 485–489.
- [6] G. Anand, N. Hasan, S. Jayapal, Z. Huma, T. Ali, J. Hull, E. Blair, T. McShane, S. Jayawant, *Dev. Med. Child Neurol.* 54 (2012) 187–189.
- [7] A. Koy, F. Pillekamp, T. Hoehn, H. Waterham, D. Klee, E. Mayatepek, B. Assmann, *Pediatr. Neurol.* 46 (2012) 407–409.
- [8] A.J. Wittwer, C. Wagner, *J. Biol. Chem.* 256 (1981) 4102–4108.
- [9] R.J. Cook, K.S. Misono, C. Wagner, *J. Biol. Chem.* 259 (1984) 12475–12480.
- [10] R.J. Cook, K.S. Misono, C. Wagner, *J. Biol. Chem.* 260 (1985) 12998–13002.
- [11] F. Forneris, E. Battaglioli, A. Mattevi, C. Binda, *FEBS J.* 276 (2009) 4304–4312.
- [12] J. Wang, F. Lu, Q. Ren, H. Sun, Z. Xu, R. Lan, Y. Liu, D. Ward, J. Quan, T. Ye, et al., *Cancer Res.* 71 (2011) 7238–7249.
- [13] B.A. Binzak, R.A. Wevers, S.H. Moolenaar, Y.M. Lee, W.L. Hwu, J. Poggi-Bach, U.F. Engelke, H.M. Hoard, J.G. Vockley, J. Vockley, *Am. J. Hum. Gen.* 68 (2001) 839–847.
- [14] S.H. Moolenaar, J. Poggi-Bach, U.F. Engelke, J.M. Corstiaensen, A. Heerschap, J.G. de Jong, B.A. Binzak, J. Vockley, R.A. Wevers, *Clin. Chem.* 45 (1999) 459–464.
- [15] R.P. McAndrew, J. Vockley, J.J. Kim, *J. Inherit. Metab. Dis.* 31 (2008) 761–768.
- [16] E.P. Treacy, B.R. Akerman, L.M. Chow, R. Youil, C. Bibeau, J. Lin, A.G. Bruce, M. Knight, D.M. Danks, J.R. Cashman, et al., *Hum. Mol. Gen.* 7 (1998) 839–845.
- [17] M. Eschenbrenner, M.S. Jorns, *Genomics* 59 (1999) 300–308.
- [18] A. Sreekumar, L.M. Poisson, T.M. Rajendiran, A.P. Khan, Q. Cao, J. Yu, B. Laxman, R. Mehra, R.J. Lonigro, Y. Li, et al., *Nature* 457 (2009) 910–914.
- [19] L. Bohm, A.M. Serafini, P. Fernandez, G. Van der Watt, P.J. Bouic, J. Harvey, *S. Afr. Med. J.* 102 (2012) 677–679.
- [20] H.J. Issaq, T.D. Veenstra, *J. Sep. Sci.* 34 (2011) 3619–3621.
- [21] G. Lucarelli, M. Fanelli, A.M. Larocca, C.A. Germinario, M. Rutigliano, A. Vavallo, F.P. Selvaggi, C. Bettocchi, M. Battaglia, P. Dittono, *Prostate* 72 (2012) 1611–1621.
- [22] P. Frosst, H.J. Blom, R. Milos, P. Goyette, C.A. Sheppard, R.G. Matthews, G.J. Boers, M. den Heijer, L.A. Kluijtmans, L.P. van den Heuvel, et al., *Nat. Gen.* 10 (1995) 111–113.
- [23] P.M. Ueland, S. Hustad, J. Schneede, H. Refsum, S.E. Vollset, *Trends Pharmacol. Sci.* 22 (2001) 195–201.
- [24] K. Yamada, Z. Chen, R. Rozen, R.G. Matthews, *Proc. Natl. Acad. Sci. USA* 98 (2001) 14853–14858.
- [25] D. Leclerc, A. Wilson, R. Dumas, C. Gafuik, D. Song, D. Watkins, H.H. Heng, J.M. Rommens, S.W. Scherer, D.S. Rosenblatt, et al., *Proc. Natl. Acad. Sci. USA* 95 (1998) 3059–3064.
- [26] M.L. Ludwig, R.G. Matthews, *Annu. Rev. Biochem.* 66 (1997) 269–313.
- [27] H. Olteanu, R. Banerjee, *J. Biol. Chem.* 276 (2001) 35558–35563.
- [28] A. Wilson, R. Platt, Q. Wu, D. Leclerc, B. Christensen, H. Yang, R.A. Gravel, R. Rozen, *Mol. Gen. Metab.* 67 (1999) 317–323.
- [29] K. Yamada, R.A. Gravel, T. Toraya, R.G. Matthews, *Proc. Natl. Acad. Sci. USA* 103 (2006) 9476–9481.
- [30] N.A. Leal, H. Olteanu, R. Banerjee, T.A. Bobik, *J. Biol. Chem.* 279 (2004) 47536–47542.
- [31] P.E. Mera, J.C. Escalante-Semerena, *J. Biol. Chem.* 285 (2010) 2911–2917.
- [32] H.A. Dailey, *Biochem. Soc. Trans.* 30 (2002) 590–595.
- [33] S. Arnould, M. Takahashi, J.-M. Camadro, *Proc. Natl. Acad. Sci. USA* 96 (1999) 14825–14830.
- [34] J.C. Deybach, V. da Silva, B. Grandchamp, Y. Nordmann, *Eur. J. Biochem.* 194 (1985) 431–435.
- [35] S. Sassa, *Br. J. Haematol.* 135 (2006) 281–292.
- [36] H. Puy, L. Gouay, J.C. Deybach, *Lancet* 375 (2010) 924–937.
- [37] I. Macalpine, R. Hunter, *Br. Med. J.* 1 (1966) 65–71.
- [38] J.C.G. Röhl, M.J. Warren, D.M. Hunt, *Purple Secret, Genes, “Madness” and the Royal Houses of Europe*, Bantam Press, London, 1998.
- [39] T.M. Cox, N. Jack, S. Lofthouse, J. Watling, *Lancet* 366 (2005) 332–335.
- [40] X. Qin, Y. Tan, L. Wang, Z. Wang, B. Wang, X. Wen, G. Yang, Z. Xi, Y. Shen, *FASEB J.* 25 (2011) 653–664.
- [41] R. Percudani, A. Peracchi, *EMBO Rep.* 4 (2003) 850–854.
- [42] F.N. Musayev, M.L. Di Salvo, T.-P. Ko, V. Schirch, M.K. Safo, *Protein Sci.* 12 (2003) 1455–1463.
- [43] M.K. Safo, F.N. Musayev, M.L. Di Salvo, V. Schirch, *J. Mol. Biol.* 310 (2001) 817–826.
- [44] M.L. Di Salvo, R. Contestabile, M.K. Safo, *Biochim. Biophys. Acta* 1814 (2011) 1597–1608.
- [45] A. Ruiz, J. Garcia-Villoria, A. Ormazabal, J. Zschocke, M. Fiol, A. Navarro-Sastre, R. Artuch, M.A. Vilaseca, A. Ribes, *Mol. Gen. Metab.* 93 (2008) 216–218.
- [46] P.B. Mills, R.A. Surtees, M.P. Champion, C.E. Beesley, N. Dalton, P.J. Scambler, S.J. Heales, A. Briddon, I. Scheimberg, G.F. Hoffmann, et al., *Hum. Mol. Gen.* 14 (2005) 1077–1086.
- [47] F.N. Musayev, M.L. Di Salvo, M.A. Saavedra, R. Contestabile, M.S. Ghatge, A. Haynes, V. Schirch, M.K. Safo, *J. Biol. Chem.* 284 (2009) 30949–30956.
- [48] J.H. Kang, M.L. Hong, D.W. Kim, J. Park, T.C. Kang, M.H. Won, N.I. Baek, B.J. Moon, S.Y. Choi, O.S. Kwon, *Eur. J. Biochem.* 271 (2004) 2452–2461.
- [49] E.O. Ngo, G.R. LePage, J.W. Thanassi, N. Meisler, L.M. Nutter, *Biochemistry* 37 (1998) 7741–7748.
- [50] M. Daugherty, B. Polanuyer, M. Farrell, M. Scholle, A. Lykidis, V. de Crecy-Lagard, A. Osterman, *J. Biol. Chem.* 277 (2002) 21431–21439.
- [51] N. Manoj, S.E. Ealick, *Acta Crystallogr.* 59 (2003) 1762–1766.
- [52] S. Steinbacher, P. Hernandez-Acosta, B. Bieseler, M. Blaesse, R. Huber, F.A. Culianez-Macia, T. Kupke, *J. Mol. Biol.* 327 (2003) 193–202.
- [53] T.P. Begley, C. Kinsland, E. Strauss, *Vitam. Horm.* 61 (2001) 157–171.
- [54] B. Zhou, S.K. Westaway, B. Levinson, M.A. Johnson, J. Gitschier, S.J. Hayflick, *Nat. Gen.* 28 (2001) 345–349.
- [55] M. Ozeir, U. Muhlenhoff, H. Webert, R. Lill, M. Fontecave, F. Pierrel, *Chem. Biol.* 18 (2011) 1134–1142.

- [56] S.F. Heeringa, G. Chernin, M. Chaki, W. Zhou, A.J. Sloan, Z. Ji, L.X. Xie, L. Salviati, T.W. Hurd, V. Vega-Warner, et al., *J. Clin. Invest.* 121 (2011) 2013–2024.
- [57] W.J. van Berkel, N.M. Kamerbeek, M.W. Fraaije, *J. Biotech.* 124 (2006) 670–689.
- [58] G. Gibbons, K. Mitropoulos, N. Myant, *Biochemistry of Cholesterol*, Elsevier Biomedical, Amsterdam, 1982.
- [59] S. Yamamoto, K. Bloch, *J. Biol. Chem.* 245 (1970) 1670–1674.
- [60] M. Nagai, J. Sakakibara, K. Wakui, Y. Fukushima, S. Igarashi, S. Tsuji, M. Arakawa, T. Ono, *Genomics* 44 (1997) 141–143.
- [61] N.S. Ryder, M.C. Dupont, *Biochem. J.* 230 (1985) 765–770.
- [62] A. Belter, M. Skupinska, M. Giel-Pietraszuk, T. Grabarkiewicz, L. Rychlewski, J. Barciszewski, *Biol. Chem.* 392 (2011) 1053–1075.
- [63] A. Chugh, A. Ray, J.B. Gupta, *Prog. Lipid Res.* 42 (2003) 37–50.
- [64] I. Greeve, I. Hermans-Borgmeyer, C. Brellinger, D. Kasper, T. Gomez-Isla, C. Behl, B. Levkau, R.M. Nitsch, *J. Neurosci.* 20 (2000) 7345–7352.
- [65] R. Mirza, S. Qiao, K. Tateyama, T. Miyamoto, L. Xiuli, H. Seo, J. Bone Miner. Metab. 30 (2012) 144–153.
- [66] X. De Deken, D. Wang, M.C. Many, S. Costagliola, F. Libert, G. Vassart, J.E. Dumont, F. Miot, *J. Biol. Chem.* 275 (2000) 23227–23233.
- [67] C. Dupuy, R. Ohayon, A. Valent, M.S. Noel-Hudson, D. Deme, A. Virion, *J. Biol. Chem.* 274 (1999) 37265–37269.
- [68] J. Nunez, J. Pommier, *Vitam. Horm.* 39 (1982) 175–229.
- [69] J.E. Friedman, J.A. Watson Jr., D.W. Lam, S.E. Rokita, *J. Biol. Chem.* 281 (2006) 2812–2819.
- [70] G. Afink, W. Kulik, H. Overmars, J. de Randamie, T. Veenboer, A. van Cruchten, M. Craen, C. Ris-Stalpers, *J. Clin. Endocrinol. Metab.* 93 (2008) 4894–4901.
- [71] J.C. Moreno, W. Klootwijk, H. van Toor, G. Pinto, M. D'Alessandro, A. Leger, D. Goudie, M. Polak, A. Gruters, T.J. Visser, *N. Engl. J. Med.* 358 (2008) 1811–1818.
- [72] S.E. Calvo, E.J. Tucker, A.G. Compton, D.M. Kirby, G. Crawford, N.P. Burtt, M. Rivas, C. Guiducci, D.L. Bruno, O.A. Goldberger, et al., High-throughput, pooled sequencing identifies mutations in NUBPL and FOXRED1 in human complex I deficiency, *Nat. Gen.* 42 (2010) 851–858.
- [73] C.J. Dunning, M. McKenzie, C. Sugiana, M. Lazarou, J. Silke, A. Connelly, J.M. Fletcher, D.M. Kirby, D.R. Thorburn, M.T. Ryan, *EMBO J.* 26 (2007) 3227–3237.
- [74] E. Fassone, A.J. Duncan, J.W. Taanman, A.T. Pagnamenta, M.I. Sadowski, T. Holand, W. Qasim, P. Rutland, S.E. Calvo, V.K. Mootha, et al., *Hum. Mol. Gen.* 19 (2010) 4837–4847.
- [75] R. Ensenauer, M. He, J.M. Willard, E.S. Goetzman, T.J. Corydon, B.B. Vandahl, A.W. Mohsen, G. Isaya, J. Vockley, *J. Biol. Chem.* 280 (2005) 32309–32316.
- [76] J. Zhang, W. Zhang, D. Zou, G. Chen, T. Wan, M. Zhang, X. Cao, *Biochem. Biophys. Res. Commun.* 297 (2002) 1033–1042.
- [77] J. Nouws, L. Nijtmans, S.M. Houten, M. van den Brand, M. Huynen, H. Venselaar, S. Hoefs, J. Gloerich, J. Kronick, T. Hutchin, et al., *Cell. Metab.* 12 (2010) 283–294.
- [78] A. Mostowska, B. Biedziak, I. Dunin-Wilczynska, A. Komorowska, P.P. Jagodzinski, *Birth Defects Res. A Clin. Mol. Teratol.* 91 (2011) 169–176.
- [79] A. Mostowska, K.K. Hozyasz, B. Biedziak, J. Misiak, P.P. Jagodzinski, *Eur. J. Oral. Sci.* 118 (2010) 325–332.
- [80] A. Mostowska, K.K. Hozyasz, P. Wojcicki, M. Dziegielewska, P.P. Jagodzinski, *J. Med. Genet.* 47 (2010) 809–815.
- [81] A.R. Johnson, C.N. Craciunescu, Z. Guo, Y.W. Teng, R.J. Thresher, J.K. Blusztajn, S.H. Zeisel, *FASEB J.* 24 (2010) 2752–2761.
- [82] A.R. Johnson, S. Lao, T. Wang, J.A. Galanko, S.H. Zeisel, *PLoS ONE* 7 (2012) e36047.

Collapse of the native structure by a single amino acid exchange in human NAD(P)H:quinone oxidoreductase (NQO1)

Wolf-Dieter Lienhart^{a†}, Venugopal Gudipati^{a†}, Michael K. Uhl^b, Alexandra Binter^a, Sergio Pulido^c, Robert Saf^d, Klaus Zangger^c, Karl Gruber^b and Peter Macheroux^{a*}

Running title: collapse of native structure in human NQO1

^a Graz University of Technology, Institute of Biochemistry, Petersgasse 12, A-8010 Graz, Austria.

^b University of Graz, Institute of Molecular Biosciences, Humboldtstr. 50, A-8010 Graz, Austria.

^c University of Graz, Institute of Chemistry, Heinrichstr. 28, A-8010 Graz, Austria.

^d Graz University of Technology, Institute for Chemistry and Technology of Materials, Stremayrgasse 9, A-8010 Graz, Austria.

†The first two authors (W.-D.L. and V.G.) have equally contributed to this work

Author contributions

K.G. and P.M. initiated the project; W.-D.L., V.G., K.Z., M.K.U., K.G. and P.M. designed experiments, and analysed data; W.-D.L. and V.G. expressed and purified proteins; M.K.U. and K.G. crystallized proteins and determined the crystal structures. W.-D.L., V.G. and A.B. performed biochemical experiments, determined binding constants as well as kinetic parameters; V.G. and R.S. performed mass spectrometry; K.Z. and S.P. performed NMR-experiments; K.Z., K.G. and P.M. wrote the manuscript.

* Corresponding author: Prof. Dr. Peter Macheroux, Graz University of Technology, Institute of Biochemistry, Petersgasse 12, A-8010 Graz, Austria, Tel.: +43-316-873 6450, Fax: +43-316-873 6952, Email: peter.macheroux@tugraz.at

Abstract

Human NAD(P)H:quinone oxidoreductase (NQO1) is essential for the antioxidant defence system, stabilization of tumor suppressors (e.g. p53, p33 and p73) and activation of quinone based chemotherapeutics. Overexpression of NQO1 in many solid tumours coupled with its ability to convert quinone-based chemotherapeutics into potent cytotoxic compounds made it a very attractive target for anti-cancer drugs. A naturally occurring single nucleotide polymorphism (transition from C609T) leading to an amino acid exchange (P187S) has been implicated in development of various cancers and poor survival rates following anthracyclin based adjuvant chemotherapy. Despite the importance for cancer prediction and therapy, the exact molecular basis for the loss of function in NQO1 P187S is currently unknown. Therefore we solved the crystal structure of NQO1 P187S. Surprisingly, this structure is virtually identical to NQO1. Employing a combination of NMR spectroscopy and limited proteolysis experiments we demonstrate that the single amino acid exchange destabilizes interactions between the core and C-terminal domain leading to depopulation of the native structure in solution. This collapse of the native structure diminishes cofactor affinity and leads to a less competent FAD binding pocket thus severely compromising the catalytic capacity of the variant protein. Hence our findings provide a rationale for the loss of function in NQO1 P187S due to a frequently occurring single nucleotide polymorphism. This leads us to propose that stabilisation of the native structure by molecular chaperones might be a valuable approach to rescue catalytic activity and thus enhance quinone-based chemotherapies.

Significance statement

Chemotherapeutics against cancer are generally designed against validated targets disregarding individual genetic dispositions. Recent progress in genetics and DNA-sequencing led to the identification of numerous single nucleotide polymorphisms (SNP), which may affect the efficiency of drug treatments. A frequent SNP in the human *NQO1* gene was shown to be involved in cancer progression and poor response to some chemotherapeutics. Current models attempting to rationalize the loss of function due to the resulting proline to serine exchange in the encoded enzyme are inconclusive mainly due to the lack of structural information. Our study provides biochemical and structural evidence that this single amino exchange destabilizes the three-dimensional structure thus severely compromising the catalytic properties of the enzyme.

Introduction

NAD(P)H:quinone oxidoreductase (NQO1; EC 1.6.99.2) is a cytosolic FAD-dependent enzyme catalysing the two-electron reduction of quinones to hydroquinones. NQO1 is an essential component of the antioxidant defence system preventing the formation of potentially harmful semiquinone radicals (1). Additionally, NQO1 stabilises several tumour suppressors, p33ING1b, p53 and p73 thereby exerting an antineoplastic effect (2–5) and also activates quinone based chemotherapeutics by reducing the quinone pharmacophore to a cytotoxic hydroquinone form (6). Due to a frequent single nucleotide polymorphism (SNP) in the *NQO1* gene (on human chromosome 16q22.1), nucleotide C609 is changed to T, resulting in the replacement of proline 187 to serine in the protein (7). The frequency of the *NQO1**2 homozygous genotype was estimated to be between 4% and 20% depending on the ethnic group with the highest prevalence in Asian populations (8). The *NQO1**2 genotype is associated with increased benzene hematotoxicity (9) and poor survival rates of women with breast cancer (10). It was proposed that occurrence of the *NQO1**2 genotype is a prognostic and predictive marker for breast cancer (10).

Despite the importance for cancer prediction and therapy, the exact structural and molecular basis for the loss of function in NQO1 P187S is currently unknown. The site of amino acid exchange (P187S) is neither in the active site of the enzyme, nor near the FAD and NAD(P)H binding sites. Therefore it was speculated that the proline to serine replacement leads to a local perturbation of a central β -sheet reducing the affinity of FAD thus lowering catalytic activity (11). It was also proposed that FAD acts as a chemical chaperone, maintaining the properly folded state of NQO1 (12). Our findings establish that the amino acid replacement destabilizes the native fold of the enzyme thus contradicting previous assumptions proposed to rationalize the loss of function in the NQO1 P187S variant.

Results and discussion

In view of the important cellular functions of NQO1 and the high frequency of the *NQO1**2 genotype, we studied the biochemical and structural properties of NQO1 P187S in comparison to NQO1. During purification of the recombinant NQO1 proteins by Ni-NTA affinity and size exclusion chromatography we noticed that NQO1 P187S was partially depleted of the FAD cofactor indicating lower cofactor binding affinity as compared to NQO1. Therefore we prepared the apo-forms of NQO1 and NQO1 P187S and studied the binding of the FAD cofactor to the apo-forms by monitoring difference absorption changes. As shown in (Fig.1, left diagrams, page 74) the spectral perturbations observed for NQO1 and NQO1 P187S show clear

differences in their absorption minima and maxima as well as their isosbestic points. However, both titrations produced sharp end points (Fig. S1, page 78), indicating that dissociation constants of FAD binding are below the micromolar range for both NQO1 and NQO1 P187S. Since the dissociation constants for both proteins are in the same range we assumed that reduced activity in P187S cannot be explained solely by the loss of FAD as suggested in previous studies (12). For the accurate determination of dissociation constants FAD was titrated with apo-NQO1 and apo-NQO1 P187S in a microcalorimeter (for details see Materials & Methods, page 85). These ITC measurements showed that each protomer of the dimeric proteins has a single FAD binding site, albeit NQO1 P187S exhibits an increase of the dissociation constant (K_d) by a factor of 7 compared to NQO1 ($K_d = 64 \pm 23$ nM and 428 ± 90 nM for NQO1 and NQO1 P187S, respectively; Fig.1, right diagrams, page 74). Thus, our experiments show that FAD binding is not only affected qualitatively in terms of the mode of physical interactions but also quantitatively (*i.e.* lower affinity).

Furthermore, rapid reaction measurements demonstrated that the reductive half reaction of the catalytic cycle is severely affected in NQO1 P187S. The bimolecular rate constants for NQO1 P187S were decreased by a factor of 300 and 70 with NADH and NADPH, respectively (Table S1, page 83). On the other hand, the oxidative half reaction, *i.e.* reduction of a quinone substrate (*e.g.* benzoquinone or menadione) by the reduced FAD cofactor was still very rapid in NQO1 P187S and complete within the dead time of the stopped-flow instrument (approx. 5 ms). Since the reductive half reaction is the rate-limiting step in the catalytic cycle the lower rate of reduction leads directly to a decrease of catalytic turnover in NQO1 P187S. It should be noted in this context that the much lower rate of reduction strongly indicates that the FAD binding site is catalytically less competent, corroborating the conclusion that the mode of FAD binding is different in NQO1 P187S.

The observed qualitative and quantitative differences in physical properties of FAD binding and catalysis suggested structural perturbations in the FAD binding pocket of NQO1 P187S. To analyse these putative structural differences we solved the X-ray crystal structure of NQO1 P187S (Fig. S2, panel B, page 79) (for data collection and refinement statistics see, Table S2, page 84). The first crystallisation attempts were successful in the presence of dicoumarol, a competitive inhibitor of NQO1. These crystals diffracted to 2.7 Å and revealed a structural topology (Fig. 2A, page 75) virtually identical to the NQO1 crystal structure (13, 14) with a root-mean-square-deviation of 0.33 Å for 249 C atoms. NQO1 P187S exists as a dimer in the crystal (Fig. S2, panel B, page 79) and in solution. The FAD binding site of NQO1 P187S exhibited no discernible differences with the flavin isoalloxazine ring as well as the AMP moiety

engaging in the same interactions as NQO1 (Fig. 2B, page 75). The same is true for the region around the amino acid exchange site where no significant structural differences between NQO1 and NQO1 P187S were observed (Fig. 2C, page 75). In the absence of Cibacron blue, slowly growing crystals were obtained for NQO1 P187S, which diffracted to 2.2 Å (Fig. S2, panel C, page 79) (for data collection and refinement statistics see, Table S2, page 84). With these crystals no electron density was obtained for the last 50 C-terminal amino acids (Fig. 3B, page 76). Apart from the missing C-terminus, NQO1 P187S shows no differences to NQO1 in the topology of the structure and the active site (Fig. S2, panel C, page 79). ESI-MS analysis of a protein crystal taken from the same crystallisation drop confirmed that the protein was truncated indicating that the C-terminus was lost due to proteolytic cleavage. Closer inspection of the missing C-terminal amino acids revealed that the cleavage of NQO1 P187S had occurred at amino acid 224 (Fig. 2C, page 75). It appears that the proline to serine replacement weakens the interaction of the core domain with the C-terminal domain and leads to a higher mobility in both domains. A plausible explanation for this destabilisation is that the replacement of the hydrophobic proline which is surrounded by mainly hydrophobic residues (Leu145, Ile147, Leu169, Leu189 and Ile170, Fig. 2C, page 75), by a hydrophilic serine residue leads to perturbations in the hydrophobic pocket thereby affecting the interactions with the C-terminus.

To further investigate this phenomenon, we performed limited proteolysis experiments and analysed the tryptic fragments by MALDI-TOF MS. As shown in (Fig. 3A, page 76) NQO1 P187S was rapidly cleaved by trypsin while NQO1 was much less susceptible to proteolytic cleavage. Complete in-gel tryptic digestion of the main fragments (inset 1 and 2, Fig. 3A, page 76) and subsequent peptide fingerprinting confirmed that the C-terminus was completely digested within 5 minutes in NQO1 P187S but still present in NQO1 (Fig. S3, page 80). The C-terminus of NQO1 is digested much more slowly than in NQO1 P187S, *i.e.* more than half of the protein retained the C-terminus even after 160 minutes of incubation. A recent proposition that NQO1 P187S adopts a native conformation in the presence of excess FAD (12) was not confirmed in our limited proteolysis experiments (Fig. S4, page 81). To assess the role of the C-terminus in catalysis, we generated truncated variants, NQO1 Δ 50 and NQO1 P187S Δ 50 in which 50 amino acids were deleted at the C-terminus. In the case of NQO1 Δ 50 the bimolecular rate constant for FAD reduction dropped drastically whereas the truncated NQO1 P187S Δ 50 was only marginally affected by the C-terminal deletion (Table S1, page 83).

Although our spectroscopic and kinetic measurements have documented the effects of the proline to serine exchange on catalytic function the determined crystal structure of NQO1 P187S is virtually identical to NQO1 and hence does not provide a structure based explanation

for the loss of enzymatic activity. This prompted us to employ NMR-spectroscopy to characterize the structural properties of NQO1 and NQO1 P187S in solution.

Both one-dimensional proton spectra (Fig. S5, page 82) as well as 2D ^1H - ^{15}N -HSQC measurements (Fig. 4 A and C, page 77), obtained with uniformly ^{15}N -labelled proteins, revealed significant structural differences between NQO1 and NQO1 P187S. Signals indicative of a well folded protein (e.g. peaks below 0 ppm in the ^1H -NMR spectrum) and well dispersed signals beyond ~ 8.5 ppm in ^1H - ^{15}N -HSQC spectra were significantly more pronounced in NQO1 (Fig. S5, page 82). To gain further insight into the dynamic behaviour, we carried out ^{15}N relaxation measurements. Histograms showing the distribution of rotational correlation times τ_c are presented in (Fig. 4B and D, page 77). Short correlation times (< 20 ns) are indicative of highly flexible residues, while the well-structured regions of a protein in the molecular mass range of NQO1 should give rise to values around 30-40 ns. In the case of NQO1 P187S very short correlation times were observed whereas much longer correlation times of up to 58 ns were observed for NQO1 (compare panels B and D in Fig. 4, page 77). Using ^{13}C , ^{15}N double-labelled NQO1 several of the peaks for flexible residues could be assigned and they all lie either in the N-terminal hexahistidine-tag or the last ten C-terminal residues. Peaks missing in the ^1H - ^{15}N -HSQC of NQO1 P187S (Fig. 4C, page 77) are likely in the intermediate-fast motional regime ($k_{\text{ex}} \sim \text{ms}$), leaving only the very flexible residues observable. Since we know from X-ray crystallography that the NQO1 P187S adopts a structure identical to NQO1 in the crystal we assume that disordered and more flexible conformations seen in NMR-spectroscopy are in equilibrium with the native conformation. However, it is apparent that the percentage of NQO1 P187S exhibiting native conformation is negligible since rapid reaction experiments (Table S1, page 83) show that the catalytic activity of NQO1 P187S is severely compromised.

Predictable efficacy and preventing adverse side effects are major goals in anticancer drug discovery and chemotherapy. The overexpression of NQO1 in various solid tumours and its ability to activate quinone based chemotherapeutics rendered it an attractive target for anticancer treatment (6). Recently, EPI-743 a quinone based drug targeting NQO1 was granted orphan designation for treating mitochondrial diseases. Yet no information is currently available on how patients with homozygous NQO1*2 genotype respond to this drug (15). On the other hand the effects of NQO1 polymorphism and its implications for anti-cancer chemotherapy has been well studied for over a decade (8). A recent study reported the association of the NQO1*2 homozygous genotype to adverse breast cancer outcome as well as poor survival rates after anthracycline-based chemotherapy (17% for NQO1*2 versus 75% for other genotypes) (10). The wealth of information on the involvement of the NQO1 P187S variant in cancer

development and the failure to active chemotherapeutics was contrasted by a lack of knowledge to rationalize the loss of function on a molecular level. Our study has remedied this situation and provides a structural and biochemical basis for further explorations to use NQO1 as a drug target.

In summary, the experimental findings reported in this study have established the molecular cause of the severely compromised enzymatic activity and stability of NQO1 P187S. The single amino acid substitution of proline 187 to serine destabilises a crucial interdomain contact and results in a higher mobility of the C-terminal and core domain, which in turn leads to the depopulation of a highly ordered (native) state, consequently compromising cofactor binding and catalytic efficiency. This study also emphasizes the importance of combining structural methods to enhance our understanding of the effects SNP have on protein properties, in particular folding dynamics. In the case of NQO1, it is conceivable that efforts to reinforce interdomain contacts, for example by small molecular chaperones, may lead to a repopulation of the catalytically competent native structure thus paving the way for more efficient treatment with quinone based anti-cancer drugs.

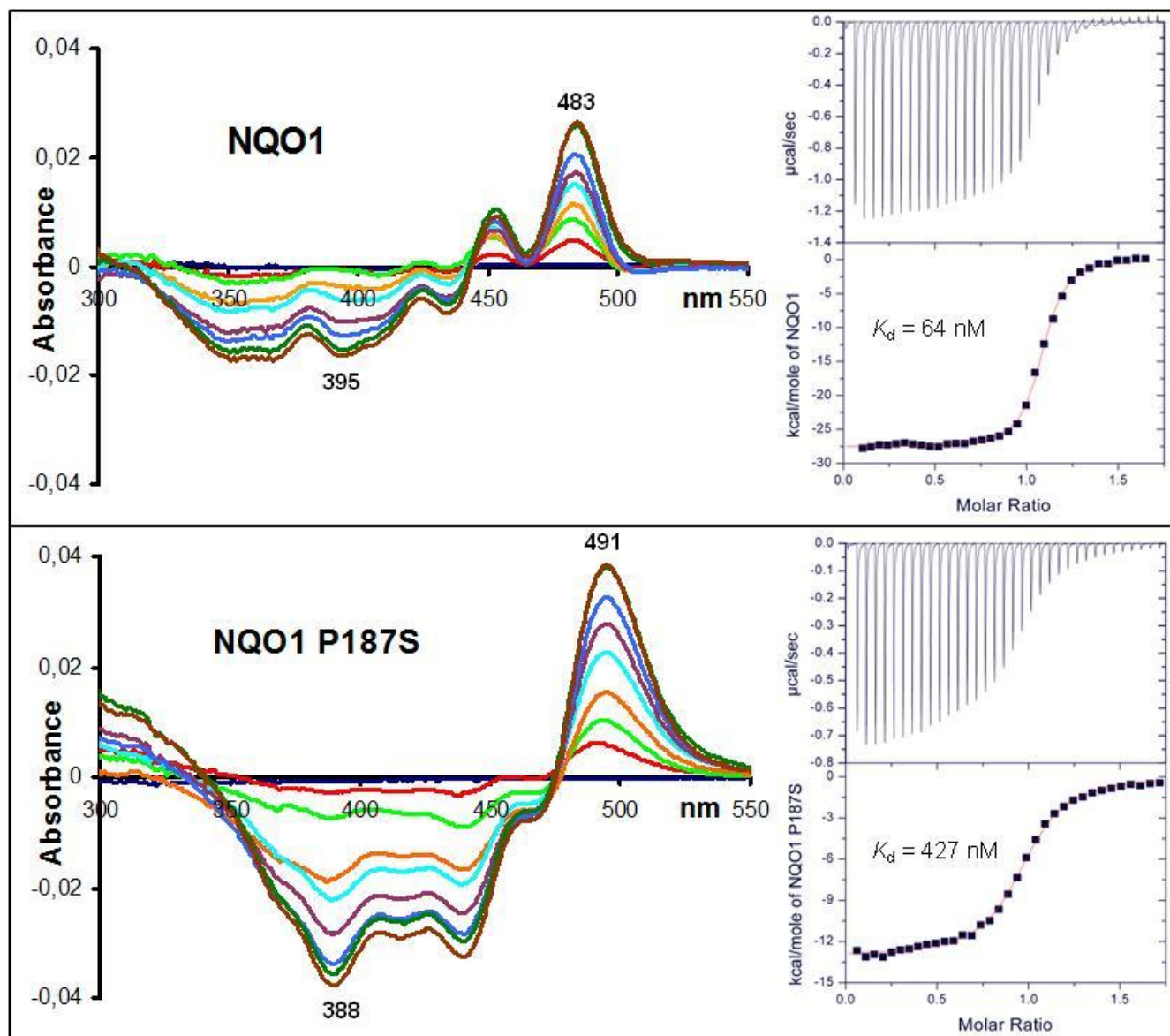


Fig. 1. The binding mode and affinity of Fad towards NQO1 P187S are different compared to that of NQO1. **Left diagrams:** UV/Vis difference absorption spectra. Representative difference absorption spectra obtained from the difference titration of apo-NQO1 and apo-NQO1 P187S with the FAD cofactor in the spectral range of 300 nm to 550 nm.

Right diagrams: Isothermal titration calorimetry. NQO1 (top right) and NQO1 P187S (bottom right) were titrated into a FAD solution. The upper panel in each diagram shows the time-dependent release of heat during the titration (exothermic). Peak integrals as a function of the FAD to protein molar ratio are shown in the bottom panel of each diagram.

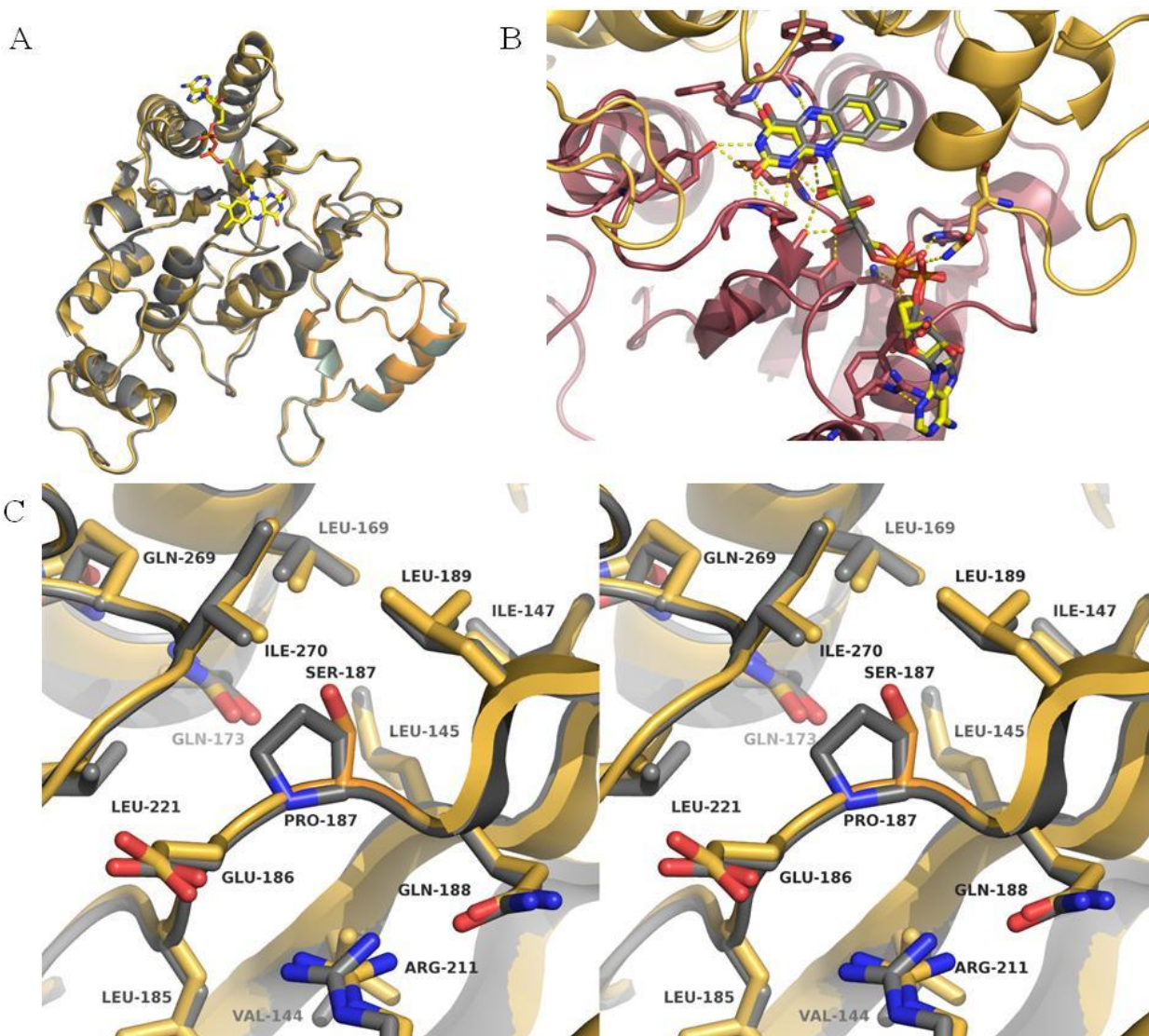


Fig. 2. Crystal structure of the NQO1 P187S is virtually identical to NQO1. **(A)** Crystal structure of a NQO1 P187S (gold) subunit superimposed on NQO1 (grey) (PDB: 1d4a) **(B)** Close-up view of the FAD binding site in NQO1 P187S. FAD molecule is represented as ball and stick model, while the two subunits of NQO1 are represented as cartoon and shown in red and gold colours. Hydrogen bonds between FAD and protein backbone are depicted as yellow dashed lines. **(C)** Stereo representation showing the site of the amino acid replacement, NQO1 P187S (gold) is superimposed on NQO1 (grey)

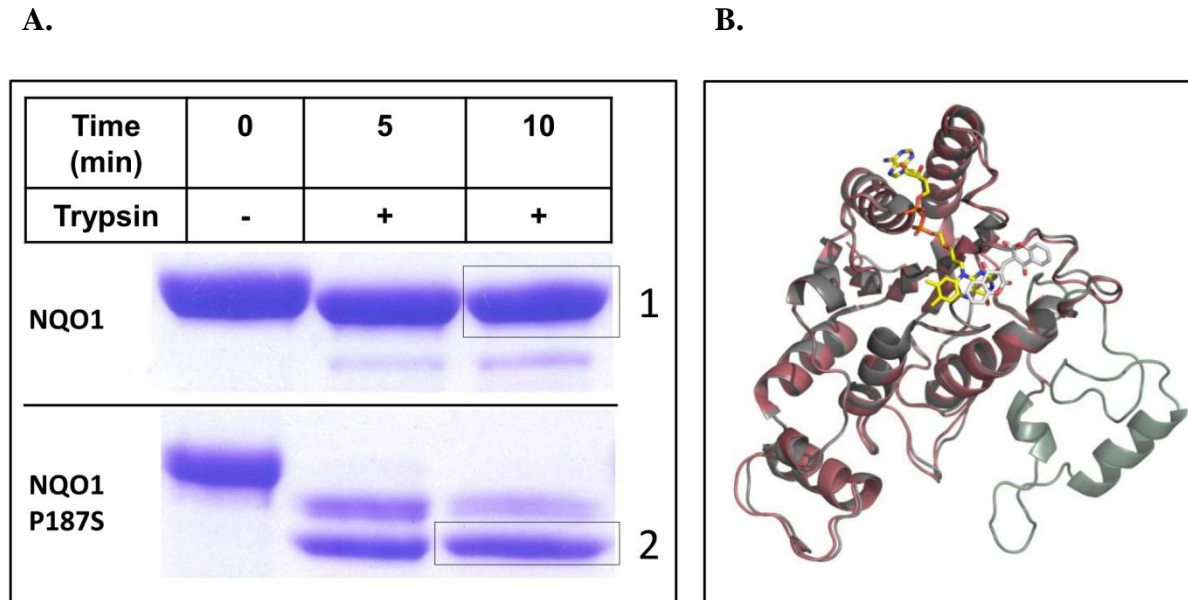


Fig. 3. The C-terminus of NQO1 P187S is flexible. **(A)** Limited proteolysis of NQO1, and NQO1 P187S by trypsin analysed by SDS-PAGE. The C-terminal region of NQO1 P187S was proteolysed within 5 minutes indicating that it is flexible. **(B)** Superimposed X-ray crystal structures of NQO1 (grey) and NQO1 P187S (C-terminal truncation), (magenta). The C-terminus of NQO1 P187S was randomly cleaved by an unknown protease during the crystallization procedure confirming our hypothesis that the C-Terminus is flexible.

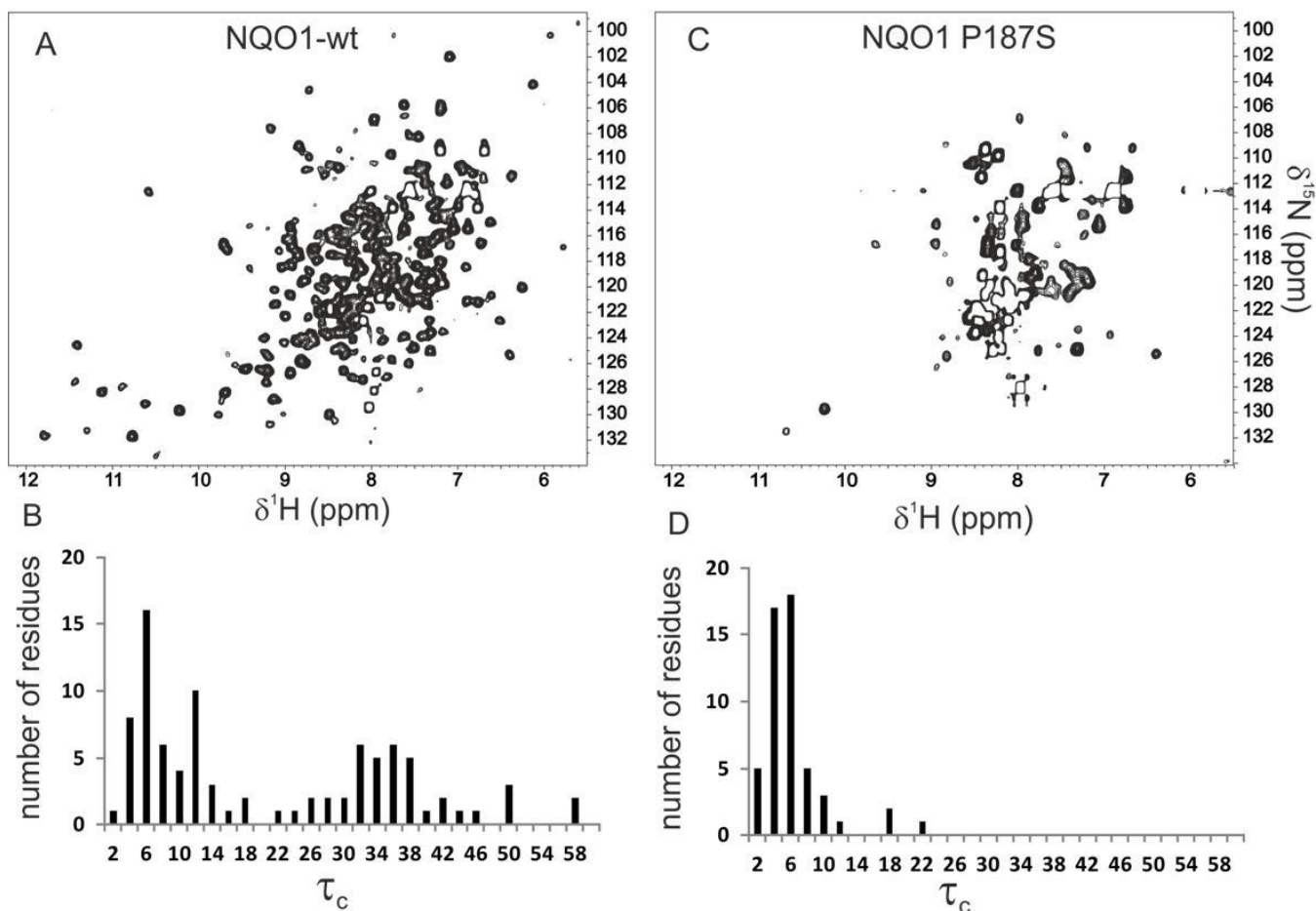


Figure 4: NQO1 P187S loses its structure in solution. 2D ^1H - ^{15}N HSQC spectra of NQO1 and the NQO1 P187S are shown in panels (A and C) respectively. In the panels below (B and D) the distribution of rotational correlation times (τ_c in ns) for NQO1 and the NQO1 P187S are shown. Almost complete absence of well dispersed signals in the HSQC spectrum and of long τ_c values are indicative of increased mobility in the NQO1 P187S.

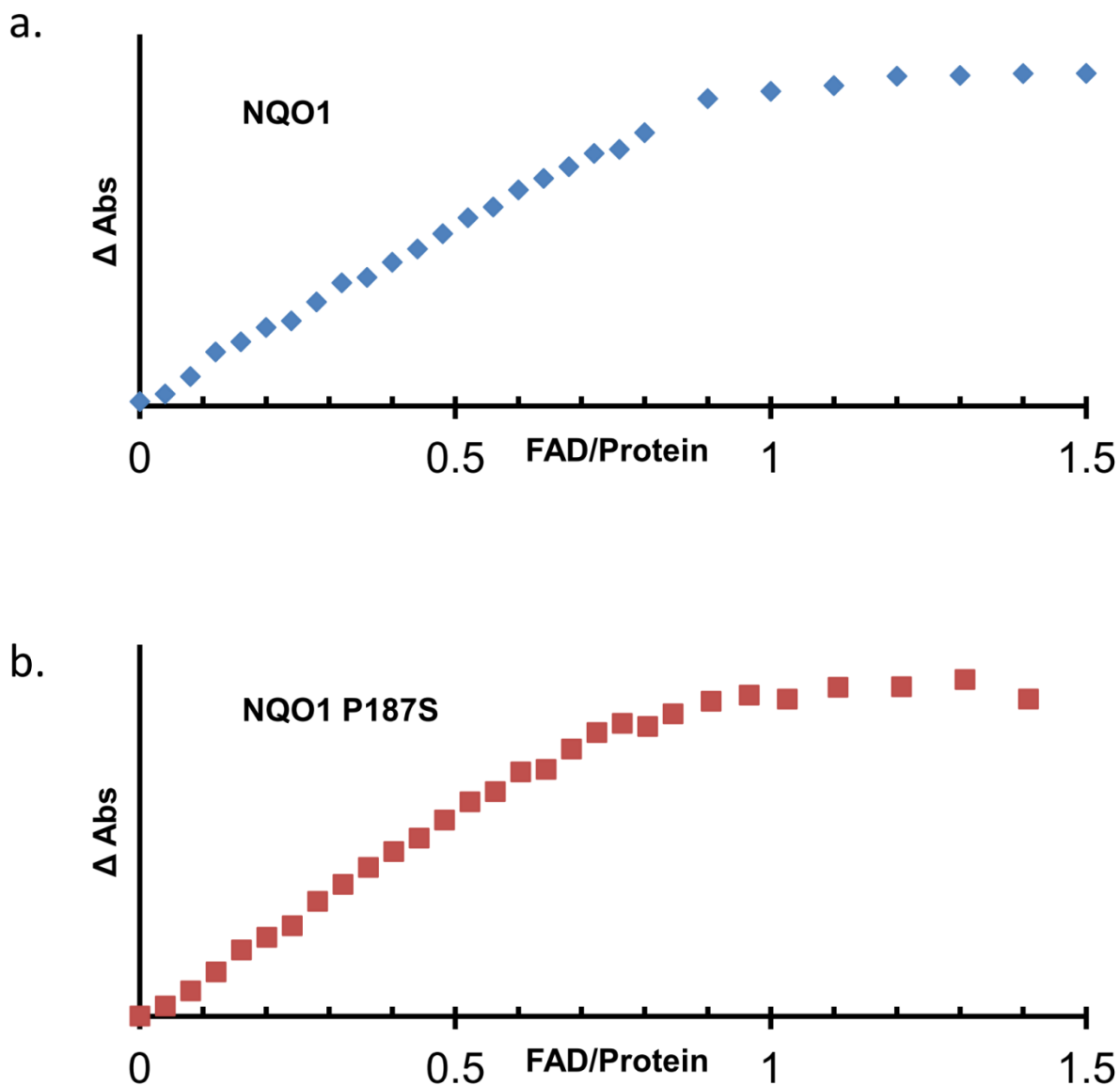


Fig. S1. Differential titration of NQO1 and NQO1 P187S, The spectral change (Fig. 1, left diagrams) was monitored by plotting the sum of the absolute value at 435 and 483nm (NQO1) or 437 and 491nm (NQO1 P187S) of all the spectra against the ratio of FAD to protein The data indicates a binding ratio of one FAD per subunit for both NQO1 and NQO1 P187S.

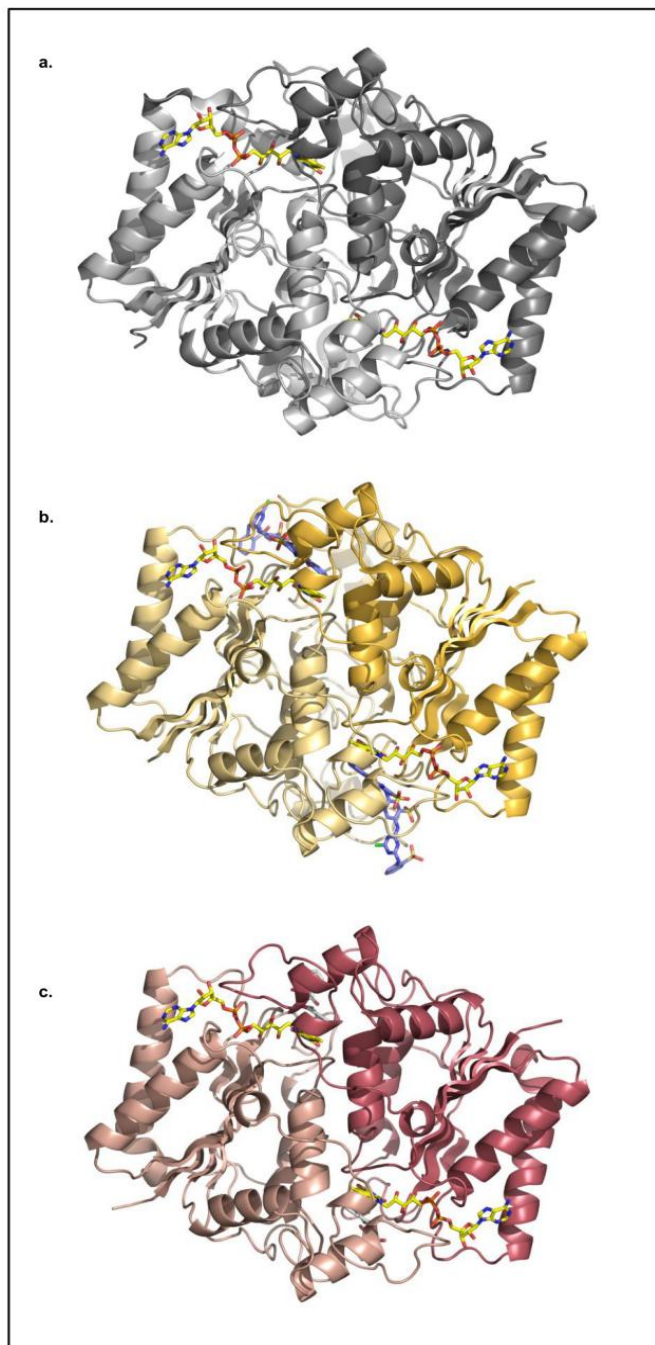


Fig. S2. Comparison of the X-ray crystallographic dimeric structures of NQO1, NQO1 P187S and NQO1 P187S. All three proteins exist as dimers in the crystal structure and exhibit similar structural topology. **(A)** X-ray crystal structure of NQO1 (PDB code: 1d4a). **(B and C)** X-ray crystal structures of NQO1 P187S and NQO1 P187S Δ 50, respectively. FAD cofactor (**A, B** and **C**) and Cibacron Blue (**B**) are shown as stick models.

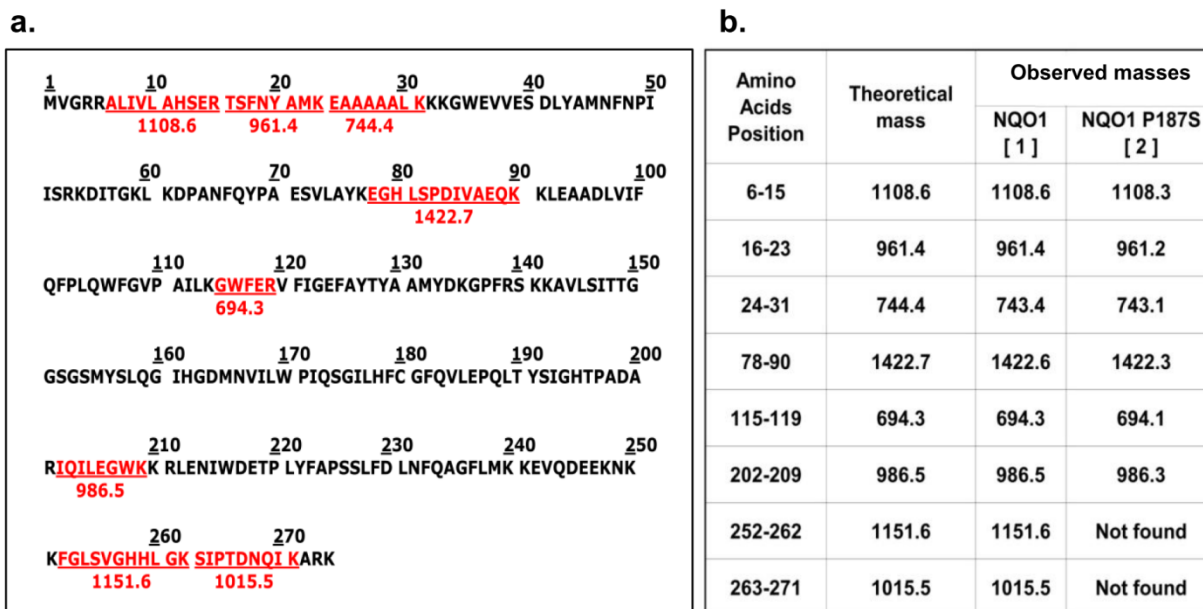


Fig. S3: MALDI-TOF MS analysis of NQO1 proteins after limited proteolysis. The C-terminus of NQO1 P187S is rapidly proteolysed compared to that of NQO1. **(A)** Theoretical tryptic digest of NQO1 generated by ExPASy PeptideCutter tool; peptide sequences colored in red are used as a peptide fingerprint for analyzing the MALDI-TOF MS data. **(B)** Tabular form listing the observed peptides after MALDI-TOF MS of NQO1 and NQO1 P187S protein from SDS-PAGE bands (Inset 1 & 2, Fig. 3A)

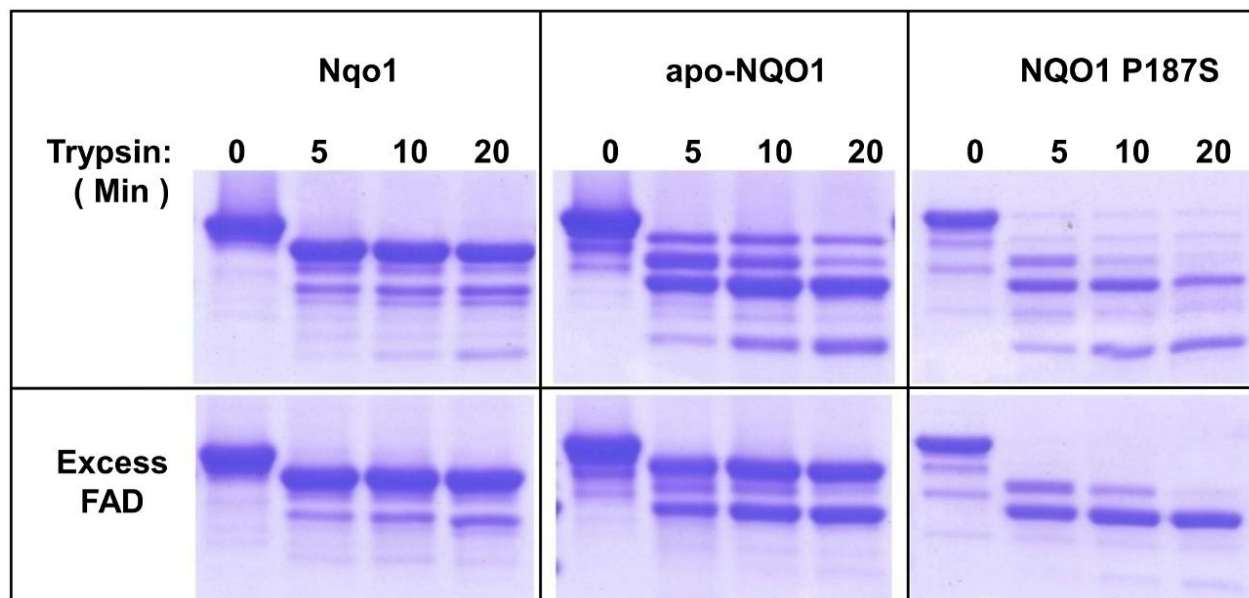


Fig. S4: Inter-domain association between C-terminus and core domains of NQO1 P187S is not stabilized by the presence of FAD. NQO1, apo-Nqo1 and NQO1 P187S were subjected to limited tryptic digestion, in the presence (bottom panel) or absence (top panels) of excess FAD. 30 μ M protein solution was digested with 2 ng/ μ l of sequencing grade modified trypsin in the presence or absence of 300 μ M FAD and analyzed by SDS-PAGE. In the presence of FAD, apo-NQO1 was stabilized whereas the C-terminus of NQO1 P187S is completely cleaved within 5 minutes. NQO1 P187S was stabilised after proteolysis of the C-terminus indicating that FAD does not stabilise the interaction between the C-terminus and the core domain.

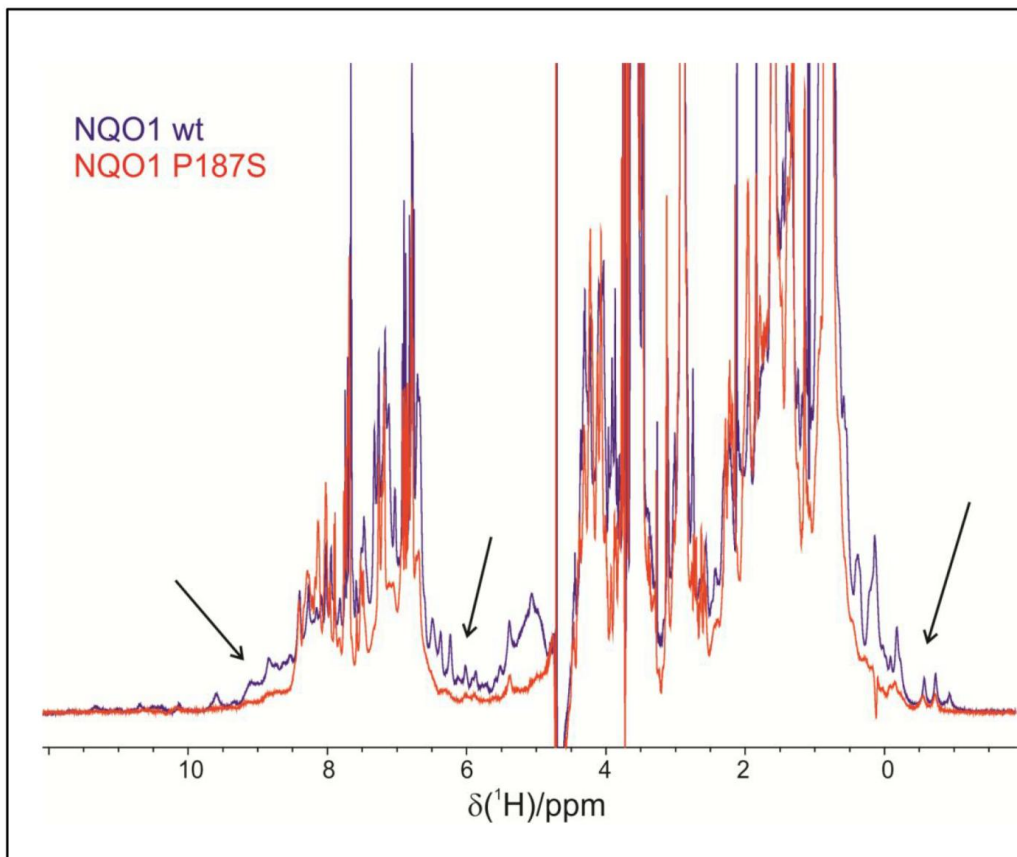


Fig. S5: NQO1 P187S exhibits different structural topology in solution to that of NQO1. Intensities of ¹H NMR spectra NQO1 (blue) and NQO1 P187S (red) were normalized on the methyl region (0.9 p.p.m) and superimposed. Signals outside the random coil regions (Arrows), which reflect tertiary structure, are much more pronounced for NQO1 than NQO1 P187S indicating its loss of structure in solution.

<u>Protein</u>	$\frac{\text{NADH}}{k_{\text{red}}}$ (M min ⁻¹)	$\frac{\text{NADPH}}{k_{\text{red}}}$ (M min ⁻¹)
NQO1	$2.1 \cdot 10^8 \pm 0.6 \cdot 10^8$	$3.4 \cdot 10^8 \pm 1.6 \cdot 10^8$
NQO1 P187S	$7.1 \cdot 10^5 \pm 1.0 \cdot 10^5$	$5.1 \cdot 10^6 \pm 1.1 \cdot 10^6$
NQO1 Δ50	$2.8 \cdot 10^5 \pm 0.4 \cdot 10^5$	$8.0 \cdot 10^5 \pm 0.7 \cdot 10^5$
NQO1 P187S Δ50	$1.9 \cdot 10^5 \pm 0.1 \cdot 10^5$	$4.9 \cdot 10^5 \pm 0.1 \cdot 10^5$

Table S1: Rapid Reaction kinetics. Bimolecular rate constants (M⁻¹ min⁻¹) determined for NQO1 proteins using NADH or NADPH as reducing agent. The absorbance change of protein bound FAD at 445 nm was monitored in a stopped-flow instrument at 4 °C.

	NQO1 P187S	NQO1 P187S $\Delta 50$
Data collection		
X-ray source	ESRF ID-29	ELETTRA XRD1
Wavelength (Å)	0.9724	1.1354
Temperature	100 K	100 K
Space group	I222	P4 ₁ 2 ₁ 2
Cell dimensions		
<i>a, b, c</i> (Å)	104.17, 104.56, 118.57	51.05, 51.05, 169.04
Resolution (Å)	26.74 - 2.69	33.81 - 2.20
high resolution shell	2.84 - 2.69	2.26 - 2.20
Total no. reflections	114922 (16147)	144289 (7592)
Unique no. reflections	18149 (2523)	12127 (843)
Multiplicity	6.3 (6.4)	11.9 (9.0)
Completeness (%)	99.5 (97.0)	99.8 (98.0)
<i>R</i> _{p.i.m.} (%)	6.4 (31.4)	3.5 (21.0)
<i>R</i> _{meas} (%)	16.0 (80.7)	12.4 (65.5)
<i>I</i> / σ (<i>I</i>) average	9.3 (2.4)	18.3 (3.2)
Refinement		
Resolution (Å)	46.22 - 2.69	33.20 - 2.20
high resolution shell	2.83 - 2.69	2.42 - 2.20
<i>R</i> _{work}	0.1847 (0.3102)	0.1755 (0.2292)
<i>R</i> _{free}	0.2074 (0.3448)	0.2239 (0.2955)
No. atoms	4531	2004
Protein	4316	1787
Cofactor/substrate	208	78
Water	7	139
Protein residues	541	222
B-factors (total)		
Protein (Å ²)	41.9	34.1
Cofactor/substrate (Å ²)	44.2	30.3
Water (Å ²)	38.0	37.8
All atoms (Å ²)	42.0	34.2
R.m.s. deviations		
Bond lengths (Å)	0.003	0.004
Bond angles (°)	0.719	0.895
Ramachandran outliers (%)	0	0

*Values in parentheses are for highest-resolution shell.

Table S2: Crystallographic data and refinement statistics for NQO1 P187S and NQO1 P187S (C-terminal truncation) crystal structures.

Materials & Methods

Molecular cloning of *nqo1*

The *nqo1* gene sequence (UniProtKB/Swiss-Prot: P15559) was codon optimized for *E. coli* expression and chemically synthesized (GeneArt, Carlsbad, California, USA). The *NQO1* genes were cloned into pET28a (Merck, Darmstadt, Germany) vector using Nde1 and Xho1 restriction sites to encode for a N-terminal histidine tagged fusion protein using gene specific primers (Eurofins, Luxembourg). *NQO1 P187S*, *NQO1 Δ 50* and *NQO1 P187S Δ 50* were generated by using QuikChange® II XL Site-Directed Mutagenesis Kit (Santa Clara, California, USA)

Protein expression purification

Protein expression was carried out in LB Broth (5 g/l sodium chloride) containing (50 µg/l) kanamycin. Fresh medium was inoculated with 40 ml/l of an over night culture and grown to an OD₆₀₀ of 0.95 before induction with 0.4 mM IPTG. Cells were harvested at 17,600 g for 5 min, resuspended in 1% saline solution and pelleted at 3,700 g at 4 °C for 45 min. Cell pellets were resuspended in lysis buffer (50 mM HEPES, 150 mM NaCl, 10 mM imidazol, pH 7.0) with 2 ml buffer per 1 g pellet. A pinch of FAD (disodium salt hydrate from Sigma Aldrich, St. Louis, Missouri, USA) and 10 µl of protease inhibitor cocktail for use in purification of histidine-tagged proteins in DMSO solution (Sigma Aldrich, St. Louis, Missouri, USA) were added per 25 ml of slurry. Cell disruption was achieved by sonication with a Labsonic P instrument (Sartorius, Göttingen, Germany) with 70% intensity and 0.5 s pulses for 10 minutes on ice. The cell lysate was centrifuged at 38,759 g for 30 min and the supernatant was loaded onto a 5 ml HisTrap™ FF (GE Healthcare, Little Chalfont, UK) column previously equilibrated with 50 mM HEPES, 150 mM NaCl, 20 mM imidazole, pH 7.0. The column was washed with 50 ml of 50 mM HEPES, 150 mM NaCl, 50 mM imidazole, pH 7.0 after which proteins were eluted with 50 mM HEPES, 150 mM NaCl, 300 mM imidazole, pH 7.0. Fractions containing target proteins were pooled and concentrated with centrifugal filter units (Amicon Ultra-15, 30 k; Millipore, Billerica, Massachusetts, USA). Concentrated protein was applied onto a HiLoad 16/60 Superdex 200 prep grade column (GE Healthcare, Little Chalfont, UK) equilibrated with 50 mM sodium phosphate, 150 mM NaCl, pH 7.0 for further purification. The fractions containing target proteins were collected, followed by rebuffering with a PD-10 desalting column (GE Healthcare, Little Chalfont, UK) in 50 mM HEPES, pH 7.0. The protein solutions was shock frozen and stored at -80 °C if not used immediately.

Apoprotein preparation

NQO1 or NQO1 P187S were applied onto 5ml HisTrap™ FF (GE Healthcare, Little Chalfont, UK) column previously equilibrated with 50 mM HEPES, 150 mM NaCl, 20 mM imidazole, pH 7.0. The column was washed with 50 ml buffer containing 50 mM HEPES, 150 mM NaCl, 2 M urea, 2 M KBr, pH 7.0 and then reequilibrated with 50 mM HEPES, 150 mM NaCl, 20 mM, imidazole, pH 7.0 (approx. 25 ml). Apo-protein was then eluted with 50 mM HEPES, 150 mM NaCl, 300 mM imidazol, pH 7.0. Removal of FAD was verified spectrophotometrically after rebuffering the protein into 50 mM HEPES, pH 7.0, employing PD-10 desalting columns (GE Healthcare, Little Chalfont, UK).

Difference titration

Difference titrations were carried out in tandem cuvettes (two separated chambers in the sample and reference cuvette) using a Specord 200 plus photometer (Analytik Jena, Jena, Germany) at 25 °C. The cuvettes were filled with 800 µl of 50 µM apo-protein solution in buffer (50 mM Tris, 150 mM NaCl, pH 7.5) in one chamber and 800 µl of buffer in the other chamber. Titrations were performed by additions of a FAD solution (1 mM) to the apo-protein in the sample cuvette and to the buffer in the reference cuvette. In each step the same volume of buffer was added to the apo-protein solution in the reference cell to compensate for the dilution of the apo-protein in the sample cuvette. After completion of the additions an absorption spectrum from 250 to 800 nm was recorded.

Isothermal titration microcalorimetry (ITC)

A VP-ITC system (MicroCal, GE Healthcare, Little Chalfont, UK) was used for calorimetric determination of the dissociation constants for FAD. All experiments were performed at 25 °C in 50 mM HEPES, pH 7.0 buffer and solutions were degassed before measurements. The titration experiments were performed with 290 µM ± 10 µM apo-protein solution in the syringe and 27 µM ± 1 µM FAD solution in the measurement cell. The concentration of FAD and the apo-protein was determined spectrophotometrically. All experiments comprised 35 injections (initial injection of 2 µl, injection duration time 4 s, spacing time 300 s followed by 34 injections of 6 µl, injection duration time 5.4 s, spacing time 300 s). Standard measurements without FAD were subtracted and the first measurement point is rejected while the remaining data points were analysed assuming a single site binding model with Origin version 7.0 (MicroCal) for ITC data analysis.

Limited proteolysis

30 μM of NQO1, apo NQO1 and NQO1 P187S in 50 mM HEPES, 150 mM NaCl pH 7.5 buffer were subjected to limited proteolysis at 37 °C by adding trypsin (Promega, Madison, Wisconsin, USA) to a final concentration of 2 $\mu\text{g}/\text{ml}$. The reaction was stopped after 5, 10, 20 and 40 minutes by adding SDS sample buffer to aliquots of reaction mixture and immediately boiling at 95 °C for ten minutes. 300 μM FAD was added to the protein solution prior to the addition of trypsin (Fig. S4). The samples were analysed by performing SDS-PAGE with precast gradient gels (Thermo Scientific, Waltham, Massachusetts, USA) (Fig. 3A) or by linear 12.5 % polyacrylamide gels (Fig. S4).

Maldi-TOF MS

Coomassie stained protein gel bands (Inset 1 and 2 Fig. 3a) were excised and destained by following standard in-gel digestion protocols. The cysteine residues were in-gel alkylated and reduced using iodoacetamide and dithiothreitol, respectively. The proteins were in-gel digested with trypsin at 37 °C. Peptide mixtures were extracted after trypsin digestion and the mixture was desalted using ZipTip (Millipore, Darmstadt, Germany). The purified peptides were spotted on a MALDI target plate together with matrix α -cyano-4-hydroxycinnamic acid and the spectra were recorded on a Micromass ToFSpec 2E in reflectron mode at an accelerating voltage of +20 kV. The instrument was calibrated using polyethylene glycol mixture (Sigma-Aldrich, St. Louis, Missouri, USA). ProteoMasS ACTH Fragment 18-39 (Sigma-Aldrich, St. Louis, Missouri, USA) was used as peptide calibration standard for the instrument. The spectra were analysed by using Masslynx 4.1 software and peptide mass profiles were assigned.

Labelling of NQO1 and NQO1 P187S with ^{15}N / ^{13}C

Instead of LB broth (Lennox) a minimal medium containing 6,8 g/l Na_2HPO_4 , 3 g/l KH_2PO_4 , 0.5 g/l NaCl, 1 g/l $^{15}\text{NH}_4\text{Cl}$, 3 g/l glucose, 1 $\mu\text{g}/\text{l}$ biotin, 1 $\mu\text{g}/\text{l}$ thiamin, 50 $\mu\text{g}/\text{ml}$ kanamycin and 1 ml 1000x microsals [150 mM CaCl_2 , 20 mM, FeCl_3 , 50 mM H_3BO_3 , 150 μM CoCl_2 , 800 μM CuCl_2 , 1.5 mM ZnCl_2 , 15 μM $(\text{NH}_4)_6\text{Mo}_7\text{O}_{24}\cdot 4\text{H}_2\text{O}$] was used for protein expression as described above. For double labelling of proteins with ^{15}N and ^{13}C 0.75 g/l $^{15}\text{NH}_4\text{Cl}$ and 2 g/l ^{13}C -glucose were used (Eurisotop, Saarbrücken, Germany) in the minimal medium.

NMR spectroscopy

One-dimensional ^1H NMR spectra were recorded with a Bruker Avance III 500 MHz NMR spectrometer at 298 K (Bruker, Rheinstetten, Germany). All other NMR experiments were carried out with a Bruker Avance III 700 MHz NMR spectrometer, equipped with a cryogenically cooled, 5 mm TCI probe at 298 K. Samples containing between 20-40 mg/ml NQO1 or NQO1 P187S in 50 mM HEPES, pH 6.5 in 90% H_2O and 10% D_2O were used for NMR measurements. For ^{15}N relaxation measurements, series of ten interleaved, relaxation edited, ^1H - ^{15}N HSQC spectra were recorded. The spectra were processed with nmrPipe (16) and analysed with CcpNmr(17). Rotational correlation times were calculated from the ^{15}N T_1/T_2 ratios as described(18).

Stopped flow kinetics

Stopped flow measurements were carried out with a Hi-Tech (SF-61DX2) stopped flow device (TgK Scientific Limited, Bradford-on-Avon, UK), positioned in a glove box from Belle Technology (Weymouth, UK) at 4 °C. Buffers were flushed with nitrogen, followed by incubation in the glove box environment. The enzyme and substrate solutions were deoxygenated by incubation in the glove box environment and then diluted with buffer to the required concentrations. Enzyme and substrate were rapidly mixed in the stopped-flow device and FAD oxidation and reduction were measured by monitoring changes at A_{455} with a KinetaScanT diode array detector (MG-6560, TgK Scientific Limited). Initial rates were calculated by fitting the curves with Specfit 32, a multivariate data analysis program (Spectrum Software Associates, Chapel Hill, North Carolina, USA), using a two exponential function.

The reductive half reaction was investigated by mixing proteins (40 μM) in 50 mM HEPES (pH 7.0) with NADPH or NADH in the stopped flow device. In the case of NQO1 the NAD(P)H concentrations were in the range of 50–200 μM and in the case of NQO1 P187S, NQO1 $\Delta 50$ and NQO1 P187S $\Delta 50$ the NAD(P)H concentrations were between 50 μM and 5 mM. The absorption decrease was monitored at 455 nm. To study the oxidative half reaction, proteins (40 μM) in 50 mM HEPES (pH 7.0) were first reduced by the addition of equimolar amounts of NADH. The reduced enzymes were then mixed with either benzoquinone or menadione (30 to 100 μM) and the reoxidation of the reduced FAD cofactor was monitored at 455 nm.

Crystallization conditions used for obtaining NQO1 P187S structure

11 mg/ml of NQO1 P187S in 50 mM Hepes, pH 7.0 mixed with saturated dicoumarol and equimolar Cibacron blue was crystallized by the microbatch method in a precipitating solution containing 60% Tacsimate™, pH 7.0 (Hampton Research Index Screen, condition 29) and were incubated at 289 K. The total drop volume was 1 μ l with equal amounts of protein and precipitant solution. The bluish crystal grew to full size (~ 85 μ m) within 30 days. Crystals were harvested from their mother liquor with CryoLoops™ (Hampton Research) and flash-cooled in liquid nitrogen.

Crystallization conditions used for obtaining NQO1 P187S structure (C-terminal truncation)

11 mg/ml of NQO1 P187S in 50 mM HEPES, pH 7.0 mixed with saturated dicoumarol (3,3'-methylene-bis(4-hydroxycoumarin) was crystallized by vapour batch method in a precipitating solution containing: 5 mM cobalt(II) chloride hexahydrate, 5 mM nickel(II) chloride hexahydrate, 5 mM cadmium chloride hydrate, 5 mM magnesium chloride hexahydrate, 100 mM HEPES, pH 7.5 and 12% (w/v) PEG 3350 (Hampton Research Index Screen, condition 64) and were incubated at 289 K. The total drop volume was 1 μ L with equal amounts of protein and precipitant solution. The yellow crystals grew to full size (~ 80 μ m) within 2 months. Crystals were harvested from their mother liquor with CryoLoops™ (Hampton Research) and flash-cooled in liquid nitrogen.

Structure Determination and Refinement of NQO1 P187S (C-terminal truncation)

A complete dataset for NQO1 P187S with a C-terminal truncation was collected from a single crystal at the beamline XRD1 ($\lambda = 1.1$ Å) at ELETTRA (Trieste, Italy). The dataset was collected to 2.2 Å resolution from a tetragonal crystal (space group $P4_12_12$). The data were processed with the program XIA2(19). The calculated Matthews coefficient (20) indicated the presence of 1 molecule per asymmetric unit. The structure was solved by molecular replacement method using the programs PHENIX AutoMR (21) and PHASER(22) using the structure of the NQO1 protomer (PDB entry 1qbg) as search template. The best PHASER result (based on log-likelihood statistics) was further used as input model for the automated chain-tracing/rebuilding program BUCCANEER (23). R_{free} values were computed from 5% randomly chosen reflections which were not used during refinement(24). Structure refinement and model rebuilding were carried out with the programs PHENIX (21) and COOT (25, 26) by alternating

real-space fitting against σ_A -weighted $2F_o - F_c$ and $F_o - F_c$ electron density maps and least square optimizations. Water molecules were placed into the difference electron density map and accepted or rejected according to geometry criteria as well as refined B-factors. The final model was refined to $R = 17.6\%$ and $R_{\text{free}} = 22.4\%$. Details of the data reduction and structure refinement are listed in (table S2).

Electron density could not be observed for the first 2 and the last 51 residues (missing C-terminal region). Additional electron density in the active site was assigned to the cofactor FAD and dicoumarol. Validation of the structure was carried out with the program MOLPROBITY (27) yielding a Ramachandran plot with 97.3% of the residues in favoured regions, 2.7% in allowed and none in disallowed regions. Prediction of the biologically active form of NQO1 P187S (C-terminal truncation) was done using the PISA server(28).

Structure Determination and Refinement of NQO1 P187S

A complete dataset was collected from a single crystal at beamline ID-29 ($\lambda = 1.0 \text{ \AA}$) at the European Synchrotron Radiation Facility. The dataset was collected to 2.69 \AA resolution from an orthorhombic crystal (space group $I222$). Data were processed using the program XDS(29). Analysis of the dataset with the program PHENIX (21) showed a pseudo-merohedral twin operator with a twin law “ $-k, -h, -l$ ” and a twin fraction of 39% according to Yeates’ L-test(30). Patterson analysis revealed a significant off-origin peak of 49.5% of the origin peak, indicating pseudo translational symmetry. The calculated Matthews coefficient (20) indicated the presence of 2 molecules per asymmetric unit. The structure was solved by molecular replacement using the program PHASER (22) and the detwinned dataset produced using the program DETWIN(20). The partially refined structure of NQO1 P187S (C-terminal truncation) was used as search template. The best PHASER result (based on log-likelihood statistics) was further used as input model for the automated chain-tracing/rebuilding program BUCCANEER(23). R_{free} values were computed from 5% randomly chosen reflections which were not used during refinement(24). Structure refinement and model rebuilding were carried out with the programs PHENIX (21) and COOT (25, 26) by alternating real-space fitting against σ_A -weighted $2F_o - F_c$ and $F_o - F_c$ electron density maps and least square optimizations. 7 water molecules were manually placed into strong peaks of difference electron density map. The final model was refined to $R = 18.5\%$ and $R_{\text{free}} = 20.7\%$. Details of the data reduction and structure refinement are listed in (table S2).

Electron density could not be observed for residues 1-3 and residue 274 in one protomer and for residues 1-3 in the other protomer. The cofactor FAD and the ligand Cibacron blue were placed manually into the difference electron density map. Electron density for dicoumarol could not be identified. Validation of the structure was carried out with the program MOLPROBITY(27) yielding a Ramachandran plot with 93.5% of the residues in favoured regions, 6.5% in allowed and none in disallowed regions. Prediction of the biologically active form of NQO1 P187S was done using the PISA server ²⁸. Figures were created using the program PyMOL (31).

Acknowledgments

This work was supported by the Austrian *Fonds zur Förderung der wissenschaftlichen Forschung* (FWF) through project P22361 to P.M and K.G. and the PhD programme “Molecular Enzymology” (W901) to K.Z., K.G. and P.M. We also thank the interuniversity programme in natural sciences, NAWI Graz, for financial support.

References

1. Dinkova-Kostova AT, Talalay P (2010) NAD(P)H:quinone acceptor oxidoreductase 1 (NQO1), a multifunctional antioxidant enzyme and exceptionally versatile cytoprotector. *Arch Biochem Biophys* 501:116–23.
2. Asher G, Lotem J, Cohen B, Sachs L, Shaul Y (2001) Regulation of p53 stability and p53-dependent apoptosis by NADH quinone oxidoreductase 1. *Proc Natl Acad Sci U S A* 98:1188–93.
3. Garate M, Wong RPC, Campos EI, Wang Y, Li G (2008) NAD(P)H quinone oxidoreductase 1 inhibits the proteasomal degradation of the tumour suppressor p33(ING1b). *EMBO Rep* 9:576–581.
4. Asher G, Tsvetkov P, Kahana C, Shaul Y (2005) A mechanism of ubiquitin-independent proteasomal degradation of the tumor suppressors p53 and p73. *Genes Dev* 19:316–21.
5. Gong X, Kole L, Iskander K, Jaiswal AK (2007) NRH:quinone oxidoreductase 2 and NAD(P)H:quinone oxidoreductase 1 protect tumor suppressor p53 against 20s proteasomal degradation leading to stabilization and activation of p53. *Cancer Res* 67:5380–8.
6. Siegel D, Yan C, Ross D (2012) NAD(P)H:quinone oxidoreductase 1 (NQO1) in the sensitivity and resistance to antitumor quinones. *Biochem Pharmacol* 83:1033–40.

7. Traver RD et al. (1992) NAD(P)H:quinone oxidoreductase gene expression in human colon carcinoma cells: characterization of a mutation which modulates DT-diaphorase activity and mitomycin sensitivity. *Cancer Res* 52:797–802.
8. Kelsey KT et al. (1997) Ethnic variation in the prevalence of a common NAD(P)H quinone oxidoreductase polymorphism and its implications for anti-cancer chemotherapy. *Br J Cancer* 76:852–854.
9. Lan Q et al. (2004) Hematotoxicity in workers exposed to low levels of benzene. *Science* 306:1774–6.
10. Fagerholm R et al. (2008) NAD(P)H:quinone oxidoreductase 1 NQO1*2 genotype (P187S) is a strong prognostic and predictive factor in breast cancer. *Nat Genet* 40:844–53.
11. Chen S, Wu K, Knox R (2000) Structure-function studies of DT-diaphorase (NQO1) and NRH: quinone oxidoreductase (NQO2). *Free Radic Biol Med* 29:276–284.
12. Moscovitz O et al. (2012) A mutually inhibitory feedback loop between the 20S proteasome and its regulator, NQO1. *Mol Cell* 47:76–86.
13. Asher G et al. (2006) The crystal structure of NAD(P)H quinone oxidoreductase 1 in complex with its potent inhibitor dicoumarol. *Biochemistry* 45:6372–6378.
14. Faig M et al. (2000) Structures of recombinant human and mouse NAD(P)H:quinone oxidoreductases: species comparison and structural changes with substrate binding and release. *Proc Natl Acad Sci U S A* 97:3177–82.
15. Martinelli D et al. (2012) EPI-743 reverses the progression of the pediatric mitochondrial disease--genetically defined Leigh Syndrome. *Mol Genet Metab* 107:383–8.
16. Delaglio F et al. (1995) NMRPipe: a multidimensional spectral processing system based on UNIX pipes. *J Biomol NMR* 6:277–93.
17. Vranken WF et al. (2005) The CCPN data model for NMR spectroscopy: development of a software pipeline. *Proteins* 59:687–696.
18. Farrow N et al. (1994) Backbone dynamics of a free and phosphopeptide-complexed Src homology 2 domain studied by ¹⁵N NMR relaxation. *Biochemistry* 33:5984–6003.
19. Winter G (2009) xia2: an expert system for macromolecular crystallography data reduction. *J Appl Crystallogr* 43:186–190.
20. The CCP4 suite: programs for protein crystallography. (1994) *Acta Crystallogr D Biol Crystallogr* 50:760–3.
21. Adams PD et al. (2010) PHENIX: a comprehensive Python-based system for macromolecular structure solution. *Acta Crystallogr D Biol Crystallogr* 66:213–221.
22. McCoy AJ et al. (2007) Phaser crystallographic software. *J Appl Crystallogr* 40:658–674.

23. Cowtan K (2006) The Buccaneer software for automated model building. 1. Tracing protein chains. *Acta Crystallogr D Biol Crystallogr* 62:1002–1011.
24. Kleywegt GJ, Brünger AT (1996) Checking your imagination: applications of the free R value. *Structure* 4:897–904.
25. Emsley P, Cowtan K (2004) Coot: model-building tools for molecular graphics. *Acta Crystallogr D Biol Crystallogr* 60:2126–2132.
26. Emsley P, Lohkamp B, Scott WG, Cowtan K (2010) Features and development of Coot. *Acta Crystallogr D Biol Crystallogr* 66:486–501.
27. Chen VB et al. (2010) MolProbity: all-atom structure validation for macromolecular crystallography. *Acta Crystallogr D Biol Crystallogr* 66:12–21.
28. Krissinel E, Henrick K (2007) Inference of macromolecular assemblies from crystalline state. *J Mol Biol* 372:774–797.
29. Kabsch W (2010) XDS. *Acta Crystallogr D Biol Crystallogr* 66:125–32.
30. Padilla JE, Yeates TO (2003) A statistic for local intensity differences: robustness to anisotropy and pseudo-centering and utility for detecting twinning. *Acta Crystallogr D Biol Crystallogr* 59:1124–1130.
31. DeLano WL (2002) The PyMOL Molecular Graphics System. *Schrödinger LLC* www.pymol.org Version 1.:<http://www.pymol.org>.

Biochemical characterization of human NAD(P)H:quinone oxidoreductase (NQO1) variant NQO1 R139W

6.1 Introduction

Human cytoplasmic 2-electron reductase NAD(P)H:quinone oxidoreductase (NQO1) is essential for quinone detoxification. The ability of NQO1 to reduce quinone based anti tumour pro drugs to cytotoxic drugs, coupled with the up regulation of NQO1 in various solid tumors (e.g. lung, breast and pancreatic tumors) made it an attractive target for cancer treatment (1). Simultaneously, evidence has been increasingly emerging about multiple roles of NQO1 in cancer development and progression (2). In this context, NQO1 polymorphisms were widely researched in the last decade.

The number of single-nucleotide polymorphisms (SNPs) reported in the *NQO1* increased greatly in the last decade, 22 SNPs were reported in 2002 and this number has since increased to 91 in 2008 (3, 4). The two most commonly occurring SNPs in *NQO1* are C609T (*NQO1**2; NQO1 P187S) and C465T (*NQO1**3; NQO1 R139W). The frequency of *NQO1**2 varies between 16-49%, while that of *NQO1**3 varies between 0-5 % among different ethnic populations (4). NQO1 P187S has been extensively studied in the last few years and the effects of this amino acid exchange are discussed in detail in chapter 5. Contrastingly, NQO1 R139 has been poorly studied and information regarding how the amino acid exchange affects the protein is largely unknown.

Homozygous mutant alleles (*NQO1**3, C465T) encoding for NQO1 R139W were discovered in the HCT 116-R3OA cell line. This cell line is a mitomycin-c resistant sub line derived from human colorectal carcinoma HCT-116 cell line which is heterozygous for *NQO1**3 (5). Mitomycin-c is a quinone based cytotoxic antibiotic used for the treatment of solid tumors e.g. stomach, pancreas, breast and lung tumors (6). Gain of mitomycin-c resistance in HCT 116-R3OA cell line was initially ascribed to lower concentrations of NQO1 R139W (5). It was proposed that the depletion NQO1 R139W could be due to alternative splicing of *NQO1* pre mRNA. An alternative splicing site is present at the boundary of intron-4 and exon-4 (nucleotide position 465 in the open reading frame or amino acid position 139 in the peptide chain) (7). Alternate splicing of *NQO1* pre mRNA at this position results in a new species of mRNA, exon 4-deleted mRNA. This alternative splicing occurs in all three variants of NQO1, albeit at different

levels (8). This alternative splicing site if further modified by the SNP (C465T) resulting in much higher levels of exon 4-deleted mRNA in *NQO1*3* genotype. The ratio of full length to exon 4-deleted mRNA in HCT 116-R3OA cell line is 66:34, while the wild type *NQO1* cells have a ratio of 90:10 (8). The exon 4 of *NQO1* encodes for amino acids 102-139 (figure 1, A) (7). Even though the exon 4-deleted mRNA encodes for an open reading frame, it is highly probable that the resulting protein is dysfunctional since the amino acids 104-107 belonging to exon4 form a β -turn which is essential for the FAD cofactor binding (figure 1, B). Exchange of amino acids in a similar β -turn of Lot6p an orthologue of *NQO1* lead to the loss of FMN cofactor and subsequently a dysfunctional enzyme (chapter 2).

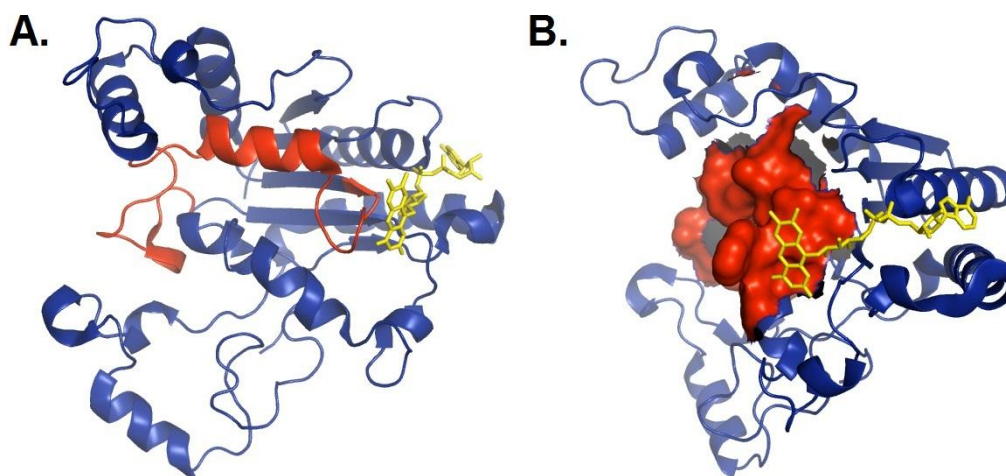


Figure 1: The amino acids encoded by exon 4 are crucial for binding of the FAD cofactor. **A.** A single protomer of *NQO1* is represented as a cartoon (blue), the FAD cofactor is shown in yellow and the amino acids encoded by exon 4 are shown in red. **B.** The amino acids of *NQO1* (104-G10) which are a part of exon 4 are represented as surface (red) forming a part of the FAD cofactor (yellow) binding pocket.

Pan et.al., showed that the loss of *in vivo* *NQO1* R139W enzymatic activity in HCT 116-R3OA cell line can be partially restored by preventing the formation of exon 4-deleted mRNA (8). It is surprising that the authors of the above mentioned study did not compare the *in vivo* enzymatic activity of *NQO1* in wild type cell line compared to that of HCT 116-R3OA cell line. It

is possible that HCT 116-R3OA cell line will have comparable enzymatic activity to that wild type cell line since full length mRNA (90% *NQO1*:34% *NQO1**3) is present in both cell lines.

Intriguingly, no evidence was available as to how the HCT 116-R3OA cell line responds to other quinone based drugs (e.g. β -lapachone and benzoquinone ansamycins) shown to be activated by NQO1. It is still unknown how the HCT 116-R3OA gained the resistance to mitomycin-C while the parent cell line HCT 116 is susceptible to mitomycin-c. It is possible that NQO1 R139W enzyme is unable to reduce mitomycin-c. Since, HCT 116-R3OA cells are resistant to mitomycin treatment even though they possess 34% of full length mRNA encoding for NQO1 R139W. In this context it would be interesting to biochemically characterize NQO R139W and evaluate its ability to reduce mitomycin-c.

6.2 Results, discussion and future work

NQO1 R139W enzyme was cloned, expressed and purified in a similar fashion to NQO1 P187S mentioned in chapter 5. Preliminary, difference titration, isothermal calorimetry, rapid reaction measurements, partial proteolysis and X-ray crystallography experiments indicated that NQO1 R139W exhibits similar biochemical and structural properties to that of NQO1 (data not shown). The data obtained from difference titration and isothermal calorimetry experiments is only indicative but not conclusive, hence these experiments will be repeated in the near future. The X-ray crystal structure of NQO1 R139W has yet to be refined in order to arrive at proper conclusions. On the other hand, partial proteolysis and rapid reaction measurements conclusively showed that NQO1 R139W behaves similarly to NQO1.

Reduction of quinone moiety to cytotoxic hydroquinone is essential for cytotoxicity of many quinone based anti cancer drugs. NQO1 was known to efficiently reduce quinones to hydroquinones. However, evidence regarding NQO1's ability to activate prodrugs is still inconclusive with many studies reporting contrasting results. Several quinone based chemotherapeutics were reported to be activated by NQO, e.g. alkylators mitomycin-c, RH1(2,5-diaziridinyl-3-(hydroxymethyl)-6-methyl-1,4-benzoquinone), indolequinone EO9 and redox cycling compounds streptonigrin and β -lapachone (9). Currently, unequivocal evidence showing that these compounds are activated by NQO1 but not other reductases (e.g. cytochrome P450 reductase, cytochrome b5 reductase, NQO2, carbonyl reductases, and thioredoxin reductase) is not available since the majority of conclusions were based on experiments performed with cell lines rather than purified enzymes (6).

In this context we have studied the biochemical and structural properties of NQO1 P187S completely and NQO1 R139W partially. It would be interesting to test the ability of NQO1 variants to activate the above mentioned chemotherapeutics, and also compare the pro-drug activating properties of NQO1 variants with that of a single electron reductase such as cytochrome P450 reductase.

References

1. Siegel, D., Kepa, J. K., and Ross, D. (2012) NAD(P)H:quinone oxidoreductase 1 (NQO1) localizes to the mitotic spindle in human cells. *PLoS One* **7**, e44861
2. Lajin, B., and Alachkar, A. (2013) The NQO1 polymorphism C609T (Pro187Ser) and cancer susceptibility: a comprehensive meta-analysis. *Br. J. Cancer* **109**, 1325–37
3. Nebert, D. W., Roe, A. L., Vandale, S. E., Bingham, E., and Oakley, G. G. NAD(P)H:quinone oxidoreductase (NQO1) polymorphism, exposure to benzene, and predisposition to disease: a HuGE review. *Genet. Med.* **4**, 62–70
4. Guha, N., Chang, J. S., Chokkalingam, A. P., Wiemels, J. L., Smith, M. T., and Buffler, P. A. (2008) NQO1 polymorphisms and de novo childhood leukemia: a HuGE review and meta-analysis. *Am. J. Epidemiol.* **168**, 1221–32
5. Pan, S. S., Forrest, G. L., Akman, S. A., and Hu, L. T. (1995) NAD(P)H:quinone oxidoreductase expression and mitomycin C resistance developed by human colon cancer HCT 116 cells. *Cancer Res.* **55**, 330–5
6. Siegel, D., Yan, C., and Ross, D. (2012) NAD(P)H:quinone oxidoreductase 1 (NQO1) in the sensitivity and resistance to antitumor quinones. *Biochem. Pharmacol.* **83**, 1033–40
7. Gasdaska, P. Y., Fisher, H., and Powis, G. (1995) An alternatively spliced form of NQO1 (DT-diaphorase) messenger RNA lacking the putative quinone substrate binding site is present in human normal and tumor tissues. *Cancer Res.* **55**, 2542–7
8. Pan, S.-S., Han, Y., Farabaugh, P., and Xia, H. (2002) Implication of alternative splicing for expression of a variant NAD(P)H:quinone oxidoreductase-1 with a single nucleotide polymorphism at 465C>T. *Pharmacogenetics* **12**, 479–88
9. Parkinson, E. I., Bair, J. S., Cismesia, M., and Hergenrother, P. J. (2013) Efficient NQO1 substrates are potent and selective anticancer agents. *ACS Chem. Biol.* **8**, 2173–83

Curriculum vitae

Personal Details:

Name: Venugopal Gudipati
Date of Birth: 30-08-83
Nationality: Indian
Address: Elisabethstraße 85, 8010, Graz, Austria.
Email: venugopal.gudipati@tugraz.at



Education:

2009 – To date: **Graz University of Technology, Austria**
Doctoral studies in Biochemistry.
Supervised by: Dr. Peter Macheroux
Expected finish date: 02/2014

05/2012-11/2012: **University of Cologne, Germany**
Research stay at the institute of genetics.
Supervised by: Dr. Jürgen Dohmen

2007 – 2008: **University of Glasgow, United kingdom**
Mres in Biomedical sciences.

2002 – 2006: **Andhra University, Visakhapatnam, India**
Bachelor of technology in Biotechnology.

Research and technical Skills:

- DNA & RNA isolation, molecular cloning and protein expression.
- Endogenous and recombinant protein purification. (FPLC)
- Purification of macromolecular complexes. (Affinity chromatography & FPLC)
- Biochemical characterization of proteins.
(UV-Vis, fluorescence spectroscopy, SDS-PAGE and Immuno blotting)

- Characterizing Protein-Protein interactions.
(Pull-down assays, Co-Immuno precipitation and MALDI-Tof)
- Enzyme kinetics. (ITC, SPR and Stopped flow)
- Enzyme activity assays & protein stability assays.
- *Saccharomyces cerevisiae* and *Escherichia coli* cell culture.
- Bacteriophage decontamination.
- Scientific writing & communication, critical evaluation and mentoring.

Publications:

- Gudipati, V., Koch, K., Lienhart, W.-D. & Macheroux, P. The flavoproteome of the yeast *Saccharomyces cerevisiae*. *Biochim. Biophys. Acta* (2013).
- Lienhart, W.-D., Gudipati, V. & Macheroux, P. The human flavoproteome. *Arch. Biochem. Biophys.* 535, 150–62 (2013).
- Craig, A., Ewan, R., Mesmar, J., Gudipati, V. & Sadanandom, A. E3 ubiquitin ligases and plant innate immunity. *J. Exp. Bot.* 60, 1123–32 (2009).

Publications in submission:

- Collapse of the native structure by a single amino acid exchange in human NAD(P)H:quinone oxidoreductase (NQO1). **Wolf-Dieter Lienhart, Venugopal Gudipati, Peter Macheroux et al., (Co first authors)**

Posters and Oral Presentations:

- Protein Quality Control and Ubiquitin Systems in Health and Disease, Kusadasi, Turkey. (November 2012)
- 5th International Beilstein Symposium, Protein structure meets enzyme kinetics, Rudesheim, Germany. (September 2011)

Venugopal Gudipati